Okamoto and Tanimoto *Progress in Earth and Planetary Science* (2016) 3:34
DOI 10.1186/s40645-016-0109-2

Progress in Earth and Planetary Science

REVIEW Open Access

A review of atmospheric chemistry observations at mountain sites

Sachiko Okamoto* and Hiroshi Tanimoto*

Abstract

Located far from anthropogenic emission sources, high-altitude mountain stations are considered to be ideal sites for monitoring climatic and environmentally important baseline changes in free tropospheric trace gases and aerosols. In addition, the observations taken at these stations are often used to study the long-range transport of dust as well as anthropogenic and biomass burning pollutants from source regions and to evaluate the performance of global and regional models. In this paper, we summarize the results from past and ongoing field measurements of atmospheric constituents at high-altitude stations across the globe, with particular emphasis on reactive trace species including tropospheric ozone, along with its precursors such as carbon monoxide, nitrogen oxides, total reactive nitrogen, and nonmethane hydrocarbons. Over the past decades, our understanding of the temporal variability and meteorological mechanisms of long-range transport has advanced in tandem with progress in instrumentation and modeling. Finally, the future needs of atmospheric chemistry observations at mountain sites are addressed.

Keywords: Atmospheric observation, High-altitude station, Long-range transport, Seasonal cycle, Long-term trend, Biomass burning, Anthropogenic pollution

Introduction

Trace gases and aerosols present in the atmosphere are responsible for global changes in the environment and climate of the Earth. These changes include global warming, which has caused a temperature increase of 0.85 °C during the period from 1880 to 2012, primarily due to increases in the atmospheric concentrations of greenhouse gases (GHGs) since the pre-industrial era (Intergovermental Panel on Climate Change 2013), poor air quality associated with high levels of photo-oxidants, and fine particulate matter with particle diameters of less than 2.5 μm ($PM_{2.5}$). These changes have been traced to high population densities and hasty industrialization in rapidly developing regions (World Health Organization 2006). Such air pollution problems, which can cause damage to human health and to vegetation growth, are now recognized as important, and robust evidence based on reliable observations is needed to support related policymaking processes.

Located far from anthropogenic emissions, high-altitude mountain stations are ideal sites for monitoring the temporal variations of trace gases and aerosols in the atmosphere at background levels. As a result, atmospheric monitoring programs have been established at a substantial number of mountain stations in order to obtain information on the levels, variability, and trends of trace gases and aerosols in the free troposphere (FT), as well as to assess the influence of anthropogenic and natural emission sources. It is widely accepted that observations at mountain sites are affected by the horizontal and vertical transport of polluted air masses from the ground surface (Henne et al. 2004; Trickl et al. 2003). Based on the analysis of tropospheric ozone (O_3) data collected at 27 stations located in mountainous and rural areas in Western Europe at altitudes ranging from 115 to 3550 m above sea level (a.s.l.), Chevalier et al. (2007) suggested that ground-based stations devoted to the monitoring of background free tropospheric O_3 should be settled, if possible, above 2000 m a.s.l.

Tropospheric O_3, which is an important GHG, has an estimated radiative forcing (RF) of 0.40 ± 0.20 W m^{-2} (Intergovermental Panel on Climate Change 2013). The RF from tropospheric O_3 depends strongly on altitude and latitude due to the coupling of O_3 changes with temperature, water vapor, and clouds (Bowman et al.

* Correspondence: okamoto.sachiko@nies.go.jp; tanimoto@nies.go.jp
Center for Global Environmental Research, National Institute for Environmental Studies, 16-2 Onogawa, Tsukuba, Ibaraki 305-8506, Japan

2013; Worden et al. 2008, 2011). O_3 is the main source of hydroxyl radicals (OH), which drive the oxidizing capacity of the atmosphere. It is widely accepted that tropospheric O_3 has two sources: subsidence transport from the stratosphere and in situ photochemical production, which occurs when carbon monoxide (CO) and hydrocarbons are photo-oxidized in the presence of nitrogen oxides ($NO_x = NO + NO_2$) (Crutzen 1974; Monks et al. 2009). The major loss pathways for O_3 in the troposphere include dry deposition to the Earth's surface, chemical destruction via photolysis to $O(^1D)$ which reacts with water vapor, and chain reaction with hydroperoxyl radicals (HO_2) and OH (Seinfeld and Pandis 2006). The lifetime of O_3 in the troposphere varies strongly in different seasons and locations, ranging from a few days in the tropical boundary layer to 1 year in the upper troposphere. The modeled mean lifetime of tropospheric O_3 has been reported as 22.3 ± 2 days (Stevenson et al. 2006).

Although CO is not a radiatively active gas, it affects the climate indirectly via its interaction with OH radicals, which are the primary CO sink. The oxidation of CO by OH leads to the formation of HO_2, which then can become involved in reactions to produce O_3 in NO_x-rich environments. In contrast, CO oxidation by OH radicals can lead to O_3 destruction through catalytic cycles of HO_x in low-NO_x environments (Kanakidou and Crutzen 1999). The changes in the OH radical concentration due to changes in CO can perturb the concentrations of GHGs such as methane (CH_4) (Thompson and Cicerone 1986) and chlorofluorocarbon (CFC) along with others such as hydrochlorofluorocarbons (HCFCs) and hydrofluorocarbons (HFCs). The major sources of CO emissions into the atmosphere are direct emissions from incomplete combustion of biomass and fossil fuels associated with in situ production via the oxidation of hydrocarbons such as CH_4 and isoprene (C_5H_8). Global estimates for anthropogenic and biomass burning emissions for 2000 were 611 and 459 Tg (CO) $year^{-1}$, respectively (Lamarque et al. 2010). The global mean tropospheric lifetime of CO is relatively long at approximately 2 months (e.g., Prather 1996) and seasonal and spatial CO lifetime variations have been reported in the study of Duncan et al. (2007). In the Northern Hemisphere winter season, the lifetime tends to be long, so CO from fossil fuels and industry accumulates. Conversely, in the Southern Hemisphere, CO approaches its seasonal minimum in austral summer because its lifetime is short and biomass burning activities are at a minimum. This latitudinal gradient becomes weak as summer approaches because the CO lifetime declines, over a scale of weeks to months, across most of the Northern Hemisphere. Simultaneously, however, the CO lifetime increases at southern mid-latitudes since the biomass-burning season is beginning in the Southern Hemisphere.

The term "background" concentrations have been used with various definitions in the literature over time. Calvert (1990) described "background concentration" as "the concentration of a given species in a pristine air mass, in which anthropogenic impurities of a relatively short lifetime are not present". However, because the troposphere is globally influenced by the long-range transport of pollution, Parrish et al. (2012) adopted the term "baseline," which refers to measurements obtained when local emission influences are determined to be negligible. Since remote coastal or mountainous sites are regarded as having no direct influence from local sources/sinks, such sites are the primary choices when looking to obtain representative data on continental to hemispheric scales. The US Environmental Protection Agency (EPA) defined the "Policy Relevant Background (PRB)" concentration as the concentration that would occur in the USA in the absence of anthropogenic emissions in continental North America (U.S. Environmental Protection Agency, 2006). Hence, since the sources of PRB concentrations include natural emissions and long-range transport of pollutants, they cannot be controlled by domestic regulations in the USA and/or neighboring countries.

Most studies have assumed the representativeness of mountain sites without providing evidence to support the assumption. Nappo et al. (1982) suggested that "representativeness is the extent to which a set of measurements taken in a space-time domain reflects the actual conditions in the same or different space-time domain taken on a scale appropriate for a specific application". However, representativeness not only varies with time, it also strongly depends on the trace gases because the concentration within a certain volume is controlled by vertical/horizontal transport and mixing, chemical transformations, surface deposition, and emissions.

The spatial representativeness of monitoring sites has been assessed by different approaches, primarily in Europe (e.g., Henne et al. 2010; Joly and Peuch 2012; Kovač-Andrić et al. 2010; Spangl et al. 2007; Tarasova et al. 2007). In addition, observations at mountain-based stations provide information of the lower FT, which is located between the planetary boundary layer (PBL) and the tropopause. Many species in the FT, such as O_3, have longer lifetimes than those in the PBL owing to the lower temperatures and lack of deposition in the FT, which is also where most of the transport of chemical species within the atmosphere occurs. The combination of long-range transport and longer chemical lifetimes in the FT indicates that the chemistry of this zone is an important factor when determining the chemical composition of regions remote from pollutant sources (Hemispheric Transport of Air Pollution 2007).

However, observations at ground-based stations can often be influenced by local sources. The objective of

data selection is to differentiate the concentrations representative of well-mixed air masses near the site from those substantially affected by local sources or meteorology. Data selection can be performed on the basis of independently measured parameters such as wind direction and speed, statistical approaches for rejecting particular data, or combined meteorological and statistical filters. For example, statistical approaches have been applied to trend analyses of trace gases (e.g., Novelli et al. 1998, 2003; Ruckstuhl et al. 2012; Schuepbach et al. 2001; Thoning et al. 1989; Zellweger et al. 2009) in order to evaluate source regions and their emission estimates (e.g., Greally et al. 2007; Prinn et al. 2001) and to model the long-range transport of trace gases (Balzani Lööv et al. 2008).

When using measurements at mountainous sites, it is necessary to consider upslope flow, which often imposes pollution from local anthropogenic sources located in the foothills. This source is the most likely factor in the contamination of clean air masses arriving at the site from the FT. Conversely, in the absence of emission sources near the site, the upslope flow can transport clean air masses from the boundary layer that have atmospheric compositions that are different from that from the FT (e.g., Hahn et al. 1992; Oltmans et al. 1996b; Peterson et al. 1998).

Upslope flow on isolated mountains results from two primary mechanisms: mechanically forced lifting and buoyant upslope flow. Mechanically forced lifting is caused by the deflection of strong winds by a mountain slope. The importance of this mechanism differs among mountains and depends mainly on the height of the mountain and the mean speed of the wind. Buoyant upslope flow is caused by the daytime solar heating of air near the surface of the mountain. During the day, warmed air masses rise toward the summit. At night, flows down the mountain occur due to radiative cooling of the ground surface. Both the upslope and downslope flows are important for mountain meteorology and the transport of local pollution (e.g., Furger et al. 2000). In practice, however, determination of baseline concentrations is difficult because the nature and magnitude of such local influence depend on the mountain topography, local wind patterns, and the characteristics of local emission sources.

The World Meteorological Organization (WMO) launched the Global Atmosphere Watch (GAW) Programme in 1989 to promote systematic and reliable observations of the chemical composition of the atmosphere. Currently, the GAW has the most extensive measurement program. Its focal areas include aerosols, GHGs, selected reactive gases, O_3, ultraviolet (UV) radiation, and precipitation chemistry. In October 1990, WMO designated the Japan Meteorological Agency (JMA) in Tokyo as the World Data Centre for Greenhouse Gases (WDCGG) and tasked it with collecting, archiving, and providing data related to GHGs and reactive gases in the atmosphere and oceans from observation sites throughout the world that participate in the GAW and other scientific monitoring programs.

Since its establishment, WDCGG has provided users with data and other information through its regular publications and the WDCGG website (http://ds.data.jma.go.jp/gmd/wdcgg/). In addition, observational data is currently provided by many regional monitoring programs worldwide including the European Monitoring and Evaluation Programme (EMEP; http://www.emep.int) in the European region, the Clean Air Status and Trends Network (CASTNET; http://www.epa.gov/castnet), the Interagency Monitoring of Protected Visual Environments (IMPROVE; http://vista.cira.colostate.edu/improve/) in North America, which monitors visibility conditions, tracks changes in visibility, and works to identify sources and causes of regional haze in class I areas (including national parks, wilderness areas, and national memorial parks), and the Acid Deposition Monitoring Network in East Asia (EANET; http://www.eanet.asia/).

In this paper, we describe past and current atmospheric observations conducted at high-altitude stations on mountains, the data of which are available in public databases or published papers. First, overviews of the individual mountain stations above 1500 m a.s.l. are given. Next, we review temporal variations, particularly the long-term trends and seasonal variations of reactive species including tropospheric O_3, and its precursors such as CO, NO_x, total reactive nitrogen (NO_y), and nonmethane hydrocarbons (NMHCs), but excluding long-lived GHGs. Since observations of aerosol optical properties at high-altitude stations are well described by Andrews et al. (2011), short-lived species—with the exceptions of carbon dioxide (CO_2) and mercury (Hg) described in association with the analysis of reactive species—are mainly discussed here. We will review previous observations of the long-range transport of pollutants from anthropogenic and biomass burning sources, desert dust, and volcanic plumes from eruption events, along with the downward transport of stratospheric air masses into the troposphere as important sources of O_3. Moreover, we also review the modeling studies using photochemical box models and chemical transport models.

Review

High-elevation mountain sites

The ground-based stations for atmospheric chemistry observations presented in this study are located at high altitudes above 1500 m a.s.l., as shown in Fig. 1; detailed site information is listed in Table 1. In total, the list contains 31 stations. These stations were selected because

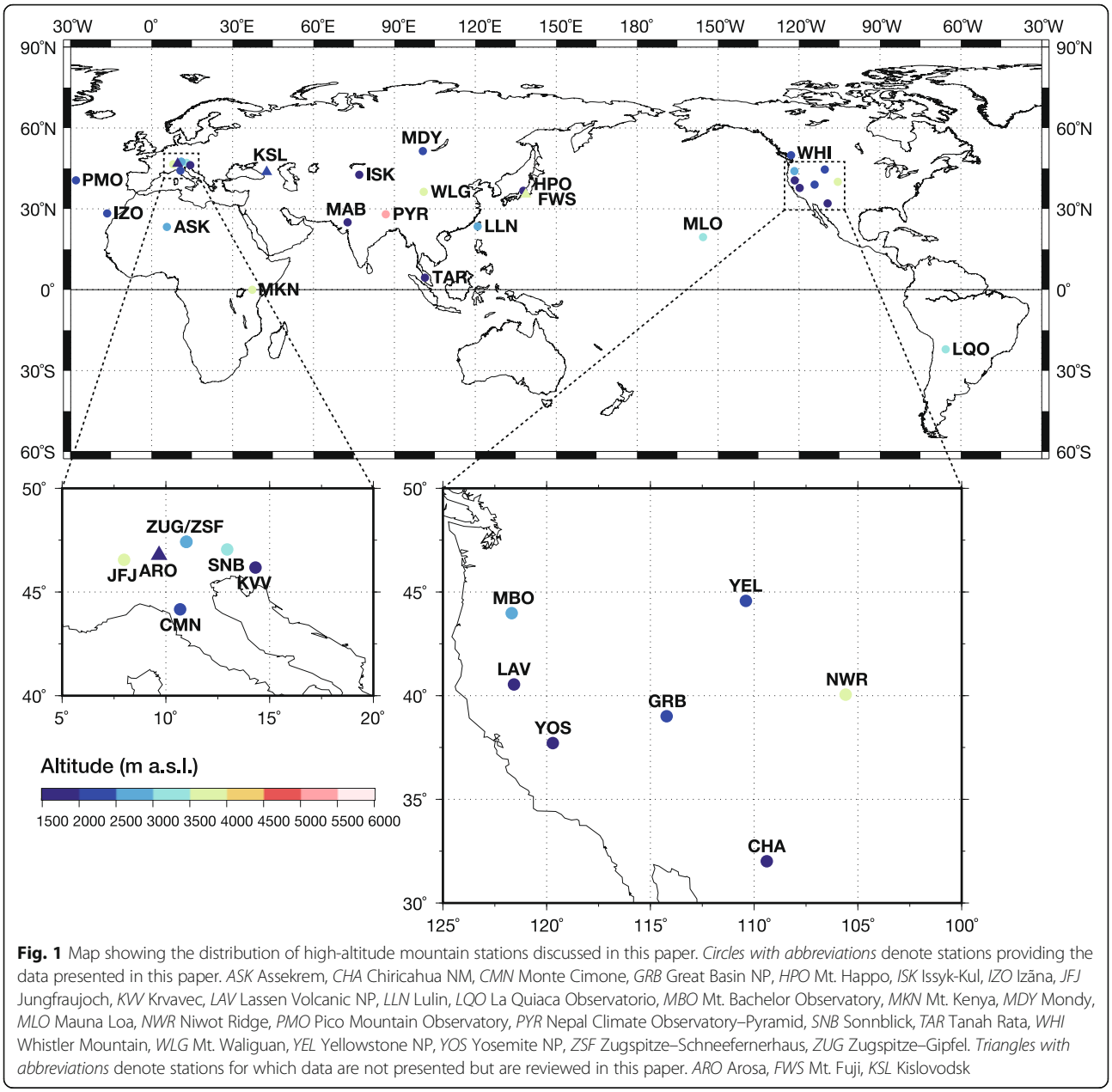

Fig. 1 Map showing the distribution of high-altitude mountain stations discussed in this paper. *Circles with abbreviations* denote stations providing the data presented in this paper. *ASK* Assekrem, *CHA* Chiricahua NM, *CMN* Monte Cimone, *GRB* Great Basin NP, *HPO* Mt. Happo, *ISK* Issyk-Kul, *IZO* Izãna, *JFJ* Jungfraujoch, *KVV* Krvavec, *LAV* Lassen Volcanic NP, *LLN* Lulin, *LQO* La Quiaca Observatorio, *MBO* Mt. Bachelor Observatory, *MKN* Mt. Kenya, *MDY* Mondy, *MLO* Mauna Loa, *NWR* Niwot Ridge, *PMO* Pico Mountain Observatory, *PYR* Nepal Climate Observatory–Pyramid, *SNB* Sonnblick, *TAR* Tanah Rata, *WHI* Whistler Mountain, *WLG* Mt. Waliguan, *YEL* Yellowstone NP, *YOS* Yosemite NP, *ZSF* Zugspitze–Schneefernerhaus, *ZUG* Zugspitze–Gipfel. *Triangles with abbreviations* denote stations for which data are not presented but are reviewed in this paper. *ARO* Arosa, *FWS* Mt. Fuji, *KSL* Kislovodsk

they provide reliable observational data that have been utilized in numerous previous studies. Furthermore, we tried to cover the entire world except for Arctic and Antarctic Polar Regions. Many stations are located in northern mid-latitudes, particularly in central Europe and western North America. Compared to the Northern Hemisphere, significantly fewer stations are in the Southern Hemisphere, and no high-altitude stations are present in the Oceania region.

Region I: Africa

Assekrem (ASK), Algeria ASK is a GAW Global station operated by the Déportent Météorologique Régional Sud of the Office National de la Météorologie (ONM), Algeria, and is located on the summit of the second highest point of the Hogger Mountain Range in the Sahara Desert (Zellweger et al. 2007). It plays an important role in capturing air pollutants from continental Africa.

Mt. Kenya (MKN), Kenya MKN is a GAW Global station that has been designated for long-term measurements of various chemical compounds and physical and meteorological parameters in the lower troposphere. The main office is the Kenya Meteorological Department (KMD). MKN is located on the northwestern slope of Mt. Kenya

Table 1 List of stations mentioned in this paper

Station	ID	Country	Latitude	Longitude	Altitude (m)	Data source
Region I: Africa						
Assekrem	ASK	Algeria	23.27° N	5.63° E	2710	WDCGG[a]
Mt. Kenya	MKN	Kenya	0.06° S	37.30° E	3678	WDCGG[a]
Izaña (Tenerife)	IZO	Spain	28.31° N	16.50° W	2373	NMHCs: Schmitt and Schultz et al. (1998) Other: WDCGG[a]
Region II: Asia						
Mt. Waliguan	WLG	China	36.29° N	100.90° E	3810	WDCGG[a]
Issyk-Kul	ISK	Kyrgyzstan	42.62° N	76.98° E	1640	WDCGG[a]
Nepal Climate Observatory–Pyramid	PYR	Nepal	27.96° N	86.81° E	5079	WDCGG[a]
Lulin	LLN	Taiwan	23.47° N	120.87° E	2862	LLN website[b]
Mondy	MDY	Russian Federation	51.65° N	100.92° E	2006	EANET[c]
Mt. Abu	MAB	India	24.65° N	72.78° E	1680	Naja et al. (2003)[d]
Mt. Happo	HPO	Japan	36.70° N	137.80° E	1850	CO: Kato et al. (2000); Narita et al. (1999); Pochanart et al. (2004)[e] NMHCs: Sharma et al. (2000) Other: EANET[c]
Mt. Fuji	FWS	Japan	35.37° N	138.73° E	3776	–
Region III: South America						
La Quiaca Observatorio	LQO	Argentina	22.10° S	65.60° W	3459	WDCGG[a]
Region IV: North and Central America						
Whistler Mountain	WHI	Canada	50.06° N	122.96° W	2182	Macdonald et al. (2011)[f]
Great Basin NP	GRB	USA	39.01° N	114.22° W	2060	CASTNET[g]
Mt. Bachelor Observatory	MBO	USA	43.98° N	121.69° W	2743	Gratz et al. (2015); Weiss-Penzias et al. (2007)[h]
Niwot Ridge	NWR	USA	C1: 40.04° N T-van: 40.05° N	C-1: 105.54° W T-van: 105.59° W	C-1: 3021 T-van: 3523	WDCGG[a]
Chiricahua NM	CHA	USA	32.01° N	109.39° W	1570	CASTNET[g]
Lassen Volcanic NP	LAV	USA	40.54° N	121.58° W	1756	O_3: CASTNET[g] Aerosol: IMPROVE[i]
Yellowstone NP	YEL	USA	44.57° N	110.40° W	2430	CASTNET[g]
Yosemite NP	YOS	USA	37.71° N	119.71° W	1605	CASTNET[g]
Region V: South–West Pacific						
Tanah Rata	TAR	Malaysia	4.48° N	101.37° E	1545	WDCGG[a]
Mauna Loa	MLO	USA	19.54° N	155.58° W	3397	NO_x and NO_y: Ridley et al. (1998) Aerosol: IMPROVE[i] Other: WDCGG[a]

Table 1 List of stations mentioned in this paper *(Continued)*

Region VI: Europe						
Sonnblick	SNB	Austria	47.05° N	12.96° E	3106	WDCGG[a]
Zugspitze–Gipfel	ZUG	Germany	47.42° E	10.99° E	2962	WDCGG[a]
Zugspitze–Schneefernerhaus	ZSF	Germany	47.42° N	10.98 °E	2671	WDCGG[a]
Monte Cimone	CMN	Italy	44.17° N	10.68° E	2165	NMHCs: EBAS[j] Other: WDCGG[a]
Kislovodsk	KSL	Russian Federation	43.73° N	42.66° W	2070	–
Krvavec	KVV	Slovenia	46.18° N	14.32° E	1720	WDCGG[a]
Arosa	ARO	Switzerland	46.78° N	9.67° E	1840	–
Jungfraujoch	JFJ	Switzerland	46.55° N	7.99° E	3580	Aerosol: EBAS[j] Other: WDCGG[a]
Pico Mountain Observatory	PMO	Portugal	38.47° N	28.40° W	2225	NMHCs: WDCGG[a] NO_x and NO_y: Val Martin et al. (2008b)

[a]World Data Centre for Greenhouse Gases (http://ds.data.jma.go.jp/gmd/wdcgg/)
[b]Data available at http://lulin.tw
[c]Acid Deposition Monitoring Network in East Asia (http://www.eanet.asia/)
[d]Data obtained from M. Naja
[e]Data obtained from S. Kato
[f]Data obtained from A. M. Macdonald
[g]Clean Air Status and Trends Network (http://www.epa.gov/castnet)
[h]Data obtained from D. Jaffe
[i]Interagency Monitoring of Protected Visual Environments (http://vista.cira.colostate.edu/improve/)
[j]EBAS (http://ebas.nilu.no)

and in a protected portion of the Mount Kenya National Park. The climate of equatorial East Africa is dominated by seasonal displacement of the intertropical convergence zone (ITCZ). During boreal summer, the ITCZ is situated far to the north, resulting in southerly to southeasterly winds over Kenya. From September onward, the ITCZ begins to retreat southward, followed by a rainy period from mid-October to December over Kenya. Throughout boreal winter, the ITCZ is situated south of the equator. As a result, a northeasterly monsoon circulation dominates East Africa. When the ITCZ begins to progress northward again, it brings a second rainy period from mid-March to the beginning of June to equatorial East Africa. One noteworthy feature of the boreal monsoon circulation is the East African low-level jet (EALLJ), which develops from May onward in the southeast trade winds over Madagascar. With the northward transition of the ITCZ, the EALLJ strengthens and extends northward, reaching its maximum extent in June or July. Its counterpart, blowing from the north along the East African coast during boreal winter, is less pronounced (Henne et al. 2008).

Izaña (IZO), Spain IZO is a GAW Global station operated by the Agencia Estatal de Meteorología (AEMET) for long-term measurements of various chemical compounds and physical and meteorological parameters. The station is located on the Island of Tenerife roughly 300 km west of the African coast. As typically occurs in subtropical oceanic atmospheres to the west of continents, the low troposphere in this region is strongly stratified owing to the synoptic-scale subsidence conditions. Two air masses are well differentiated by the presence of a temperature inversion layer: the marine boundary layer (MBL) and the FT (Rodríguez et al. 2009).

In the moist and cool MBL, the north to northeast trade wind blows. Because the condensation level is usually lower than the inversion level under the trade wind regime, the top of the MBL, which is frequently located just below the temperature inversion layer, is characterized by a layer of stratocumulus clouds formed by the condensation of water vapor onto available pre-existing particles. The presence of this stratocumulus layer creates a quasi-continuous foggy and rainy regimen throughout the year at altitudes between 800 and 2000 m a.s.l. on the island.

In the FT, northwest subsiding dry airflows dominate throughout the year, except in summer, when they frequently alternate with southeast airflows laden with Saharan mineral dust particles (Chiapello et al. 1999). In winter (January to March), air masses originate from the North Atlantic, North America, and the Sahara (Cuevas et al. 2013). In spring (April to June), a pattern similar to that in winter is observed. The contributions from the Sahara and the southern part of the North Atlantic are weaker, and the transport from North America is more well-defined than that in winter. In summer (July to September), essentially only two geographical sectors of the air mass pathways are identified: that from North America and that from the Sahara and Northern Sahel. Air masses from North America and the North Atlantic travel at relatively high altitudes, whereas those from the Sahara originate from low levels.

The observational records of a Fourier transform infrared (FTIR) spectrometer that began routine operation in March 1999 have been utilized in many studies (García et al. 2012; Schneider et al. 2005a, b, 2008; Sepúlveda et al. 2012; Viatte et al. 2011). The instrument is part of the Total Column Carbon Observation Network (TCCON), which is a network of ground-based Fourier transform spectrometers designed to retrieve precise and accurate column abundances of atmospheric constituents including CO_2, CH_4, nitrous oxide (N_2O), hydrogen fluoride (HF), CO, and water vapor isotopologues (Wunch et al. 2011). The TCCON was established in 2004 and is currently affiliated with 26 sites. In addition, other remote sensing observations have been conducted by lidar (Welton et al. 2000), multipass optical absorption spectroscopy (MOAS) (Armerding et al. 1997; Comes et al. 1995, 1997), differential optical absorption spectrometry (DOAS) (Carslaw et al. 1997; Gil et al. 2000, 2008), and multi axis-DOAS (MAX-DOAS) (Puentedura et al. 2012).

Region II: Asia

Mt. Waliguan (WLG), China WLG is a GAW Global station operated by the China Meteorological Administration (CMA). This station is located at the edge of the northeastern boundary of the Qinghai–Tibetan Plateau. Mt. Waliguan is 90 km from Xining and 260 km from Lanzhou, which are the main industrial and most populated regions of central–eastern China. The wind patterns near WLG are controlled by the Qinghai–Tibetan Plateau monsoon and are thus associated with seasonal variations. The predominant wind directions are from the southwest in cold seasons and from the east in warm seasons. Locally, WLG is affected by the mountain–valley breezes (Fu et al. 2012). Xue et al. (2011) identified three major types of air masses at WLG in summer: those originating from the east and southeast having passed over populated regions of China, those originating from the west having passed over remote regions of central Asia and Xinjiang, and those originating mainly from the north having passed over regions of Siberia and Mongolia. During a recent 10-year period (2000 to 2009); the transport regime at WLG in summer was dominated by air originating from the east that may have passed over populated regions in China.

Issyk-Kul (ISK), Kyrgyzstan ISK is located in the northern Tien-Shan Mountains along the shoreline of Lake Issyk-Kul. The Issyk-Kul lake region is surrounded

by two giant mountain chains including Kungey Ala-Too to the north and Terskey Ala-Too to the south, which together form a closed area. The mountain chains impede the transport of the polluted air from Chu Valley in Bishkek, the capital of Kyrgyzstan, and from Almaty, a huge industrial center in Kazakhstan (Semenov et al. 2005). Observations of a long-term total O_3 column (Aref'ev et al. 1995; Visheratin et al. 2006), total NO_2 column (Aref'ev et al. 1995, 2009; Ionov et al. 2008), total CO column (Aref'ev et al. 2013), and height mean concentrations of CO_2 (Kashin et al. 2007, 2008) have been reported along with atmospheric spectral transparency observations (Aref'ev and Semenov 1994, Aref'ev et al. 2008; Semenov et al. 2005).

Nepal Climate Observatory–Pyramid (PYR), Nepal PYR is a GAW Global station installed within the framework of the Stations at High Altitude for Research on the Environment (SHARE) project of Everest-K2 National Research Council (Ev-K2-CNR) and the atmospheric brown cloud (ABC) project of the United Nations Environmental Programme (UNEP) in order to obtain information on the atmospheric background conditions in this region (Bonasoni et al. 2008). This station is located at the confluence of the secondary Lobuche valley and the main Khumbu valley in Sagarmatha National Park in the eastern Nepal Himalaya.

In the Himalayan region, a 3 km thick brownish layer of pollutants known as Asian brown clouds has been observed to extend from the Indian Ocean to the Himalayan range (Ramanathan and Crutzen 2003). This phenomenon strongly affects the air quality, visibility, and the energy budget of the atmosphere over the entire Indian subcontinent. The high-altitude meteorology in the Himalayas is strongly influenced by the Asian monsoon circulation and by local mountain wind systems (Bollasina et al. 2002). The mountain–valley wind system is predominant, with a strong valley wind from the south to southwest during daytime and a weak mountain wind at night. In summer, the valley wind prevails throughout the day.

Nepal, including its borders with India and Bangladesh, is the most frequent origin of air masses transported in the PBL that reach PYR throughout the year (Gobbi et al. 2010). The atmospheric conditions in the Himalayas are influenced by the transport of polluted air masses from South Asia and the Indo–Gangetic Plains, the northwest-to-northeast region extending from eastern Pakistan across India to Bangladesh and Myanmar. Occurrences of brown clouds over the Himalayan foothills and Northern Indo–Gangetic Plains have been identified by high aerosol optical depth (AOD) values >0.4 and are associated with high concentrations of pollutants measured at PYR, as characterized by an up-valley breeze circulation (Bonasoni et al. 2010).

Lulin (LLN), Taiwan LLN is located inside Jade Mountain National Park, which is part of the Central Mountain Range. This station is operated by National Central University (NCU), Taiwan. Owing to the mountain–valley circulation, LLN is frequently located in the FT, particularly during the winter, and is generally free from surface pollution in the boundary layer (Ou-Yang et al. 2014; Sheu et al. 2010; Wai et al. 2008). Taiwan is located at the edge of the western Pacific Ocean and is southeast of the East Asian continent. The southwest monsoon prevails in summer, whereas the northeast monsoon prevails between late fall and spring. Additionally, since the Westerlies prevail at a higher elevation in spring (Ou Yang et al. 2012), LLN is affected by pollution outflows from Southeast Asia and the Asian continent.

Mondy (MDY), Russian Federation MDY is located in central Eastern Siberia near the Russia–Mongolia border, which is known to be a very lightly populated continental area of the world. MDY is operated by the Limnological Institute, Russian Academy of Sciences, and contributes to the EANET program. Air masses reaching MDY are typically classified into four groups: long-range transport from Europe, Siberia east of the Ural Mountains, high-latitude polar regions, and much shorter-range transport usually less than several hundred kilometers from the southwest (Pochanart et al. 2003).

Mt. Abu (MAB), India MAB is located at a mountaintop known as Guru Shikhar, which is the highest peak in the southern end of Aravalli Mountain Range in western India. In this region, northwest winds dominate in winter (November to February) and southwest winds dominate in summer (May to August) (Kumar and Sarin 2010; Naja et al. 2003; Ram et al. 2008; Ram and Sarin 2009; Rastogi and Sarin 2005, 2008). Diurnal O_3 concentration variations in spring and summer at MAB show a unique pattern, whereas those in autumn and winter show a pattern typical of high-latitude sites (Naja et al. 2003). Naja et al. (2003) suggested that this seasonal change in diurnal variation might be caused by changes in the wind pattern in different seasons and changes in the boundary layer mixing height during the day and at night.

Mt. Happo (HPO), Japan HPO is operated by the Ministry of the Environment (MOE) of Japan, which contributes to the EANET program. This station is located in a mountainous area near the coast of the Japan Sea. During fall to spring, westerly winds are dominant (Pochanart et al. 1999), and most of the air masses pass over the Asian continent, particularly over Mongolia and northwestern China, driven by the Siberian High (Liu et al. 2013). The North Pacific high-pressure system is strong in summer, and the Siberian High reverses to a

low-pressure system. This behavior is typical of the summer monsoon in East Asia. Associated with the summer monsoon, pristine air masses from the Pacific are transported to HPO more frequently, particularly in the boundary layer. Domestic pollution plumes have only been observed during limited periods in summer, particularly in August, when the land–sea air circulation over Tokyo Bay occasionally transports pollution from Tokyo to cause a late-afternoon daily maximum (Chang et al. 1989).

Mt. Fuji, Japan (FWS), Japan FWS was operated by the JMA until 2004, after which the nonprofit organization (NPO) Valid Utilization of Mount Fuji Weather Station (http://npofuji3776-english.jimdo.com) assumed responsibility for its operation. Mt. Fuji, which is the highest mountain in Japan, is located in the central part of the main Japanese island of Honshu. Its summit is positioned in the FT for most of the year (Igarashi et al. 2004). Westerly winds prevail at FWS, particularly strong winds in winter, owing to the southward shift of the polar jet stream (Nakazawa et al. 1984).

Region III: South America

La Quiaca Observatorio (LQO), Argentina LQO is operated by the Servicio Meteorológico Nacional (SMNA). This station is located in the Puna–Altiplano Plateau (15–26° S, 65–69° W) in the central portion of the Andes, which is an important dust activity region (Gaiero et al. 2013; Prospero et al. 2002). The Altiplano is situated between the hyper-arid Pacific coastal desert to the west and the moist continental lowlands to the east. The prevailing flows in the middle and upper troposphere over the Altiplano are westerly from May to October in the dry season and easterly from December to March in the rainy season (Garreaud et al. 2003).

Region IV: North and Central America

Whistler Mountain (WHI), Canada WHI is located on the summit of Whistler Mountain in a part of the Coast Mountain Range approximately 100 km north of Vancouver. The station was established in 2002 to measure aerosols and trace gases in the lower troposphere and is operated by Environment and Climate Canada (Macdonald et al. 2011). In this region, synoptic scale climatology is controlled by the Aleutian Low and the Pacific High. In winter, the zonal flow is generally stronger, and the Aleutian Low causes a more southwesterly flow over British Columbia. In summer, the intensified Pacific High causes more a northwesterly flow over the south coast of British Columbia (Klock and Mullock 2001). PBL influence was found to occur mostly during spring and summer and less frequently in late autumn and winter (Gallagher et al. 2011, 2012). Biogenic processes characterized during the Whistler Aerosol and Cloud Study 2010 (WACS 2010), which was a large measurement campaign with a focus on aerosols and clouds, have also been shown to be important at the station during late spring and summer (e.g., Ahlm et al. 2013; Lee et al. 2012; Pierce et al. 2012; Wainwright et al. 2012; Wong et al. 2011).

Mt. Bachelor Observatory (MBO), USA MBO is located on the summit of an extinct volcano in the Cascade Ridge of central Oregon. This station is operated by the University of Washington. At this altitude, the flow is predominantly from the southwest to the northwest. Owing to its elevation, the prevailing westerly winds, regional topography, and the lack of large urban/industrial emission sources upwind, MBO is well positioned for sampling FT air masses near the West Coast of the USA with minimal influence from local anthropogenic emissions (Weiss-Penzias et al. 2006). Three distinct pollution influences have been identified at MBO: Asian long-range transport, North American biomass burning, and North American industry (Jaffe et al. 2005; Weiss-Penzias et al. 2007; Reidmiller et al. 2010).

Niwot Ridge (NWR), USA NWR is located approximately 35 km west of Boulder, Colorado, on the Continental Divide for North America with runoff on the two sides destined for the Colorado and Mississippi Rivers, respectively. The station is situated on land owned by the Mountain Research Station of the University of Colorado and is used as a Long-Term Ecological Research (LTER) site with support from the National Science Foundation. This site is also used by the National Oceanic and Atmospheric Administration (NOAA) Global Monitoring Division for long-term monitoring, flask sampling, and for the collection of air that is used for preparing calibration standards of trace gases. Continuous O_3 measurement has been conducted at two sites, data from both of which are available at the WDCGG website. We used the O_3 data from the C-1 research site located at 3021 m a.s.l. in a subalpine forest 10 km east of the Continental Divide of the Americas. For CO data, we used observations from the treeline van (T-van) research site at 3523 m a.s.l. located in an alpine fellfield. Weekly and bi-weekly flask samplings have been also operated at the T-van. Wind patterns at NWR are dominated by Westerlies (Haagenson 1979), although, at times, upslope flows from the south or southeast transport air from Denver to the site (Hahn 1981).

Chiricahua National Monument (CHA), USA

CHA is located in Arizona and is operated as a Clean Air Markets Program site by the EPA. CHA contributes to the CASTNET program (https://www3.epa.gov/castnet/site_pages/CHA467.html), which monitors air quality

and deposition including O_3 concentration, and to the IMPROVE program.

Great Basin National Park (GRB), USA GRB is located on the northeastern flank of the Snake Range in Nevada. This station is operated by the Great Basin National Park and is sponsored by the National Park Service (NPS) Air Resources Division. This agency administers an extensive air monitoring program that measures air pollution levels in national parks for visibility, gaseous pollutants, and atmospheric deposition. GRB contributes to the CASTNET (https://www3.epa.gov/castnet/site_pages/GRB411.html) and IMPROVE programs.

Lassen Volcanic National Park (LAV), USA LAV is located on the northwest flank of Mt. Lassen, the southernmost active volcano in the Cascade Mountain Range in northern California. This station is operated by the Lassen Volcanic National Park and is sponsored by the NPS Air Resources Division. LAV contributes to the CASTNET (https://www3.epa.gov/castnet/site_pages/LAV410.html) and IMPROVE programs.

Yellowstone National Park (YEL), USA YEL is located in Wyoming. It is operated by the Yellowstone National Park and is sponsored by the NPS Air Resources Division. YEL contributes to the CASTNET (https://www3.epa.gov/castnet/site_pages/YEL408.html) and IMPROVE programs.

Yosemite National Park (YOS), USA YOS is operated by Yosemite National Park and is sponsored by the NPS Air Resources Division. YOS is located on the western slope of the Sierra Nevada Mountains in northern California. YOS contributes to the CASTNET program (https://www3.epa.gov/castnet/site_pages/YOS404.html) and IMPROVE programs.

Region V: South–West Pacific

Tanah Rata (TAR), Malaysia TAR and the co-located Cameron Highlands Meteorological Station are operated by the Malaysian Meteorological Department (MMD) (Toh et al. 2013) and participate in the EANET program. Malaysia's climate can be categorized into four seasons: the northeast monsoon (winter monsoon) from November to early March, the southwest monsoon (summer monsoon) from late May to September, and two transition periods between the monsoons (Yonemura et al. 2002). The mean wind direction at TAR depends on the monsoon season. The prevailing winds during the northeast and southwest monsoons are from the northeast and southwest, respectively. The precipitation pattern has two maximum and two minimum periods, and temperatures are approximately constant throughout the year.

Mauna Loa (MLO), USA MLO is a GAW Global station operated by the Global Monitoring Division (GMD), NOAA Earth System Research Laboratory (NOAA/ESRL). This station is located on the slope of the active Mauna Loa volcano and is free from continental pollution sources. Atmospheric constituents have been continuously monitored since the 1950s. Currently, MLO is well known for its measurements of rising anthropogenic CO_2 (e.g., Keeling et al. 1995). Winds at MLO are controlled by several factors including the strength of synoptic scale or trade winds, the height and strength of the trade wind inversion, the flow of the synoptic winds around the island mountain topography, and the daily heating and cooling cycle on the island. At night, the station is above the inversion layer in the free tropospheric atmosphere with minimal influence from local emissions. A long-term trend analysis of aerosol optical properties (Collaud Coen et al. 2013) has shown significant negative trends for the backscatter fraction and Ångström exponent and positive trends for the scattering and absorption coefficients.

Region VI: Europe

Sonnblick (SNB), Austria SNB is located on the highest peak among the main ridges of the Austrian Alps. This station is organized by the Environment Agency, Austria, and is one of the high-altitude stations of the Monitoring Network in the Alpine Region for Persistent and other Organic Pollutants (MONARPOP). Since its foundation in 1886, most of the main meteorological parameters have been measured. These data serve as a unique long-term climate record (Schöner et al. 2012). The origins of pollution reaching SNB are typically industrial areas in southern and central Germany, most parts of northeastern Europe, and the northern parts of Italy near the Milan agglomeration (Holzinger et al. 2010). Local pollution sources reach SNB by convective mixing, particularly in the daytime, when the mixing height surpasses the altitude of SNB. Henne et al. (2010) assessed the parameters reflecting site representativeness in consideration of population (emission proxy), deposition, and transport at 34 sites in western and central Europe. They classified SNB as a "mostly remote" site where the total population influence, population variability, and total deposition influence are small.

Zugspitze–Gipfel (ZUG) and Zugspitze–Schneefernerhaus (ZSF), Germany Zugspitze is the highest mountain of the Wetterstein Mountains in the Bavarian Alps. Monitoring activities began at ZSF and were later moved to ZUG in 2001 and 2002. ZUG and ZSF are both GAW

Global stations and are located at the summit and on the southern slope of Zugspitze, respectively.

ZSF has been jointly operated by the Federal Environmental Agency (Umweltbundesamt, UBA) and the German Weather Service (Deutscher Wetterdienst, DWD). Because ZUG/ZSF, which is located at the northern flank of the Alps, is more distant from the central Alps and at a lower elevation compared with SNB, Henne et al. (2010) classified ZUG/ZSF as a "weakly influenced, constant deposition" site where the total population influence, population variability, and deposition variability are systematically larger than those at "mostly remote" sites. ZUG is a TCCON site, at which total columns of GHGs have been measured by means of FTIR spectroscopy (e.g., Angelbratt et al. 2011a, b; Rinsland et al. 2003; Vigouroux et al. 2008).

Monte Cimone (CMN), Italy CMN is a GAW Global station operated by the Institute of Atmospheric Sciences and Climate of the National Research Council of Italy (ISAC-CNR). Mt. Cimone is the highest peak of the northern Italian Apennines and is the only high mountain station for atmospheric research located between the Southern Alps and the northern Mediterranean Sea. The Apennines are the first mountain chain affected by air masses from the Sahara on their way to Europe (Bonasoni et al. 2004). The station is considered to be representative of the baseline conditions of the Mediterranean FT (Bonasoni et al. 2000a; Fischer et al. 2003). Even during the warm seasons, the influence of the boundary layer air is substantial owing to convection and the mountain breeze (Fischer et al. 2003; Van Dingenen et al. 2005). The Mediterranean basin is located at the boundary between the tropical zone and northern midlatitudes. It serves as a crossroad for air masses originating from Europe, Asia, and Africa, where anthropogenic emissions encounter natural emissions (Kanakidou et al. 2011; Lelieveld et al. 2002). Henne et al. (2010) classified CMN as a "weakly influenced, constant deposition" site.

Kislovodsk (KSL), Russian Federation KSL is organized by the Oboukhov Institute of Atmospheric Physics (IFA), Russian Academy of Sciences. This station is located on the mountain plateau at the northern slope of the side ridge in the North Caucasus. The main features of air transport to KSL in the summer are the prevailing northern components, which include the town of Kislovodsk and the Caucasus foothills, and the northeastern components, which include the northern Caspian. In the winter, the main air transport features are the prevailing southern components, which include the regions behind the Caucasus and Asia Minor deserts, and the southwestern components, which include the Mediterranean and the deserts of North Africa (Tarasova et al. 2003).

During the warm season from April to October, the mountain–valley air circulation affects the O_3 concentration (Elansky et al. 1995; Senik and Elansky 2001). Simultaneous measurements of O_3 concentration were conducted at KSL and at the nearest town located 18 km to the north (Senik et al. 2005). That study indicated that surface O_3 at KSL is only slightly influenced by the pollutants accumulated within the atmospheric boundary layer and revealed information relating primarily to the regional and global state of the troposphere. Observations of the total O_3 and NO_2 columns have also been reported (Elansky et al. 1995).

Krvavec (KVV), Slovenia KVV, managed by the Hydrometeorological Institute of Slovenia (HIS), is located on the slope of Mt. Krvavec in the Kamniško–Savinjske Alps, which are part of the southern margin of the Alps. At this station, continuous measurements of black carbon (BC) and O_3 have been conducted within the framework of the EMEP, which is a science-based and policy-driven program of the Convention on Long-Range Transboundary Air Pollution (CLRTAP) program set up to facilitate international cooperation in solving transboundary air pollution problems.

Arosa (ARO), Switzerland ARO is located within the eastern part of the Swiss Alps at the end of Plessur Valley. This station is surrounded by mountains with heights ranging from 2500 to 3000 m a.s.l. The transport of emissions from large cities such as Chur and Davos to ARO is rare due to a channeling effect (Li et al. 2005). The longest available total O_3 record in the world is from ARO, where total O_3 measurements have been conducted continuously since late 1926. The total O_3 data are based on measurements of ultraviolet (UV) radiation by Dubson spectrophotometers and have been homogenized (Staehelin et al. 1998a). These data have been utilized in numerous studies (e.g., Brönnimann et al. 2003; Hoegger et al. 1992; Krzyścin 2000; Rieder et al. 2010a, b; Scarnato et al. 2010; Staehelin et al. 1998b).

Jungfraujoch (JFJ), Switzerland JFJ is a GAW Global station located on a mountain crest on the northern edge of the Swiss Alps. As part of the station is incorporated into the Swiss National Air Pollution Monitoring Network (NABEL), a wide range of in situ trace gas observations is performed by the Swiss Federal Laboratories for Materials Science and Technology (Empa) in association with the Swiss Federal Office for the Environment (FOEN). First sporadic aerosol observations at JFJ started in the 1970s, but the majority of the operational long-term measurements of aerosols and aerosol optical properties were initiated by the Paul Scherrer Institute (PSI) in the mid-1990s (Bukowiecki et al. 2016; Collaud Coen et al. 2007; Fierz-Schmidhauser et al. 2010;

Nyeki et al. 2012). The site has been shown to be excellent for studies on new particle formation (Bianchi et al. 2016) or aerosol–cloud interaction, including mixed-phase and glaciated clouds (Hoyle et al. 2016; Verheggen et al. 2007). In addition, remote sensing investigations have been performed by FTIR spectroscopy, which allows for quasi-simultaneous investigation of total column concentrations of a large number of gaseous constituents (e.g., Barret et al. 2002, 2003a, b; De Mazière et al. 1999; Dils et al. 2011; Duchatelet et al. 2009, 2010; Krieg et al. 2005; Mahieu et al. 1997; Melen et al. 1998; Rinsland et al. 1991, 1992, 1996, 2000, 2008; Vigouroux et al. 2007; Zander et al. 2008, 2010). JFJ is exposed mostly to FT air masses in autumn and winter. In late spring and summer, it is intermittently influenced by vertically exported polluted air masses transported in the PBL over Europe (e.g., Zellweger et al. 2000, 2003). Henne et al. (2010) classified JFJ as a "mostly remote" site.

Pico Mountain Observatory (PMO), Portugal PMO is located on the summit caldera of Mt. Pico on the Azores Islands in the central North Atlantic. PMO was jointly established in 2001 by scientists from the University of the Azores and Michigan Technological University and has been operated by these two groups, along with scientists from the University of Colorado, Boulder, since then. The Azores Islands are often affected by continental outflow. Emissions from North America are transported in the lower FT to the Azores. Episodically, emissions exported from the eastern US are transported by warm conveyor belts associated with convection followed by subsidence and reach the Azores within 5 to 7 days (Owen et al. 2006). In addition, the Azores region is affected by transport from high latitudes. Trace gases and aerosols emitted from boreal wildfires in Canada, Alaska, and Siberia are transported to the Azores over long periods ranging from 6 to 15 days (Honrath et al. 2004; Lapina et al. 2008; Val Martin et al. 2008a). PMO also has the advantage of being located in the lower FT most of the time due to the mechanically forced upslope flow resulting from the deflection of strong winds by the mountain slope (Kleissl et al. 2007). In addition, the influence of local sources on the island via upslope flows is relatively small (Helmig et al. 2008; Kleissl et al. 2007; Val Martin et al. 2008b).

Instrumentation and measurement techniques for ozone and its precursors

O_3 concentrations can be measured by UV absorption, gas-phase titration, or conventionally by iodometric (KI) titration. The GAW Programme established a guideline for O_3 measurement that recommends the use of UV absorption in O_3 analyzers as a routine measurement technique for continuous in situ observation (World Meteorological Organization 2013). This measurement method is based on the absorption of radiation at 253.7 nm by O_3 in the gas cells of the instrument. An O_3 photometer is used as the primary standard, and traceability is ensured through instrument comparisons (Tanimoto et al. 2007).

The CO concentrations reported in this paper were determined by collection of discrete air samples in flasks with subsequent analysis in the laboratory, in addition to continuous measurements. GC/HgO, which refers to gas chromatography combined with mercury oxide (HgO) reduction detection, was used for measurements of CO concentrations in flasks. Non-dispersive infrared radiometry (NDIR), wavelength-scanned cavity ring down spectroscopy (WS-CRDS), or gas chromatography with flame ionization detection (GC-FID) were used for in situ measurements. All measurement methods require reference gases. In the GAW Programme, the gas standards for CO measurements have been established and maintained by the NOAA/ESRL (World Meteorological Organization 2010).

The NMHC concentrations reported in this paper were determined by collection of discrete air samples in flasks with subsequent analysis in the laboratory, in addition to continuous measurements. Gas chromatography with mass spectrometry (GC-MS) was used for in situ measurements, and GC-FID was used for in situ and laboratory measurements.

NO concentrations can be measured by ozone chemiluminescence detection (CLD), which utilizes the gas-phase reaction of ambient NO with O_3 added in excess to the air sample. NO_2 concentrations can be also measured by CLD via reduction to NO by photolytic conversion. CLD combined with a thermal Au catalytic convertor has been used for NO_y measurements. Intercomparisons of NO_y measurements were performed at IZO (Zenker et al. 1998) and MLO (Atlas et al. 1996). The NO_2 instrument at HPO uses a molybdenum (Mo) converter to thermally decompose NO_2 into NO. It has been shown that oxidized nitrogen compounds such as nitrous acid (HONO), peroxyacetyl nitrate (PAN), and nitric acid (HNO_3) are also converted to NO with high efficiency by the Mo convertor, and therefore contribute to the overestimation of NO_2 concentration under certain conditions (Fehsenfeld et al. 1987). In rural and remote sites, where NO_x is small compared to NO_y, the interference is negligible. Therefore, we regard NO_x concentrations at HPO as NO_y concentrations.

Seasonal and long-term changes

Tropospheric ozone

Stratospheric vs. tropospheric processes Numerous observations in the Northern Hemisphere have enabled the analysis of the seasonal and long-term variations in tropospheric O_3. For a long period of time, stratosphere–troposphere exchange (STE) followed by subsiding

transport to the middle and lower troposphere was considered to be the primary source of tropospheric O_3 (e.g., Danielsen 1968; Junge 1962). Junge (1962) found a uniform seasonal cycle of tropospheric O_3 with a maximum in spring and a minimum in winter within the Northern Hemisphere. Because the maximum was later than that of stratospheric O_3 by 2 months, this delay was thought to be caused by the response time that depends on the rate of O_3 destruction within the troposphere.

Seasonal cycles of radionuclides were also investigated as evidence for STE. Beryllium-7 (^{7}Be), beryllium-10 (^{10}Be), and lead-210 (^{210}Pb) radionuclides, with half-lives of 53.3 days, 1.5×10^6 years, and 22 years, respectively, are useful tracers for tracking the movement of airflow and convective activity in the atmosphere. ^{7}Be and ^{10}Be are produced by cosmic ray spallation reactions with N and O atoms in the stratosphere and upper troposphere. More than half (~67%) of the ^{7}Be and ^{10}Be sources are located in the stratosphere. The remainder are located in the troposphere, particularly in the upper troposphere (Lal and Peters 1967).

In addition to the independent use of ^{7}Be and ^{10}Be, the ^{10}Be/^{7}Be ratio has been considered as a stratospheric tracer because its value in the stratosphere is significantly higher than that in the troposphere because of the markedly longer radioactive half-life of ^{10}Be than that of ^{7}Be (Koch and Rind 1998). ^{210}Pb is a daughter nuclide of radon-222 (^{222}Rn), which is emitted from soils and has a half-life of 3.8 days (Turekian et al. 1977). Therefore, high ^{7}Be concentrations with respect to low ^{210}Pb concentrations could indicate strong air subsidence from upper altitudes, which can increase surface ^{7}Be and O_3 concentrations, because these components are produced mainly in the stratosphere/upper troposphere (Cristofanelli et al. 2006, 2015; Cuevas et al. 2013; Tsutsumi et al. 1998; Zanis et al. 1999).

Contrastingly, O_3 produced photochemically within polluted air masses in the troposphere can be traced by a high concentration of ^{210}Pb. The combined use of ^{7}Be and ^{210}Pb can clarify information about the origin of the air masses (Graustein and Turekian 1996; Heikkilä et al. 2008; Lee et al. 2007; Zanis et al. 2003b). Gros et al. (2001) utilized CO and its isotopic composition (^{13}C, ^{18}O, and ^{14}C) together with ^{7}Be as an STE tracer because ^{14}CO is produced by the neutron–proton exchange reaction in nitrogen-14 (^{14}N) prior to its oxidation. Approximately three fourths of all ^{14}CO in the atmosphere is of direct cosmogenic origin. Gros et al. (2001) determined the proportion of stratospheric air in an air mass by examining the background and stratosphere levels of ^{14}CO at SNB.

The origins of air masses associated with high-O_3 episodes and the contributions from the stratosphere and the troposphere have previously been discussed in detail, along with the correlations of O_3 with water vapor and anthropogenically emitted compounds such as CO, CO_2, NMHCs, and total atmospheric Hg (Ambrose et al. 2011; Bonasoni et al. 2000b; Cristofanelli et al. 2006, 2015; Kajii et al. 1998; Tsutsumi et al. 1998; Wang et al. 2006). Cristofanelli et al. (2006) investigated the influence of stratospheric intrusion by using ^{7}Be, relative humidity, potential vorticity (PV), and total column O_3. Based on the aforementioned methods, Cristofanelli et al. (2015) reconstructed the frequency of days influenced by stratospheric intrusion at CMN for the period from 1996 to 2011. Liang et al. (2008) utilized the oxygen isotopic ratio of atmospheric CO_2 ($\delta^{18}O(CO_2)$) as a tracer at WLG. The $\delta^{18}O(CO_2)$ and $\Delta^{17}O(CO_2)$ values were found to be enhanced by CO_2 originating in the stratosphere and to have a seasonal cycle that differed from those of surface sources (Assonov et al. 2010).

PV (1 PVU = 10^{-6} m^2 s^{-1} K kg^{-1}) analysis has also been widely used to detect the STE (Cristofanelli et al. 2006, 2009a, 2015; Cuevas et al. 2013; Ding and Wang 2006; Kentarchos et al. 2000; Leclair De Bellevue et al. 2006; Schuepbach et al. 1999; Tsutsumi et al. 1998). PV is the product of absolute vorticity and thermodynamic stability. Because PV is conserved in adiabatic, frictionless flow, the dynamical tropopause is generally considered to be a well-defined continuous surface with a quasi-material character. Air parcels can only cross the dynamical tropopause when diabatic or other non-conservative processes (such as friction) change the PV. In the atmosphere above 350 hPa, PV rapidly increases with altitude, reaching typical values from 1.0 PVU (Danielsen 1968) to 3.5 PVU (Hoerling et al. 1991).

On the other hand, during the Los Angeles smog episodes in the 1950s, it was revealed that O_3 was produced via photochemical reactions in the polluted air containing NO_x and hydrocarbons (Haagen-Smit 1952). Later in the 1970s and 1980s, photochemistry involving the oxidation of CO and hydrocarbons in the remote atmosphere had been regarded as the major source of tropospheric O_3 (e.g., Chameides and Walker 1973). The seasonal cycles of tropospheric O_3 have been argued as a clue to understanding the contributions from the stratospheric influence and the tropospheric photochemistry. The spring O_3 maximum has widely been observed at many remote sites across the mid-latitudes in the Northern Hemisphere (Monks 2000; Oltmans et al. 2004). Arguments have been presented on the possible mechanisms, sources, and processes of this variation, particularly the roles of stratospheric intrusion and tropospheric photochemistry (Monks 2000; Scheel et al. 1997).

As we discussed above, the former was considered to be more important in 1960, while the latter was considered to play a key role in later years, triggered by the finding of a springtime PAN maximum, which is an

unambiguous marker for tropospheric photochemistry. It has been suggested that the onset of photochemical O_3 production from the accumulation of O_3 precursors such as CO and NMHCs over the winter may be related to the springtime maximum of O_3 (Penkett and Brice 1986). Additionally, the lifetime of O_3 in winter is long enough to allow its accumulation once produced from the precursors emitted from anthropogenic sources (Fenneteaux et al. 1999; Liu et al. 1987). Intensive campaigns such as the Mauna Loa Observatory Photochemistry Experiment (MLOPEX) were made to gain an understanding of the detailed photochemical mechanisms of tropospheric O_3 in the pristine marine atmosphere, thereby suggesting an important role of in situ photochemical production of O_3 (e.g., Ridley and Robinson 1992).

In more recent years, chemistry transport models, evaluated against the seasonal cycles of tropospheric O_3, predicted that photochemical production and stratospheric influence were 4974 ± 223 and 556 ± 154 Tg(O_3) year^{-1}, respectively, thereby highlighting the importance of photochemical production of O_3 (e.g., Stevenson et al. 2006; Sudo and Akimoto 2007). Based on these state-of-science models, the contribution of stratospheric O_3 to the spring maximum is thought to be minor. Nagashima et al. (2010) showed the seasonal variations of the contributions from the stratosphere, PBL, and FT at 25 selected sites including ZSF, ISK, MDY, HPO, NWR, and MLO and concluded that the stratospheric contributions from surface sites, including the interior of the Eurasian continent (ISK and MDY), had a minimum in summer and autumn.

However, arguments on the role of the stratospheric O_3 in the tropospheric O_3 distributions and variations continue, with emphasis on the differences in the season, region, and altitude. Škerlak et al. (2014) compiled a global 33 year climatology of STE for the period 1979 to 2011 by using the ERA-Interim reanalysis dataset from the European Centre for Medium-Range Weather Forecasts (ECMWF) and showed the geographical and seasonal distributions of stratospheric O_3 fluxes across the tropopause and down to the top of PBL. They reported that western North America (from March to May) and the Tibetan Plateau (in except for the period from September to November) are the regions where surface O_3 levels were most likely affected by the STE, with a maximum value of more than 120 kg km^{-2} month^{-1}. This could have significant implications for surface O_3 air quality. However, these estimates could still have large uncertainties resulting from uncertainties and/or biases in the reanalysis datasets used.

Seasonal variations The seasonal cycle of O_3 is controlled by the interaction of photochemical and dynamical processes and shows clear dependences on the latitude, altitude, and availability of precursors. Figure 2 shows the seasonal cycles of O_3 at the 26 high-altitude stations around the globe. Here, we show only data that were available on the public websites or by the referred publications; the data providers are summarized in Table 1. The aforementioned typical small springtime O_3 maxima have been reported at numerous stations on remote islands such as IZO, with peak concentration of ~55 parts per billion (ppb) (Cuevas et al. 2013; Rodrıguez et al. 2004; Schmitt and Volz-Thomas 1997; Fig. 2f); MLO, at ~50 ppb (Oltmans et al. 1996a, 2006; Fig. 2q); and PMO (Kumar et al. 2013). In a later study, Hauglustaine et al. (1999) utilized a photochemical box model in conjunction with the MLOPEX 2 measurements to evaluate the processes and species controlling photochemistry and to provide insight into the O_3, odd nitrogen, and odd hydrogen budget in the FT over the Pacific. Their analysis indicated a well-balanced production and destruction of O_3 during all seasons. The net production rate of O_3 was slightly negative, indicating that this region or the tropical Pacific troposphere acted as a net photochemical sink for O_3.

In continental Europe, including stations ZSF, SNB, JFJ, KVV CMN, and KSL, the seasonal cycle of O_3 at high altitudes exhibits a minimum in winter and a broad maximum beginning in spring and extending to summer. This behavior represents a combination of the spring maximum generally observed in the Northern Hemisphere and a secondary summer maximum, which is attributed to enhanced regional pollution associated with persistent anticyclonic weather (Chevalier et al. 2007). Such broad spring/summer maxima in O_3 have been reported at SNB (~55 ppb) (Gilge et al. 2010; Fig. 2b), ZSF (~55 ppb) (Gilge et al. 2010; Schuepbach et al. 2001; Fig. 2a), CMN (~60 ppb) (Bonasoni et al. 2000a; Campana et al. 2005; Fig. 2e), KSL (Elansky et al. 1995; Senik and Elansky 2001; Senik et al. 2005; Tarasova et al. 2003, 2009), KVV (~55 ppb; Fig. 2d), ARO (Campana et al. 2005; Pochanart et al. 2001; Staehelin et al. 1994), and JFJ (~60 ppb; Balzani Lööv et al. 2008; Gilge et al. 2010; Schuepbach et al. 2001; Zanis et al. 2007; Fig. 2c). During three intensive observations known as the FREE Tropospheric Experiment (FREETEX), which covered the period of O_3 buildup from late winter to late spring, the concentrations of peroxy radicals (HO_2+RO_2) showed a gradual increase from February to May (Zanis et al. 2003a). The calculated net O_3 production rate showed an increasing seasonal trend from late winter to late spring. Zanis et al. (2003a) suggested that in situ photochemistry is important and might have played a dominant role in controlling the O_3 accumulation from winter to spring in the lower FT over the European Alps.

In East Asia, a distinct spring maximum associated with a summer minimum with a small secondary peak in autumn was reported at HPO (~70 ppb; Kajii et al.

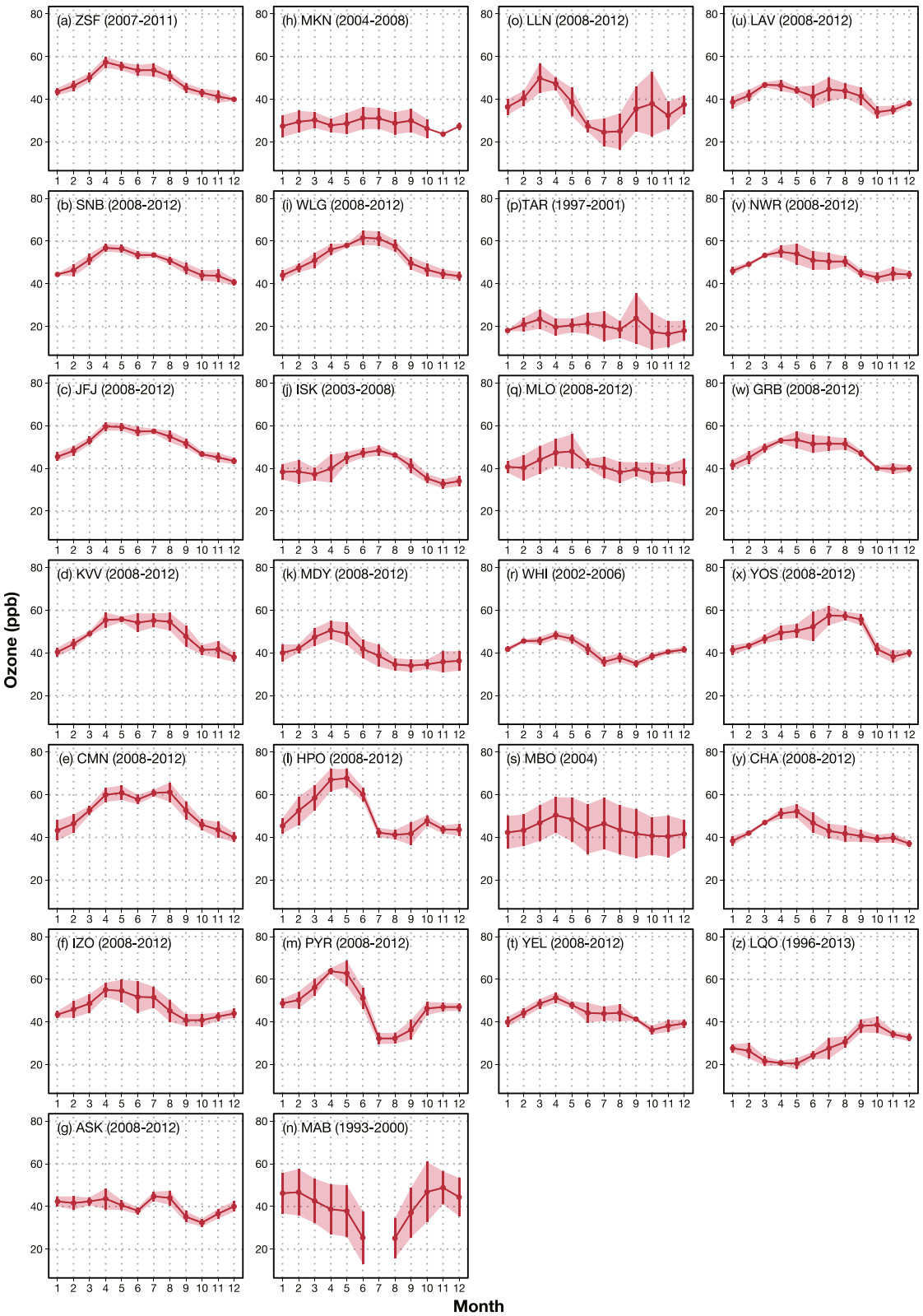

Fig. 2 Seasonal variations in tropospheric O_3 concentration at 26 mountain stations (**a**–**z**). The *lines with circles* denote the average observed O_3 concentrations during a particular period. The *years in parentheses* denote the averaging periods. The *red shaded bands* and *error bars* denote the standard deviations

1998; Pochanart et al. 2004; Fig. 2l) and FWS (Tsutsumi et al. 1994) in Japan and at LLN (~50 ppb; Ou Yang et al. 2012; Fig. 2o) in Taiwan. This seasonal pattern and magnitude are controlled by a combination of two factors. Although O_3 produced by photochemical activity accumulates from winter to summer, the East Asian monsoon brings pristine air masses from the Pacific Ocean during summer, yielding the spring maximum and the summer minimum (Tanimoto et al. 2005). It should be noted that the mean concentration at the spring peak during the period from 2008 to 2012 at HPO is 70 ppb, which is higher than those at European and North American sites owing to the substantial effects of anthropogenic activity in East Asia. It is considered likely that air mass intrusion from the stratosphere might not contribute directly to the high springtime O_3 concentration at HPO, according to analysis of the correlation between O_3 and absolute humidity (Kajii et al. 1998). In East Siberia, the seasonal cycle of O_3 at MDY showed a spring maximum and summer minimum (~50 ppb; Pochanart et al. 2003; Fig. 2k). This summer minimum is not caused by a continental–marine air mass exchange because MDY is located in the middle of Siberia. Rather, it is caused by an O_3 sink that includes surface deposition and more active vegetation (Pochanart et al. 2003). Wild et al. (2004) reported that the mean European influence on the O_3 concentration at MDY varied between 3.5 ppb in spring and 0.5 ppb in summer. In South Asia, the seasonal cycle at PYR showed a spring maximum and a summer minimum (~65 ppb; Bonasoni et al. 2010; Fig. 2m), which is similar to the case in East Asia. This likely occurred because PYR is under a greater influence from the South Asian monsoon, which brings clean maritime air masses during summer (Bonasoni et al. 2010). In addition, STE events at PYR showed frequency maxima during the dry winter and pre-monsoon spring seasons, which affected the O_3 concentration (Bracci et al. 2012; Cristofanelli et al. 2009a). The estimated average O_3 increase with respect to the average mean values by STE events for the period from 2006 to 2008 was 24 % (Bracci et al. 2012). The seasonal cycle of O_3 at MAB also depends on the South Asian monsoon. However, springtime O_3 at MAB did not show a value as high as that at PYR, and the seasonal cycle was characterized by the summer minimum and late autumn–winter maximum in the period from October to February of ~50 ppb (Naja et al. 2003; Fig. 2n). It is considered likely that one of the reasons for the disagreement is the altitude difference of approximately 3400 m. Because the stratospheric influence generally increases with an increase of altitude, PYR was frequently influenced by STE in spring (Bracci et al. 2012; Cristofanelli et al. 2009a).

In central Asia, a broad summer maximum was found in the surface O_3 concentration observed at ISK (~50 ppb; Fig. 2j) in Kyrgyzstan and at WLG on the Qinghai–Tibetan Plateau (~60 ppb; Ding and Wang 2006; Lee et al. 2007; Liang et al. 2008; Ma et al. 2005; Wang et al. 2006; Xu et al. 2015; Xue et al. 2011; Zhu et al. 2004; Fig. 2i). Analyses of the summer maximum at WLG have yielded contradicting results that have led to two competing hypotheses on its cause: long-range transport of polluted air masses from central–eastern China and intrusion of O_3-rich air masses from the stratosphere. In a three-dimensional (3D) regional chemical transport model study, Zhu et al. (2004) concluded that the seasonal O_3 transitions associated with the Asian monsoon system and transport from eastern–central China, central–South Asia, and even Europe are responsible for the distinct seasonal O_3 cycle at WLG. An alternative theory is that downward transport of air masses from the upper troposphere–lower stratosphere plays a key role in controlling the seasonal cycle of O_3 at WLG (Ma et al. 2005). An analysis of O_3 measurements and tropospheric and stratospheric tracers such as water vapor, CO, NMHCs, PV, and $\delta^{18}O$ (CO_2) attributed the summertime O_3 enhancements at WLG to stratospheric intrusion rather than the transport of anthropogenic pollution (Ding and Wang 2006; Liang et al. 2008; Wang et al. 2006). From measurements of ^{7}Be and ^{210}Pb, Lee et al. (2007) suggested that the combined processes of the downward transport of the stratospheric–upper tropospheric air masses and the long-range transport of polluted air masses from eastern–central China caused the summertime O_3 peak. A model calculation using the Nested Air Quality Prediction Modeling System (NAQPMS) estimated the contributions of the regional transport of photochemically produced O_3 and stratospheric O_3 at 10–25 and ~5 ppb, respectively (Li et al. 2009). An analysis of backward trajectories for the period from 2000 to 2009 revealed that air masses from central–eastern China dominated the airflow at WLG in summer, suggesting strong impacts of anthropogenic forcing on the surface O_3 and other trace constituents such as CO, NO, NO_2, NO_y, PAN, HNO_3, and particulate nitrate (NO_3^-) on the Tibetan Plateau (Xue et al. 2011). Using a photochemical box model constrained by observations, Xue et al. (2013) calculated the photochemical budgets of O_3 and radicals and showed that O_3 production was significantly greater than O_3 destruction during daytime in both spring and summer, which is indicative of net O_3 production in both seasons. In contrast, Ma et al. (2002) reported that the net O_3 production is positive in winter but negative in summer. Xue et al. (2013) determined that the key factor leading to this disagreement was the difference in NO levels and suggested that the transport of anthropogenic pollution from central–eastern China might perturb the chemistry in the background atmosphere over the Tibetan Plateau.

The circumstances described above indicate that the summer maximum at WLG can be attributed to the transport of anthropogenic pollution. Based on the source-receptor analysis, Nagashima et al. (2010) suggested that the summer maximum of O_3 at ISK was mainly due to the enhanced contribution of O_3 produced in the surrounding regions.

In North America, three different types of seasonal cycle were found in surface O_3. A spring maximum was observed at WHI (~50 ppb; Macdonald et al. 2011; Fig. 2r) and CHA (~55 ppb; Fig. 2y). A broad spring–summer maximum was observed at GRB (~50 ppb; Fig. 2w), LAV (~45 ppb; Fig. 2u), MBO (~50 ppb; Gratz et al. 2015; Weiss-Penzias et al. 2007; Fig. 2s), NWR (~55 ppb; Oltmans and Levy 1994; Fig. 2v), and YEL (~50 ppb; Fig. 2t). A distinct summer maximum was observed at YOS (~60 ppb; Fig. 2x). It is possible that these types of seasonal cycle in western North America reflect a difference in the influence of the boundary layer at each site. All high-O_3 events at MBO were observed between early March and late September and were caused by the Asian long-range transport, the subsidence of O_3-rich air from the upper troposphere–lower stratosphere, and the mixed influence of these two mechanisms (Ambrose et al. 2011). Therefore, the seasonal cycle at MBO might have been caused by the spring peak of background O_3 in the Northern Hemisphere and high O_3 events occurring between early spring and late summer.

Compared with the Northern Hemisphere, O_3 seasonal cycle observations have not been conducted extensively in the Southern Hemisphere and the equatorial regions, and the O_3 seasonal cycles observed at MKN and TAR, which are located in the tropics, appear to be rather flat relative to those at other mid-latitude sites. The O_3 concentrations at MKN exhibit little variation, with a minimum in November and a broad maximum in boreal summer (Henne et al. 2008). This cycle can be explained by the seasonal variation of monsoon flow over equatorial East Africa, which is driven by seasonal displacement of the ITCZ. Although the seasonal variations in O_3 at TAR were not pronounced (Fig. 2p), based on observations from 2006 to 2008, Toh et al. (2013) reported a substantial seasonal cycle associated with a minimum that occurred twice a year in the November–December and March–April timeframes, along with a maximum that occurred in the summer monsoon season in late May–September, which that coincided with the regional biomass burning period. This discrepancy is likely to be due to the interannual variability of O_3 in tropical regions. The seasonal cycle at ASK, which is located in the Sahara Desert of Algeria between IZO and MKN, has an autumn minimum and a summer maximum in the July–August timeframe (~45 ppb; Fig. 2g). In South America, the seasonal cycle of O_3 observed at LQO is characterized by an autumn minimum in the March to May period and a spring maximum in September–October timeframe (~40 ppb; Fig. 2z). It should be noted that while these O_3 maximum periods coincide with the August to October biomass burning season in the Southern Hemisphere (Duncan et al. 2003), the actual mechanism involved in the seasonal cycles has not been investigated.

The latitudinal gradient in tropospheric O_3 has also been discussed in previous research. For example, Scheel et al. (1997) found that the O_3 seasonal cycle amplitude was smaller in the northwest area than in the southeast area within Europe, and Winkler (1988) showed that the surface O_3 concentration over the Atlantic Ocean, which was twice as high in the Northern Hemisphere as that in the Southern Hemisphere, generally increased with latitude, and then dropped rapidly at 70° N. Figure 3 shows the annual mean concentrations and the amplitude (annual maximum and minimum) of the seasonal cycles of tropospheric O_3 observed at the mountain sites as a function of latitude or altitude for the period of 2008 to 2012. As can be seen in this figure, the mean O_3 concentrations and the seasonal amplitude generally increased with latitude for the range of 0°–40° N and decreased or stabilized at higher latitudes (Fig. 3c). The means were ~50 ppb in Europe and 30–45 ppb in Africa. Those in Asia were 35–50 ppb depending on the location, although three maxima were noted above 45 ppb at WLG, PYR, and HPO. In particular, the maxima at HPO and PYR were higher than those at other sites. Although one of the reasons for such a high value at PYR is believed to be its altitude at 5079 m a.s.l., no altitude dependency was observed for the annual mean O_3 concentration (Fig. 3a). Therefore, the high maximum values at PYR and HPO are associated with their seasonal cycle spring maxima. The minima were in the range of 30–50 ppb for all of the mid-latitude stations except for LLN. The tropical sites differed from other mid-latitude sites, showing small variability over the course of the year. Insufficient data were available to discuss the latitudinal gradient south of ~20° N. The seasonal amplitude for the 22 stations was 10–20 ppb, and again, the magnitude was generally dependent on the latitude. Moreover, the seasonal amplitude at MAB, LLN, HPO, and PYR, at ~25–30 ppb (Fig. 3d) was substantially larger than that at the other stations. This result was caused by either a larger spring or autumn maximum due to intense photochemical production, and a smaller summer minimum due to the Asian monsoon, than those reported at other sites. No altitude dependency was observed for the amplitude of the O_3 concentration (Fig. 3b).

Long-term trends The long-term trends for tropospheric O_3 have been actively examined and summarized in many studies (e.g., Cooper et al. 2014; Oltmans et al.

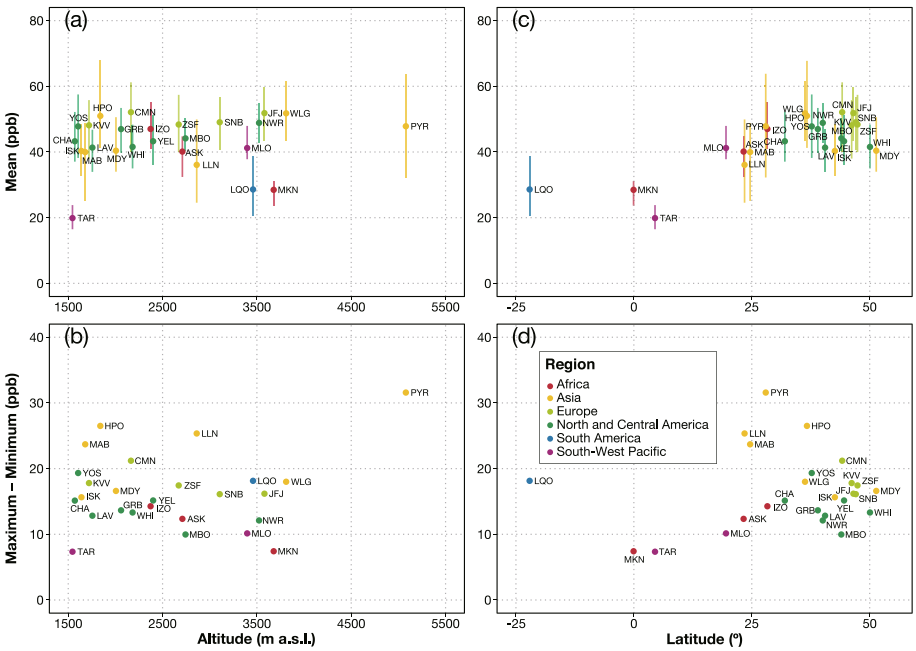

Fig. 3 Annual mean concentration and range (maximum–minimum) of seasonal cycles of tropospheric O_3 observed at mountain sites with respect to latitude and altitude of station (**a**–**d**). The *error bars* denote the maxima and minima

2006, 2013; Vingarzan 2004). The abundance of O_3 was first observed in the 19th century. The relevancies of old measurement data were examined and an apparent increase in the background O_3 levels was observed throughout the 20th century in Europe (Marenco et al. 1994; Volz and Kley 1988). More recently, Gilge et al. (2010) calculated the long-term trends for surface O_3 at SNB, ZUG/ZSF, and JFJ to be 0.22 ± 0.17 ppb year^{-1} (1989–2007), 0.42 ± 0.09 ppb year^{-1} (1975–2007), and 0.26 ± 0.16 ppb year^{-1} (1986–2007), respectively. During the past 40 years, the O_3 concentrations at ZUG/ZSF showed significant increases in the 1980s that slowed in the 1990s (Gilge et al. 2010; Logan et al. 2012; Oltmans et al. 2013; Parrish et al. 2012). In the 1990s, O_3 increases at European stations including SNB, CMN, ARO, ZUG/ZSF, and JFJ were broadly observed, indicating that the increasing trend of O_3 is a regional-scale phenomenon. The O_3 concentrations at European stations peaked in the late 1990s or early 2000s, followed by the current decreasing trend (Brönnimann et al. 2002; Cristofanelli et al. 2015; Cui et al. 2011; Gilge et al. 2010; Logan et al. 2012; Parrish et al. 2012; Oltmans et al. 2013; Staehelin et al. 1994). For the period from 2000 to 2009, Logan et al. (2012) calculated the mean rate of O_3 decrease at seven European alpine sites including SNB, ZUG/ZSF, and JFJ to be -0.16 ± 0.14 ppb year^{-1}. They discussed possible contributing factors to the O_3 changes in central Europe, including changes in stratospheric input and in O_3 precursors. In addition, they showed that emissions of NO_x from both the USA and Europe were almost constant in the 1980s but decreased in the 1990s. Model studies have suggested that variations in domestic emissions should have the largest influence on O_3 in summer, whereas variations in emissions in North America and Asia should have the largest influence in spring and late autumn over Europe (Fiore et al. 2009; Jonson et al. 2010). Such studies concluded that CO and CH_4 emissions should have only a minor influence on O_3 trends. However, the relationship between the observed O_3 trends and anthropogenic emission changes is complex. Although total anthropogenic NO_x emissions at northern mid-latitudes increased by only ~14 % for the period from 1980 to 2010, long-term O_3 trends showed remarkable increases (Parrish et al. 2014). The long-term trend for surface O_3 at KSL in Caucasus differed from that in central and southern Europe (Senik and Elansky 2001; Tarasova et al. 2003, 2009) with the former showing a decreasing trend in the 1990s (Senik and Elansky 2001; Tarasova et al. 2003). For the period from 1991 to 2001, a strong concentration change of -0.91 ± 0.17 ppb year^{-1} was observed, after which the O_3 changes decreased to -0.37 ± 0.14 ppb year^{-1} for the period from 1997 to 2006 (Tarasova et al. 2009). Tarasova et al. (2009) reported that the O_3 surface trend difference was caused by differences in the station locations relative to the source areas affecting the O_3 variations. The decreasing O_3 trend at KSL was caused by both substantial emission decreases in the 1990s due to the breakdown of the former USSR and emission control measures implemented in Europe.

In the North Atlantic, the surface O_3 record at IZO showed a slightly positive trend at 0.09 ± 0.02 ppb year^{-1} for the period from 1988 to 2009 with a rapid increase between 1996 and 1998 (Cuevas et al. 2013). Cuevas et al. (2013) suggested that the abrupt changes in the O_3 levels reflect a phase shift of the North Atlantic Oscillation (NAO), which altered the transport pattern to IZO. The predominant high positive phase of the NAO changed from 1995 to 1996. IZO is influenced by flow from both the mid-latitudes and the subtropics and NAO changes have resulted in an increased flow of the Westerlies in the mid-latitude subtropical North Atlantic, thus favoring the transport of O_3 and its precursors from North America. This process increased the tropospheric O_3 in the subtropical North Atlantic region after 1996.

In East Asia, a positive O_3 surface trend at 0.25 ± 0.17 ppb year^{-1} was observed at WLG for the period from 1994 to 2013 (Xu et al. 2015), and an especially strong increase was found in autumn, followed by spring. HPO in Japan experienced a generally large increase in springtime O_3 compared with the increases over Europe and North America during the 2000s (Tanimoto 2009; Parrish et al. 2012). The mean growth rate in springtime O_3 was ~1 ppb year^{-1} for the period from 1998 to 2006 (Tanimoto et al. 2009). Tanimoto et al. (2009) showed that variations in NO_x emissions and satellite observations of tropospheric NO_2 for East Asia were consistent with a remarkable increase of O_3 at HPO. Although this increasing trend is consistent with the increasing anthropogenic emissions in East Asia, it can only explain half of the observed increase by the model calculation. In the western USA, positive trends in springtime O_3 concentrations have been reported (e.g., Cooper et al. 2014; Jaffe et al. 2003b; Jaffe and Ray 2007; Parrish et al. 2012; Vingarzan 2004). Jaffe and Ray (2007) reported positive trends in O_3 concentration at LAV and at YEL in all seasons with growth rates of 0.33 and 0.50 ppb year^{-1}, respectively, based on the analysis of deseasonalized monthly mean O_3 concentrations (daytime data only) for the period from 1987 to 2004. Moreover, they proposed possible explanations for these O_3 trends that include (1) increases in regional emissions, (2) changes in the distribution of emissions, (3) increases in biomass burning in the western USA, and (4) increases in global background O_3. Jaffe et al. (2008) showed that the increase in fires is largely responsible for the increase in summertime O_3, but fires could not explain the trend in O_3 for other seasons. Jaffe (2011) found statistically significant correlations between springtime O_3 at 11 sites in the western USA including CHA, GRB, and YEL and free tropospheric O_3, as measured by an ozonesonde in Boulder. This correlation indicates a downward transport of enhanced O_3 from the FT to the surface. In summer, free tropospheric and surface O_3 concentrations and the number of days exceeding the US National Ambient Air Quality Standards (NAAQS) threshold were all significantly correlated with emissions from biomass burning in the western USA. This also indicates that wildfires had a large impact on O_3 concentrations in the western USA. The mean springtime O_3 at MBO showed significant increases of 0.73 ± 0.54 ppb year^{-1} for the period from 2004 to 2013, whereas the annual mean O_3 did not show a significant trend (Gratz et al. 2015). An analysis of transport patterns by Gratz et al. (2015) suggested that long-range transport from Asia has a dominant influence on the increasing springtime O_3. At HPO and MBO, which are both strongly influenced by springtime outflow from East Asia, the O_3 levels showed larger increases at higher percentile levels than those at lower percentile levels (Gratz et al. 2015; Tanimoto 2009). A statistically significant positive trend in the mean maximum daily 8-h average (MDA8) O_3 concentration at 0.12 ppb year^{-1} was observed at CHA for the period from 1989 to 2010 (Chalbot et al. 2013). The surface O_3 recorded at MLO in the Northern Pacific has shown a significant increase of 0.16 ± 0.04 ppb decade^{-1} (Oltmans et al. 2013). Oltmans et al. (2013) showed an increasing trend into the early 2000s followed by a decline in later years. In the earliest period, the increase was observed primarily in spring, but in the most recent decade, increases during autumn and early winter were observed to be greater. This change is attributed to a shift in the transport pattern associated with greater outflow from higher latitudes north of 30° N (Oltmans et al. 2006). Such a seasonal shift in the O_3 maximum has not been observed at most stations in the mid-latitudes, but shifts in the seasonal cycle to an earlier time of the year were observed at ZUG/ZSF, at 5.1 ± 3.5 days decade^{-1} (Parrish et al. 2013); JFJ, at 5.6 ± 4.1 days decade^{-1} (Parrish et al. 2013); and LAV, at 14 ± 19 days decade^{-1} (Cooper et al. 2014; Parrish et al. 2013). Additional studies are needed to determine why the seasonal O_3 cycle shifts across northern mid-latitudes are only seen at some sites and not others. Parrish et al. (2014) showed comparisons of long-term O_3 records observed at northern mid-latitude sites with three chemistry–climate model results. Some disagreement was noted between the observed and modeled results, suggesting that only limited confidence can be placed in the estimates of the present RF of tropospheric O_3 derived from modeled historic concentration changes and in the prediction of future O_3 concentrations.

Some differences between the changes in O_3 concentrations at high-altitude sites and those at low-latitude sites have been observed. The temporal behavior at Mace Head, which is a remote site in western Ireland, was similar to that at the alpine site, even though the O_3 increase in the late 1990s occurred earlier at ZUG/ZSF

than at Mace Head (Logan et al. 2012). Parrish et al. (2012) showed the long-term O_3 trends of 11 datasets regarded as baseline conditions. These datasets covered the range from low level to FT level, and included ZUG/ZSF, ARO, JFJ, HPO, and LAV data. They showed that both absolute O_3 concentrations and positive trends in O_3 generally increased with the altitude of the measurement site. In addition, they suggested that the changes in O_3 concentration showed a high degree of longitudinal uniformity over the last half of the 20th century at northern mid-latitudes.

Carbon monoxide

In the Northern Hemisphere, the seasonal maximum of CO occurs in late winter and early spring, and the seasonal minimum occurs in summer (Novelli et al. 1998); the maximum occurs 3 to 4 months after the seasonal minimum in OH radicals. The summer minimum in CO is explained well by the maximum occurrence of OH radicals, which are a CO main sink in the troposphere. The time lag for the CO maximum in late winter–early spring reflects the mixed effects of the seasonal variations in OH radical concentrations and CO emissions. The slower chemical destruction of CO by OH leads to a longer CO lifetime in winter, which allows more accumulation. Because the lifetime of CO is long enough for it to be transported across the globe, the long-range transport of industrial and biomass burning emissions originating on the Asian and North American continents can have substantial impacts on seasonal variations, depending on the location of the observation site (Novelli et al. 2003; Pfister et al. 2006; Yurganov et al. 2004, 2005).

Figure 4 shows seasonal cycles of CO at 16 high-altitude stations around the globe. The aforementioned, well-known seasonal cycles of CO have been reported at numerous stations on remote islands such as at IZO, with a peak concentration of ~115 ppb (Gomez-Pelaez et al. 2013; Fig. 4f); PMO (Kumar et al. 2013), and MLO at ~105 ppb (Greenberg et al. 1996; Jaffe et al. 1997; Fig. 4m). The seasonal cycle at ASK, at ~115 ppb (Fig. 4g), is similar to that at IZO.

In continental Europe including ZUG, SNB, JFJ, KVV, and CMN, the seasonal cycle of CO at high altitudes exhibits a maximum in late winter–early spring and a minimum in summer. The levels, amplitude, and timing differ slightly among sites, with SNB at ~160 ppb (Gilge et al. 2010; Gros et al. 2001; Fig. 4b), ZUG at ~180 ppb (Gilge et al. 2010; Fig. 4a), CMN at ~150 ppb (Cristofanelli et al. 2013; Fig. 4e), KVV at ~180 ppb (Fig. 4d), and JFJ at ~140 ppb Balzani Lööv et al. 2008; Dils et al. 2011; Forrer et al. 2000; Gilge et al. 2010; Zellweger et al. 2009; Fig. 4c).

Maxima in late winter–early spring and minima in summer also occur in North America, with WHI at ~180 ppb (Macdonald et al. 2011; Fig. 4n), NWR at ~135 ppb (Turnbull et al. 2007; Fig. 4p), and MBO at ~150 ppb (Weiss-Penzias et al. 2007; Fig. 4o).

In East Asia, the timing of the maximum shifts late toward the spring in association with a summer minimum and shows a small secondary peak in autumn, as observed at HPO with ~225 ppb (Kajii et al. 1998; Kato et al. 2000, 2002; Narita et al. 1999; Pochanart et al. 2004; Fig. 4j), and LLN with ~215 ppb (Cheng et al. 2013; Lin et al. 2010; Ou-Yang et al. 2014; Fig. 4l). Similar to that of O_3, the seasonal pattern and magnitude are controlled by a combination of two factors: the impact of continental outflow from the Asian continent from winter to spring and the East Asian monsoon that brings pristine air masses from the Pacific Ocean during summer. It should also be noted that the mean concentration of the spring peak during the period from 2008 to 2012 at HPO and LLN was between 200 and 250 ppb, which is higher than those at European and North American sites, due to substantial impacts from anthropogenic activities in East Asia in the case at HPO (Pochanart et al. 2004), and Southeast Asia biomass burning activities in the case at LLN (Cheng et al. 2013; Ou-Yang et al. 2014). The seasonal cycle at MAB, at ~180 ppb (Naja et al. 2003; Fig. 4k), shows a different pattern, with the maximum occurring after the monsoon season, as observed with O_3, due to transported pollution from the northeast.

In inland Asia, two types of seasonal cycle were found. The seasonal cycle at MDY is a typical pattern with a spring maximum and a summer minimum (Pochanart et al. 2003). Wild et al. (2004) reported that the mean European influence on the CO concentration at MDY varied between 30 ppb in spring and 10 ppb in summer. However, the seasonal pattern at WLG (Zhang et al. 2011) has a broad spring and summer maximum, which is similar to that of O_3 at WLG, thereby suggesting that both O_3 and CO are controlled by the same mechanism. At WLG, the CO data plotted in the present study showed a different seasonal cycle from that found by Zhang et al. (2011), which showed a late winter and early spring maximum. This discrepancy is likely caused by large interannual variability and variance in the flask sampling data (Fig. 4i).

In the tropics, the seasonal cycle of MKN, located in the equatorial region, differs from that at other stations. The maximum CO levels occur in January to March, followed by a sharp decrease toward April and May and an increase by the end of the year (Henne et al. 2008). Henne et al. (2008) determined that this seasonal cycle is associated with two maxima in February and August and is caused by the oscillation of monsoon circulation. The winter and spring maximum is caused by advection of CO-enriched air masses in the Northern Hemisphere during boreal

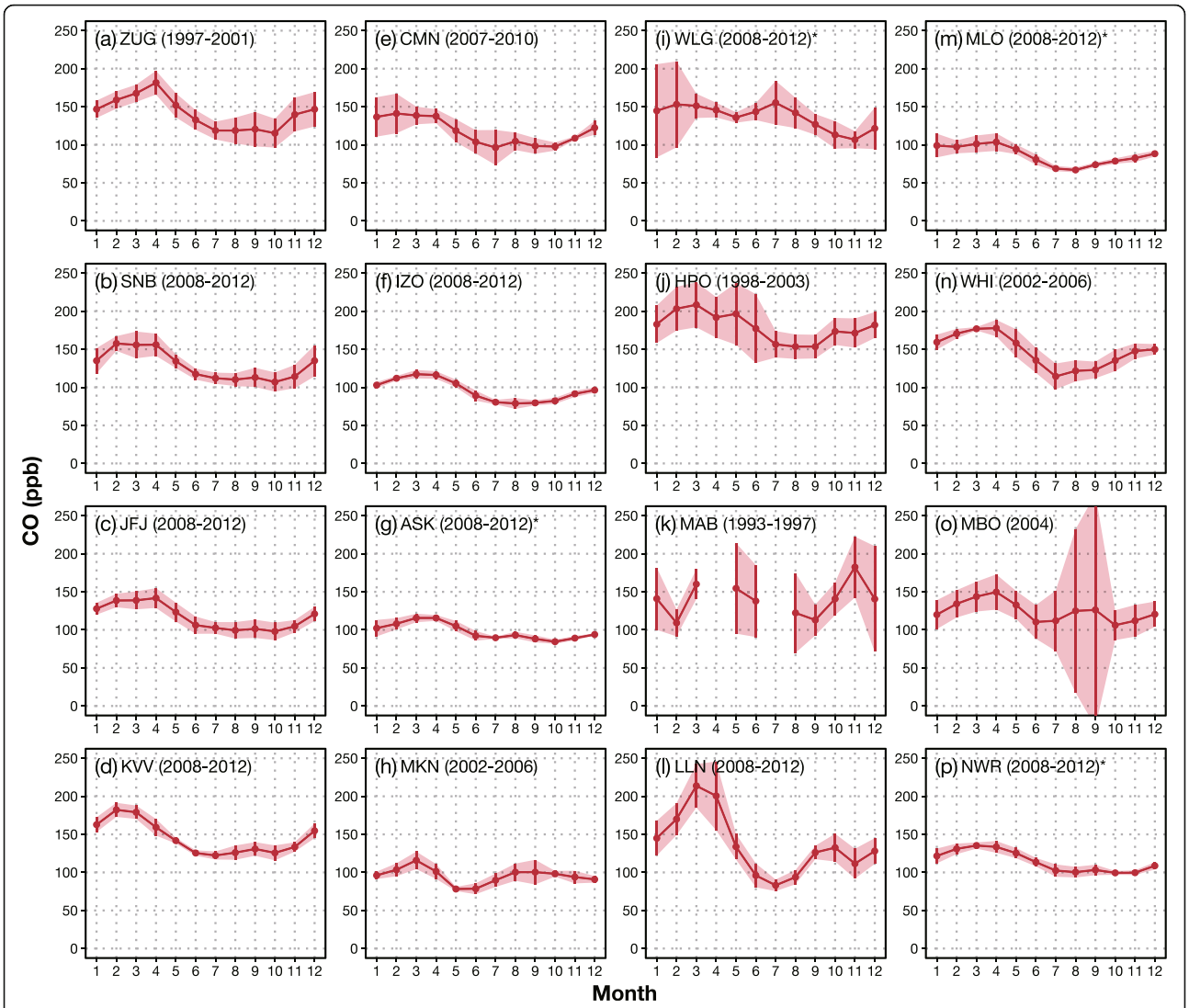

Fig. 4 Seasonal variations in CO concentration at 16 mountain stations (**a**–**p**). The *lines with circles* denote the average observed CO concentrations during a particular period. The *years in parentheses* denote the averaging periods. The *asterisks* denote CO data obtained by flask sampling. The *red shaded bands* and *error bars* denote the standard deviations

winter. In contrast, the summer maximum was observed during advection of air masses from the Southern Hemisphere that were affected by biomass-burning emissions in southern Africa.

Similar to O_3, CO also shows a gradient from south to north and greater seasonal amplitude in the Northern Hemisphere than that in the Southern Hemisphere. Based on the analysis of the global distribution of surface CO determined by flask sampling, Novelli et al. (2003) revealed a gradient between the Northern and Southern Hemispheres, with a greater seasonal amplitude in the Northern Hemisphere than that in the Southern Hemisphere and greater interannual variations in CO concentrations in the Southern Hemisphere than that in the Northern Hemisphere. Figure 5 shows the annual mean concentrations and amplitude of the seasonal cycles of tropospheric CO observed at the mountain sites as a function of altitude or latitude for the period from 2008 to 2012. The annual mean concentrations and amplitude (annual maximum/minimum) of the seasonal cycles of CO generally increased with latitude (Fig. 5c, d). This is a reverse latitudinal distribution of tropospheric OH (e.g., Spivakovsky et al. 1990). The annual mean concentrations and amplitude of the seasonal cycles of CO generally decreased with altitude (Fig. 5a), reflecting the fact that the emission sources of CO are located at the ground surface. The means were from 120 to 180 ppb in Europe and Asia and 100 ppb in Africa, and the maxima at HPO

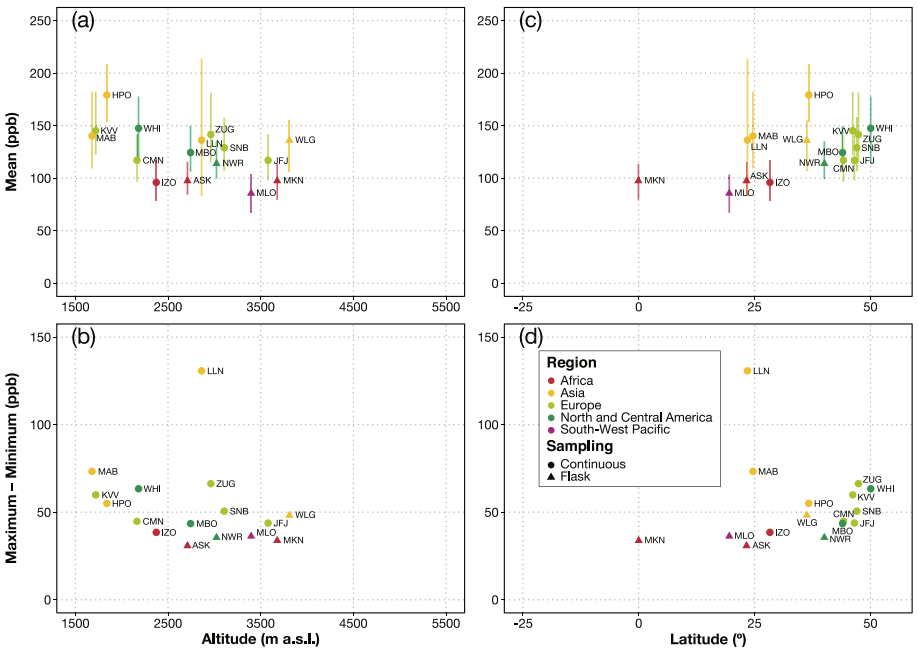

Fig. 5 Annual mean concentration and range (maximum–minimum) of seasonal cycles of tropospheric CO observed at mountain sites with respect to latitude and altitude of station (**a**–**d**). The *error bars* denote the maxima and minima

and LLN were higher than those at other sites. One of the reasons for such a high value at HPO is believed to be its averaging of the period from 1998 to 2003. The seasonal amplitude for the 15 stations except for LLN fell into the range of 85 to 180 ppb (Fig. 5b, d). The large seasonal amplitude at LLN was caused by a high spring maximum of ~215 ppb due to biomass burning activity in Southeast Asia (Ou-Yang et al. 2014), rather than the low CO of ~85 ppb in summer due to the Asian monsoon, because the summertime CO concentration at LLN was not significantly lower than that at other stations.

The CO levels increased in the Northern Hemisphere from the 1950s to the 1980s and then decreased in the late 1980s (Khalil and Rasmussen 1994; Novelli et al. 1998, 2003; Zander et al. 1989). Based on observations from NOAA Climate Monitoring and Diagnostics Laboratory sites, Novelli et al. (2003) estimated that the global mean CO concentrations decreased at a rate of -0.52 ± 0.10 ppb year^{-1} for the period from 1991 to 2001. Worden et al. (2013) examined satellite observation data for total column CO recorded by the Measurements of Pollution in the Troposphere (MOPITT) instrument from 2000 through 2011 and reported a continued decreasing trend in the Northern Hemisphere. They stated that further studies are needed in order to understand the trends and the contributions from anthropogenic emissions and possible changes in atmospheric chemistry through reactions with OH radicals. Few records of continuous observations of CO are available beginning in the 1990s at high-altitude stations other than MLO (Novelli et al. 1998, 2003) and JFJ (Dils et al. 2011; Gilge et al. 2010; Zellweger et al. 2009). The trend of CO at JFJ for the period 1996–2007 has been determined to be -3.36 ± 1.08 ppb year^{-1} (Gilge et al. 2010) and -2.65 ± 0.04 ppb year^{-1} (Zellweger et al. 2009) calculated using background data, respectively. At MBO in the western USA, the mean springtime CO showed a significant decrease for the period from 2004 to 2013, whereas the annual average CO did not show a significant trend (Gratz et al. 2015).

Other trace gases: NMHCs, NO_x, and NO_y

NMHCs Atmospheric NMHCs show considerable variation on spatial and temporal scales, but it is difficult to determine these variations on a regional basis because of the limited observational data on NMHCs available from high-altitude stations. In the troposphere, NMHCs are predominantly transformed not only by the chemical processes of photolysis and reaction with OH radical typically during daytime but also by reaction with the NO_3 radical during nighttime, and reaction with O_3 for unsaturated species, in addition to coastal and marine area reactions with chlorine (Cl) atoms, during daytime (Atkinson 2000). The reaction rate constants increase with molecular weight within a given class of NMHCs, causing lighter, saturated NMHCs to exhibit slower atmospheric decay and longer lifetimes (Atkinson and Arey 2003). NMHC concentrations are determined by the strength of the emission sources and their atmospheric removal processes. Generally, the seasonal cycles

of NMHCs show a maximum in winter and a minimum in summer owing to reaction with OH radicals. NMHC concentration ratios are useful indicators of the degree of photochemical processing or aging because NMHCs are removed at different rates, and their concentration patterns change during transport due to reaction rate differences, which span several orders of magnitude (e.g., Helmig et al. 2008, 2015).

Figure 6 shows the seasonal cycles of NMHCs at eight high-altitude stations. In this paper, only relatively long-lived species that are subject to intercontinental transport are shown, based on the lifetime or rate constant data reported by Atkinson and Arey (2003). Ethane (C_2H_6) with a lifetime of ~47 days showed a distinct seasonal cycle with a winter–spring maximum and a summer minimum with peak concentrations of ~1870 ppt at JFJ (Fig. 6a), ~1390 ppt at PMO (Helmig et al. 2008, 2015; Fig. 6b), ~1910 ppt at HPO (Sharma et al. 2000; Fig. 6c), ~1240 ppt at IZO (Schmitt and Volz-Thomas 1997; Fig. 6d), ~1210 ppt at ASK (Fig. 6e), and ~950 ppt at MLO (Greenberg et al. 1996; Fig. 6f) in the Northern Hemisphere. The seasonal cycle at MKN in the equatorial region showed two minima in April and October and two maxima in January and August, with a peak concentration of ~690 ppt (Fig. 6g). This pattern corresponds to the climate pattern in equatorial East Africa induced by the displacement of the ITCZ. Acetylene (C_2H_2), with a lifetime of ~16 days, showed a distinct seasonal cycle with a winter maximum and summer minimum at CMN with ~340 ppt (Fig. 6h), IZO with ~250–280 ppt (Schmitt and Volz-Thomas 1997; Fig. 6j), and MLO with ~260–320 ppt (Greenberg et al. 1996; Fig. 6k). The seasonal cycle at HPO showed a summer maximum with ~800 ppt, which might be the result of a local source (Sharma et al. 2000; Fig. 6i). However, based on data that eliminated the polluted air masses, Sharma et al. (2000) showed a distinct seasonal cycle of C_2H_2 with a maximum in winter and a minimum in summer. Propane (C_3H_8), with a lifetime of ~11 days, also shows a distinct seasonal cycle with a maximum in late winter–spring and a minimum in summer with ~720 ppt at JFJ (Fig. 6l), CMN with ~770 ppt (Fig. 6m), PMO with ~380 ppt (Helmig et al. 2008, 2015; Fig. 6n), HPO with ~790 ppt (Sharma et al. 2000; Fig. 6o), ~440 ppt at IZO (Schmitt and Volz-Thomas 1997; Fig. 6p), ~265 ppt at ASK (Fig. 6q), and ~140 ppt at MLO (Fig. 6r). The seasonal cycle at MKN showed two minima in April and October and two maxima in January and June at ~95 ppt (Fig. 6s). Benzene (C_6H_6), with a lifetime of ~10 days, showed a distinct seasonal cycle with a winter maximum and summer minimum at JFJ with ~105 ppt (Fig. 6t), CMN with ~150 ppt (Fig. 6u), IZO with ~90–110 ppt (Fig. 6v), and MLO with ~40–60 ppt (Fig. 6w). Generally speaking, the amplitudes of the seasonal cycles of C_2H_6 and C_3H_8 depend on the latitude, with smaller amplitudes at the lower-latitude sites and higher amplitudes at the higher-latitude sites (Fig. 7c, d). This feature is caused by a larger seasonal contrast of photochemical removals at higher latitudes than at lower latitudes. Li et al. (2005) showed that the concentrations of NMHCs, including C_6H_6 at ARO, were higher than those at JFJ because the contributions from the boundary layer emissions were generally higher at ARO due to the lower altitude. The annual maximum concentrations of C_2H_6 and C_3H_8 at higher-altitude stations are higher than those at lower-altitude stations within each latitudinal band (Fig. 7a, b).

NO_x and NO_y NO_x in the troposphere are important precursors for tropospheric O_3 and also affect OH and peroxy radicals (RO_x) concentrations, which govern the lifetimes of various gases in the troposphere (e.g., Levy 1971). In the troposphere, nitrogen species are primarily emitted in the form of NO_x from anthropogenic sources and are subsequently oxidized to other reactive nitrogen species along numerous different pathways (Fahey et al. 1986). The atmospheric lifetime of NO_x is generally in the order of hours to a day (Seinfeld and Pandis 2006). NO_y, which includes the sum of NO_x and its oxidation products such as PAN, dinitrogen pentoxide (N_2O_5), nitrous acid (HNO_2), HNO_3, and particulate nitrate (NO_3^-), plays an important role in the overall oxidizing capacity of the troposphere (Logan 1983).

In European countries, NO_x emissions declined significantly in the early 1990s due to the mandated installation of catalytic converters in vehicles and other emission reduction measures. Long-term measurements of NO_y, NO_x, and NO have been conducted at JFJ (Gilge et al. 2010; Pandey Deolal et al. 2012). For the period from 1998 to 2009, the overall annual averages of O_3 and NO_y were the highest in 2003, which was the hottest year in recorded European history caused by an exceptionally prolonged summer heat wave (e.g., Tressol et al. 2008). For the period from 1998 to 2002, the NO_y trend was positive but not significant, whereas in the period from 2004 to 2009, a significant decreasing tendency was observed at a rate of -0.048 ± 0.012 ppb year^{-1}. For the period from 1998 to 2009, no significant trend was found (Pandey Deolal et al. 2012). The comparison of PAN concentrations between the period from 1997 to 1998 and from 2009 to 2010 has indicated slightly lower values in recent measurements (Pandey Deolal et al. 2013).

NO_y measurements showed a broad spring and summer maximum at SNB, with a peak concentration of ~1.4 ppb (Kaiser 2009; Fig. 8f); ZUG, at ~1.5 ppb (Fig. 8g); and JFJ, at ~1.1 ppb (Gilge et al. 2010; Pandey Deolal et al. 2012; Zanis et al. 2007; Fig. 8h). On the other hand, NO_x showed a minimum during these seasons at SNB, with a peak concentration of ~0.6 ppb

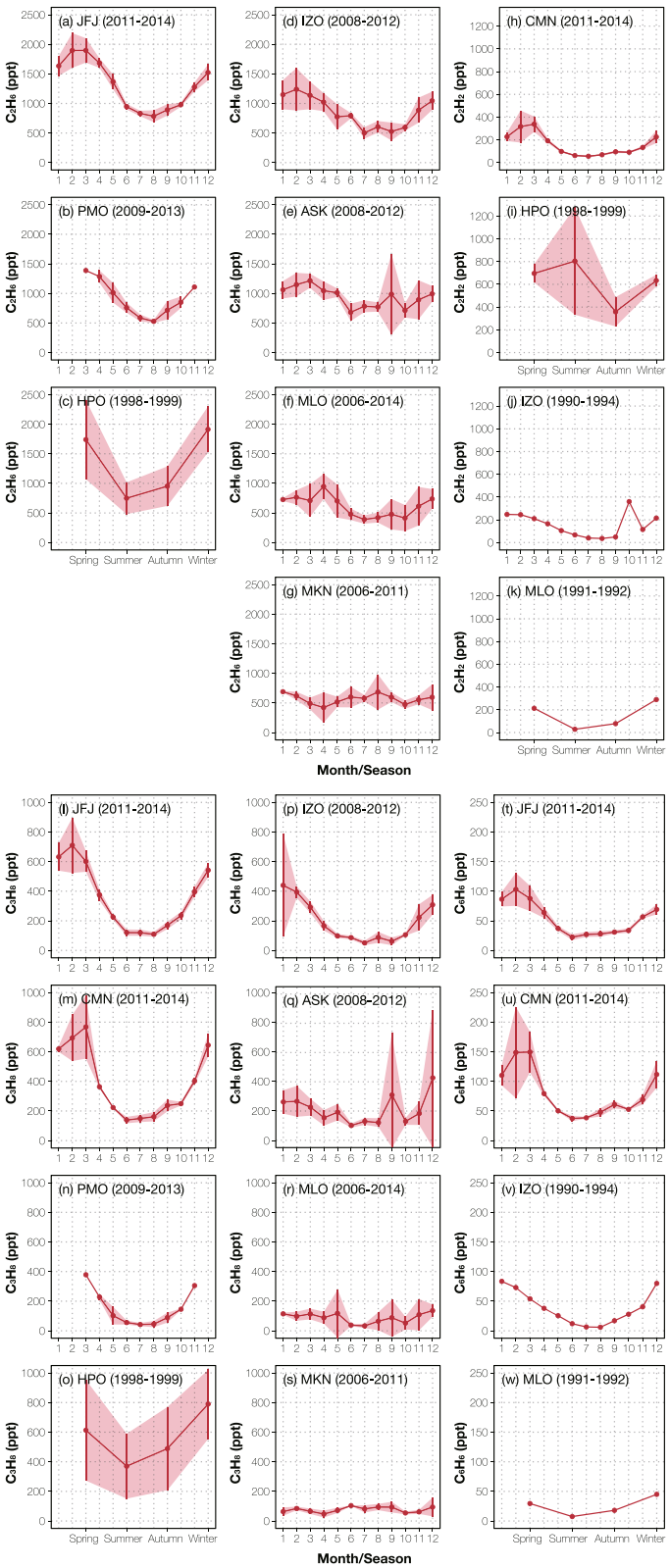

Fig. 6 Seasonal variations in C_2H_6, C_2H_2, C_3H_8, and C_6H_6 concentrations at eight mountain stations (**a**–**w**). The *lines with circles* denote the average NMHCs for observations during a particular period. The *years in parenthesis* denote the averaging periods. The *red shaded bands* and *error bars* denote the standard deviations

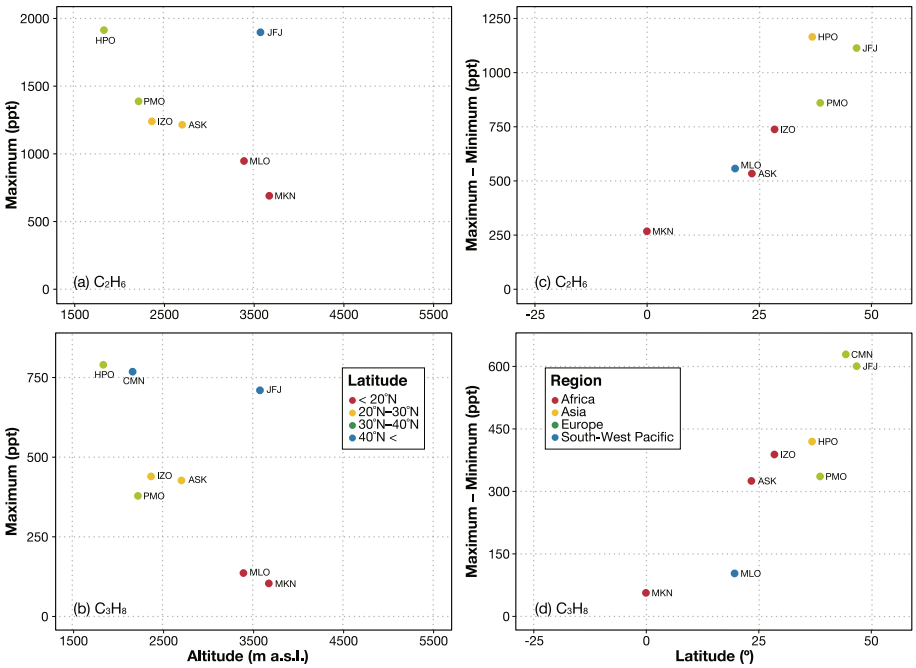

Fig. 7 Annual maximum concentration and range (maximum–minimum) of seasonal cycles of C_2H_6 and C_3H_8 observed at mountain sites with respect to latitude and altitude of station (**a**–**d**)

(Kaiser 2009; Fig. 8a); ZUG, at ~0.7 ppb (Fig. 8b); and JFJ, at ~0.4 ppb (Gilge et al. 2010; Pandey Deolal et al. 2012; Zanis et al. 2007; Fig. 8c). Because the NO_x lifetime is significantly shorter in summer than in winter (e.g., Schaub et al. 2007), NO_x concentrations are higher during the cold season. At JFJ, PAN measurements also showed a broad spring and summer maximum in the study of Pandey Deolal et al. (2013). They concluded that the mechanism of hydrocarbon accumulation in the FT in winter and the photochemically produced PAN in spring is not a dominant factor of the springtime PAN maximum. Rather, their analysis indicated a combination of strong photochemical activity in spring and summer with enhanced vertical transport from the European PBL. The seasonal cycle of NO_y at HPO showed a spring–early summer maximum at ~2.0 ppb (Fig. 8k). This cycle and level are similar to those of NO_y in Europe. At WLG, the NO_2 level did not show a minimum in summer in the study of Meng et al. (2010). Ma et al. (2002) also reported higher NO_x concentrations in July than in January. The NO_x and NO_y concentrations are low on remote islands such as IZO and MLO. At MLO, the seasonal cycle of NO_x, averaged only for free tropospheric observations, showed a spring maximum at ~0.04 ppt, and NO_y showed a maximum in spring, with a peak concentration of ~0.4 ppb (Ridley et al. 1998; Fig. 8d, h). NO_x/NO_y ratios were fairly invariant over the year, which implied that the partitioning of NO_y was near steady state (Ridley et al. 1998). NO_x observations at PMO exhibited a distinctive seasonal cycle with a July to October peak concentration of ~0.04 ppb that was larger than those in other months (Val Martin et al. 2008b; Fig. 8e). Val Martin et al. (2008b) concluded that in situ sources of NO_x such as PAN decomposition and potential photolysis of HNO_3 are required to provide NO_x levels because the lifetime of NO_x is shorter than its transit time from continental source regions. NO_y observations exhibited a distinct seasonal cycle with a peak concentration of ~0.4 ppb, which was larger from June to September than from November to March due to boreal forest wildfires and a more efficient export and transport from eastern North America (Val Martin et al. 2008a; Fig. 8j).

Long-range transport from continental sources

Anthropogenic emissions

During the past several decades, global anthropogenic emissions have increased markedly, following the dramatic growth of socioeconomic activity and energy use (e.g., Bond et al. 2007; Lamarque et al. 2010) particularly in China, which has become the largest contributor of Asian emissions. The growth rates for China's anthropogenic emissions are also the highest because of the unremitting increase in energy consumption, economic activity, and infrastructural development (e.g., Kurokawa et al. 2013). Trace gases and aerosols emitted from anthropogenic sources in East Asia have been observed at a number of mountain sites in Asia and North America including WLG (Cheng et al. 2007; Fu et al. 2012; Mu et al. 2007;

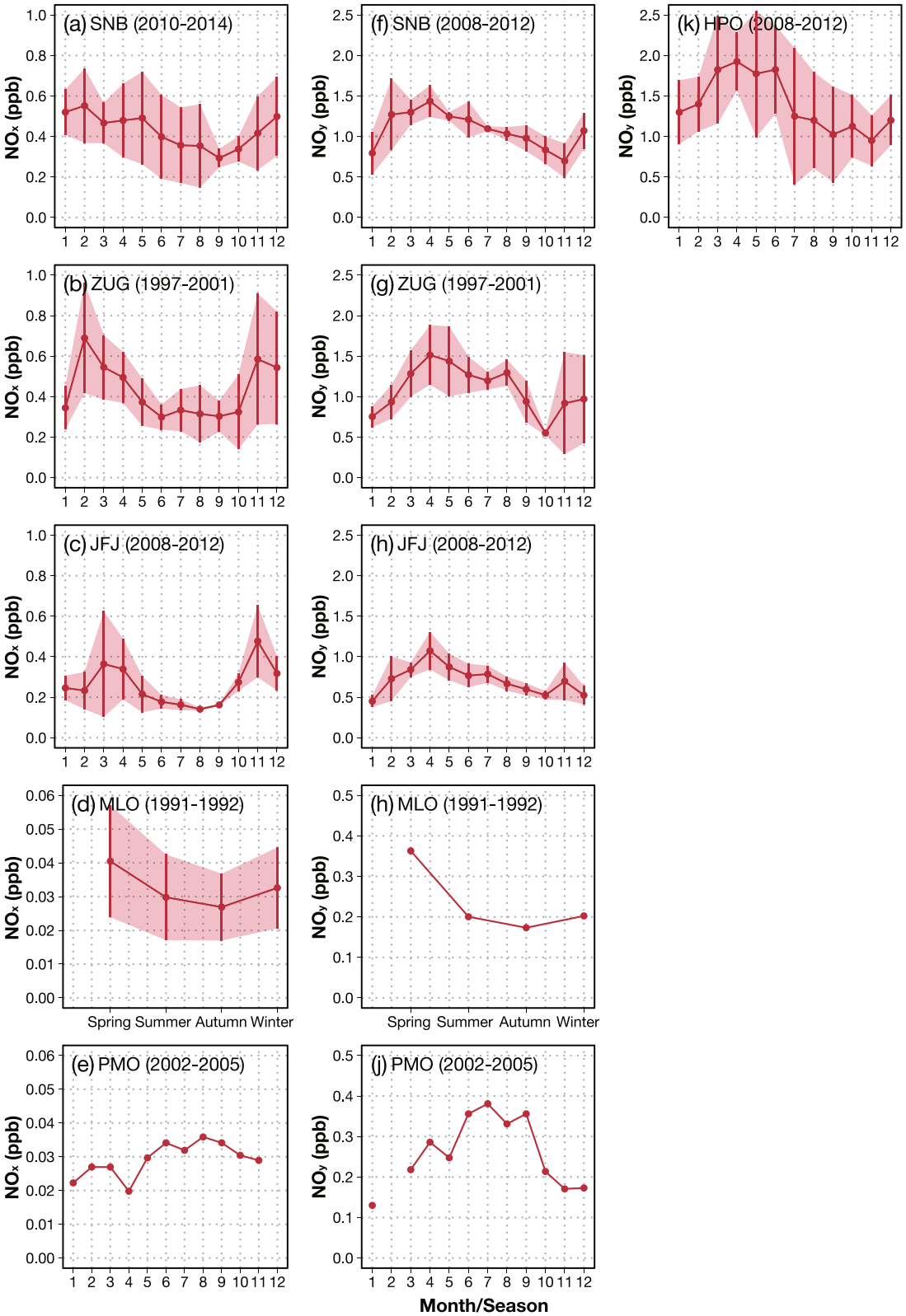

Fig. 8 Seasonal variations in NO_x and NO_y concentrations at six mountain stations. The *lines with circles* denote the average observed NO_x and NO_y concentrations during a particular period. The *years in parenthesis* denote the averaging periods. The *red shaded bands* and *error bars* denote the standard deviations. The concentrations of NO_x and NO_y were measured using photolytic (**a**–**e**), thermal Au (**f**–**j**), and Mo (**k**) convertors, followed by chemiluminescence detection

Wang et al. 2006; Xue et al. 2011, 2013; Zhang et al. 2009a, 2011), HPO (Liu et al. 2013; Pochanart et al. 2004; Sharma et al. 2000; Tanimoto 2009; Tanimoto et al. 2009), FWS (Igarashi et al. 2004, 2006), MLO (Brasseur et al. 1996; Jaffe et al. 1997; Levy and Moxim 1989; Luria et al. 1992; Perry et al. 1999), LAV (Jaffe et al. 2003a), and MBO (Ambrose et al. 2011; Fischer et al. 2010a, b; Genualdi et al. 2009; Jaffe et al. 2005; Primbs et al. 2008a, b; Reidmiller et al. 2009, 2010; Strode et al. 2008; Swartzendruber et al. 2006; Timonen et al. 2013; Weiss-Penzias et al. 2006, 2007; Wolfe et al. 2007). These emissions are illustrated in Fig. 9. HPO, which is located near the Sea of Japan, is an appropriate site for assessing the influence of air mass transport from the continent. Wild et al. (2004) estimated that local sources in Japan and regional East Asian sources contributed about 15 and 8 %, respectively, to O_3 observed at HPO in April 1996. The mass concentration of BC at HPO in a study by Liu et al. (2013) showed the highest value in spring and the lowest value in winter. By using the 3D Community Multiscale Air Quality (CMAQ) chemical transport model combined with the Process, Age, and Source Region Chasing Algorithm (PASCAL) source and process apportionment method, Liu et al. (2013) estimated that approximately 53 % of the observed BC was transported from northern China. Tanimoto et al. (2009) examined the contribution of Asian anthropogenic emissions to the observed O_3 trends at HPO by using CMAQ. However, a discrepancy was found between the observation and model results, thereby suggesting a significant underestimation of the actual growth of the Asian anthropogenic emissions or incompleteness of the modeling of pollution exported from continental Asia. MBO has proven to be effectively positioned for observing the transpacific transport of Asian plumes. Ambrose et al. (2011) described the detailed mechanism of Asian long-range transport to MBO. Surface emissions are lifted from the Asian boundary layer into the FT by convective, frontal, and orographic lifting (Bey et al. 2001; Cooper et al. 2004; Liang et al. 2004; Liu et al. 2003a). Frontal lifting is the primary mechanism for delivering eastern Asian emissions to the FT (Liu et al. 2003a). Once lifted to the FT, pollutants can be efficiently transported eastward toward North America by the prevailing westerly winds. Stohl et al. (2002) estimated the time scale of the trans-Pacific transport in the FT to be from 4 to 10 days. Subsidence wind over the northeast Pacific delivers air masses bearing Asian emissions to the lower FT over the US West Coast. This eastward export of Asian emissions is most efficient in spring due to intense frontal activity coupled with a strong westerly jet over the central Pacific (Liu et al. 2003a; Yienger et al. 2000). A calculation using the Goddard Earth Observing System chemical transport model (GEOS-Chem) revealed that, during the Intercontinental Chemical Transport Experiment Phase B (INTEX-B) period (Zhang et al. 2009b), most of the O_3 production in Asian O_3 pollution events occurred over East Asia, with maxima over northeast China and southern Japan in the spring of 2006. This model predicted significant O3 production over the North Pacific during plume transport. The plume on May 1 passed a more northerly and higher-altitude route than that on May 10, resulting in less O_3 production over the Pacific (Zhang et al. 2008). Both plumes showed a secondary O_3 production maximum at the West Coast of the USA, where the subsidence of air masses caused PAN decomposition and more O_3 production (e.g., Zhang et al. 2008). In addition to the trans-Pacific transport, regional pollution from North America has been observed

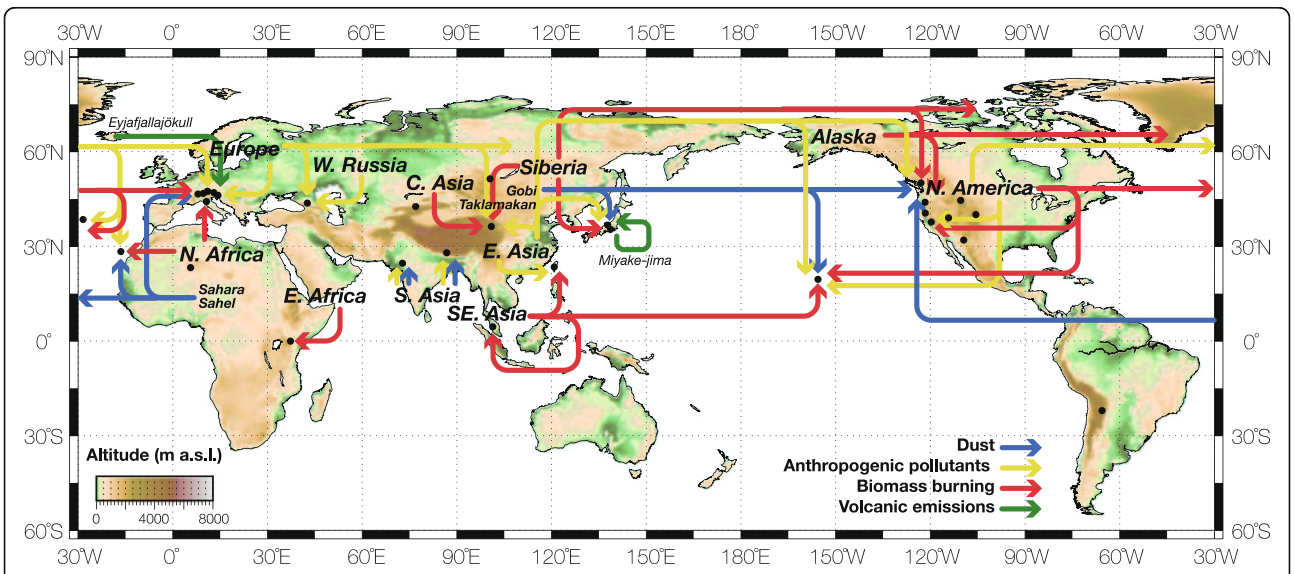

Fig. 9 Schematic overview of long-range transport pathways for dust (*blue arrows*), anthropogenic pollutants (*yellow arrows*), biomass burning (*red arrows*), and volcanic emissions (*green arrows*), which have been reported in the literature over time

at MBO (Fischer et al. 2010b; Primbs et al. 2008a, b; Reidmiller et al. 2010; Strode et al. 2008; Weiss-Penzias et al. 2006) and WHI (Macdonald et al. 2011). The influence of Asian anthropogenic emissions on MLO has been identified through observations of CO (Jaffe et al. 1997) and aerosols (Perry et al. 1999). Jaffe et al. (1997) concluded that the majority of the elevated CO events occurred during spring and were usually associated with transport from Asia. Perry et al. (1999) estimated that at least one third of the sulfate (SO_4^{2-}) species including sulfuric acid (H_2SO_4), ammonium bisulfate ($(NH_4)HSO_4$), and ammonium sulfate ($(NH_4)_2SO_4$) detected during spring from 1993 to 1996 were anthropogenic in origin. This result is consistent with the seasonal cycles of bromine (Br), lead (Pb), and zinc (Zn), high concentrations of which are found in the fine fractions of fly ash from coal-fired power plants. Levy and Moxim (1989) concluded that the NO_y maximum in the summer was caused by fossil fuel combustion in the USA, and that the Asian emissions contributed to only a small increase in spring.

Air masses affected by anthropogenic emissions have been observed at WLG by the enhancement of O_3, CO, NO_y, total gaseous mercury (TGM), and volatile organic compounds (VOCs). Backward trajectory analysis at WLG for the summers of 2000 to 2009 suggests the dominance of anthropogenic pollution transported from central and eastern China in most years (Xue et al. 2011). Fu et al. (2012) identified potential source regions of anthropogenic pollutants at WLG as eastern Gansu, eastern Qinghai, western Shanxi, Ningxia, and northern India, while Zhang et al. (2009a) described the transport mechanisms for polluted air from Lanzhou, the capital of Gansu province. They found that the plumes from Lanzhou were advected by strong easterly winds, which were vented to the FT by a belt-like mountain and were transported to WLG, either directly or by mixing, by nighttime mountain breezes. In addition, the high concentrations of organochlorine pesticides (OCPs) such as hexachlorocyclohexane (γ-HCH), dichlorodiphenyltrichloroethanes (DDTs), and polybrominated biphenyls (PBDEs) were found to be related mainly to air masses passing over Russia and Kazakhstan (Cheng et al. 2007). The particle number concentration at WLG was higher during the summer and lower during the rest of the year in the study of Kivekäs et al. (2009). Their back trajectory analysis revealed that air masses transported from the east are associated with higher particle number concentrations than those transported from other directions. As a result, they concluded that the eastern air masses might be affected by regional pollution sources such as Xining and Lanzhou.

The atmospheric conditions at PYR can be influenced by the transport of polluted air masses from South Asia and the Indo–Gangetic Plains and the ABCs extend from the Indian Ocean to the Himalayan ridge (Bonasoni et al. 2010). Bonasoni et al. (2010) showed that a mountain valley can provide an efficient channel favoring the transport of pollutants to high altitudes when the brown clouds extend as far as the Himalayan foothills under active valley breezes. They found that the most frequent direct transport of brown clouds occurred during the pre-monsoon season, occupying 20 % of total pre-monsoon days. Aerosol total number concentration, aerosol optical properties, PM_1, PM_{1-10}, and BC showed a maximum during the pre-monsoon season and a minimum during the monsoon season (Marcq et al. 2010; Marinoni et al. 2010; Sellegri et al. 2010). The monsoon minimum was attributed to wet scavenging caused by frequent clouds and precipitation. The pre-monsoon maximum was linked to an increase in anthropogenic emissions in the Indian subcontinent coupled with dry meteorological conditions, and to the large vertical extent of the regional PBL on the Indo–Gangetic Plains. At MAB, ammonium (NH_4^+), NO_3^-, and non-sea-salt SO_4^{2-} (nss-SO_4^{2-}) aerosol concentrations showed a distinctive seasonal cycle, with a decrease (increase) during the wet (dry) season (Rastogi and Sarin 2005). They attributed the low levels of NH_4^+, NO_3^-, and nss-SO_4^{2-} concentrations during the wet season to the predominance of the oceanic air mass and the high levels during the dry season to the enhanced downwind transport of pollutants and the lack of wet removal. The relative enrichment of NH_4^+ and nss-SO_4^{2-} and their linear relationship in $PM_{2.5}$ suggests that their predominant source is anthropogenic in northern India in winter (Kumar and Sarin 2010). Francis (2012) identified a high sulpher dioxide (SO_2) region surrounded by (30° N, 75° E) north of MAB by using the GEOS-Chem model and concluded that the observed spikes in SO_2 concentration at MAB were caused by the transport from that high-SO_2 region.

Emissions transported from North America have been observed at IZO (Cuevas et al. 2013; Schultz et al. 1998), PMO (Honrath et al. 2004), ARO (Huntrieser et al. 2005), ZUG/ZSF (Huntrieser et al. 2005), and JFJ (Guerova et al. 2006; Huntrieser et al. 2005; Pandey Deolal et al. 2013). Most of the elevated CO events observed at PMO during the summers of 2001 to 2003 were attributed to the outflow of North American pollution and the long-range transport of biomass-burning emissions, whereas O_3 and CO concentrations were strongly correlated with the flow from the eastern USA when the biomass-burning effects were absent (Honrath et al. 2004). The concentration ratios of NMHCs have been used as indicators of the degree of photochemical processing or aging, mainly via reaction with OH radicals, because the ratios evolve as atmospheric processing occurs depending on the individual OH rate constants (e.g., Parrish et al. (2007). Honrath et al. (2008) demonstrated that continuous measurements of NMHCs are a useful tool for identifying and characterizing pollution transport events. Owen et al. (2006) described the transport mechanisms of North American CO

emissions to PMO in the lower FT over the central North Atlantic. They found that two mechanisms were responsible for the export of pollution from the North American boundary layer that led to the enhanced CO events at PMO: direct advection from the continental boundary layer eastward over the Atlantic Ocean and uplift ahead of cold fronts. In another study, NO_y levels were significantly increased in the presence of North American anthropogenic emissions (Val Martin et al. 2008a). Zhang et al. (2014) analyzed the chemical evolution of two pollution plumes transported from North America to PMO in the summers of 2009 and 2010. They concluded that the enhanced change in O_3 relative to CO ($\Delta O_3/\Delta CO$), which has been frequently used as an indicator of O_3 production in transported plumes, might not reflect O_3 chemistry alone, and that the CO destruction in the plume could also explain the higher values. Kumar et al. (2013) showed significant decreasing trends of CO and O_3 for the period from 2001 to 2011 by in situ measurements at PMO and model simulations using GEOS-Chem. They concluded that the most important factor contributing to these decreasing trends was the decline in anthropogenic emissions from North America. Under the framework of the Convective Transport of Trace Gases into the Middle and Upper Troposphere over Europe (CONTRACE) project, aged plumes of North American pollution that passed over Europe were observed by Huntrieser et al. (2005) at ARO, ZUG/ZSF, and JFJ. They used the FLEXible PARTicle (FLEXPART) Lagrangian particle dispersion model to simulate the transport pathway of the pollution plume over the Atlantic and its dispersion over Europe. The passage of the North American plumes over Europe required almost 3 days. The time elapsed since the pollutant emission, derived by the NO_y/CO slope in the polluted plumes, was in good agreement with that simulated by the FLEXPART age spectra. Furthermore, a positive correlation between O_3 and CO in the plumes suggested that photochemical O_3 production occurred. A comparison of the model results with observations at JFJ revealed that the GEOS-Chem model tended to underestimate the O_3 concentrations (Guerova et al. 2006). Because the stratospheric contribution to the estimates based on the $^7Be/^{10}B$ ratio was shown to be reasonable (Zanis et al. 2003b), Guerova et al. (2006) suggested that this discrepancy resulted from an underestimation of the European contribution. They found that a substantial North American contribution over Europe did not always result in O_3 enhancement in summer. Cui et al. (2009) estimated the contribution of stratospheric intrusion and intercontinental transport from the North American PBL to JFJ in 2005 by using FLEXPART and the Lagrangian analysis tool (LAGRANTO) trajectory model. They determined that JFJ was influenced by stratospheric intrusion during 19 and 18 % of the total annual time and by intercontinental transport from North American PBL during 13 and 12 % of the total annual time, as indicated by FLEXPART and LAGRANTO, respectively. At IZO, a good correlation between O_3 and CO in winter and spring was observed, suggesting long-range transport of photochemically generated O_3 from North America (Cuevas et al. 2013). Sholkovitz et al. (2009) estimated that from 12 to 30 % of the annual apportionment of the soluble aerosol Fe fluxes was contributed by anthropogenic aerosols. IZO has also been influenced by North African pollution. During the summer, IZO remains in the altitude of the Saharan Air Layer (SAL), which is exported westward at low tropical latitudes (<15° N) in winter and at higher subtropical latitudes in summer (15–30° N; Rodríguez et al. 2011). Rodríguez et al. (2011) suggested that North African industrial pollutants, including emissions from crude oil refineries, the phosphate-based fertilizer industry, and power plants located at the Atlantic coast of Morocco, northern Algeria, eastern Algeria, and Tunisia might be mixed with desert dust and before being exported to the North Atlantic in the SAL. Verver et al. (2000) reported pollution outbreaks both from the Iberian Peninsula and northern or central Europe to IZO during the Second Aerosol Characterization Experiment (ACE-2) campaign.

The Alps, located in the center of Europe, are surrounded by regions of intensive air pollutant emissions. Transport of anthropogenic emissions in Europe to the high-altitude Alpine stations have been observed at SNB (Gros et al. 2001; Jabbar et al. 2012; Kaiser 2009; Kaiser et al. 2007; Karl et al. 2001a, b; Seibert et al. 1998), ZUG/ZSF (Jabbar et al. 2012; Kaiser et al. 2007), CMN (Bonasoni et al. 1997; Cristofanelli and Bonason 2009, 2013), KVV (Kaiser et al. 2007), ARO (Campana et al. 2005; Pochanart et al. 2001), and JFJ (Collaud Coen et al. 2011; Forrer et al. 2000; Kaiser et al. 2007; Kuebler et al. 2001; Lanz et al. 2009; Legreid et al. 2008; Lugauer et al. 1998; Pandey Deolal et al. 2013; Seibert et al. 1998; Tuzson et al. 2011). The Po Basin is a densely populated and highly industrialized region located immediately adjacent to the Alps that is known to have a relatively high level of air pollution. Emissions transported from the Po Basin have been observed at ARO (Campana et al. 2005), CMN (Bonasoni et al. 1997; Cristofanelli and Bonason 2009), SNB (Seibert et al. 1998), and JFJ (Lanz et al. 2009; Seibert et al. 1998). By using trajectory-based methods, Kaiser et al. (2007) showed potential source regions of air pollutants and air flow regimes connected with pollution events at ZUG, SNB, JFJ, and KVV. They determined that the influence of emissions from the Po Basin was strongest in the west Alps (JFJ), whereas the influence of emissions from Eastern Europe was strongest at SNB. In another study, the influences of meteorological processes on the regional transport to JFJ were subdivided into two categories: thermally driven

transport, which occurs on a local scale, and transport at regional (foehn) or synoptic (front) scales (Forrer et al. 2000). Thermally induced processes were observed mainly in spring and summer, and processes at the regional and synoptic scales were observed during the entire year. Continuous measurements of the total and backward scattering coefficients, absorption coefficient, condensation nuclei concentrations, epiphaniometer signals, total suspended particulate matter (TSP) mass concentrations, and major PM_1 and TSP compounds at JFJ have shown distinct seasonal cycles with a summer maximum and a winter minimum (Baltensperger et al. 1997; Cozic et al. 2008; Henning et al. 2003; Lugauer et al. 1998; Nyeki et al. 1998a, b). The seasonal cycles of SO_4^{2-}, NO_3^-, and NH_4^+ of aerosols at SNB also showed a summer maximum and a winter minimum (Kasper and Puxbaum 1998). During winter, JFJ and SNB are influenced mainly by the clean FT, resulting in low concentrations of most aerosol components. Higher mass concentrations have been found during summer when convection occasionally transports polluted air masses to JFJ and SNB. At different non-urban sites located along a west–east transect in Europe including SNB, Oliveira et al. (2007) showed year-round variations of lipophilic particulate organic compounds emitted from vehicle exhaust constituents, meat smoke tracers, phytosterols of higher photosynthetic plants, and wood smoke components. They determined that the concentrations at SNB maximized during summer, whereas an absence of seasonal variation was observed at the oceanic site. At ARO, the O_3 concentrations were found to depend significantly on the residence times of air masses over the polluted region of Europe during spring and summer (Pochanart et al. 2001). An increase in O_3 concentrations has been observed in the aged air masses, which is the result of direct photochemical accumulation of O_3 when the air masses pass over large-scale anthropogenically influenced regions in Europe. South foehn is a typical Alpine meteorological phenomenon characterized by south to north advection and is caused by a strong pressure gradient across the Alps that leads to a descending air stream northward (Seibert 1990). Campana et al. (2005) observed enhanced O_3 concentrations during south foehn events during spring and summer at ARO. In the case of the south foehn, the continental-scale influence of pollutant emissions on O_3 appeared to be far less important than the direct influence of the Po Basin emissions. The main sources of NO_x and CO are air masses with long residence times over the European continent (Kaiser et al. 2007). Kaiser et al. (2007) showed the differences between the main NO_x source regions, including northwest Europe and the region covering East Germany, the Czech Republic, and southeast Poland, and the main CO source regions including the central, northeastern, and eastern parts of Europe. The statistics for O_3 concentrations show strong seasonal effects. Near-ground air masses are poor (rich) in O_3 in winter (summer). The main source of high O_3 concentrations in winter is air masses that subside from higher elevations. During summer, the Mediterranean constitutes an important additional source of high O_3 concentrations, particularly for air masses that have crossed the Po Basin. The transport of polluted air masses from Europe and other continents can exert an influence on southern Europe and the Mediterranean basin. In particular, anthropogenic pollutants emitted from continental Europe are transported toward southern Europe and the Mediterranean basin during summer (e.g., Duncan et al. 2008; Henne et al. 2005). Based on modeled CO concentrations, Folini et al. (2009) quantified the regions of influence (ROIs) of 13 European rural background and high-altitude stations including SNB, CMN, ZUG/ZSF, and JFJ. The ROI definition of a measurement site is the area near the station from which surface emissions contribute substantially to the short-term variability of the measured trace gas concentrations. Folini et al. (2009) defined an individual site as one that roughly covers a circular area of 400 km in radius and said that large cities or other strong emission sources within 100 km from the site should be avoided. The seasonal cycle of BC at CMN was characterized by the presence of a winter minimum (December–January) and maxima in spring (April–May) and late summer (August–September), reflecting a higher efficiency of uplift during warmer months and the subsequent transport of polluted air masses from the boundary layer. In addition, a secondary minimum was observed in June, when wet deposition is expected to peak owing to maximum rainfall (Cristofanelli et al. 2013). They indicated that CMN was affected by air masses rich in anthropogenic CO during spring and summer. In addition, Cristofanelli et al. (2013) identified three main regimes of the seasonal correlation among CO, O_3, and BC at CMN: negative correlation between CO and O_3 during the period from October to December, significant positive correlation between CO and O_3 during the period from May to September, and almost no correlation between CO and O_3 and BC enhancements mainly associated with relatively old anthropogenic emissions during the period from January to April. They considered it likely that the negative correlation between O_3 and CO was attributed to the combined processes concurrent in enhanced O_3 with low CO (i.e., STE) and O_3 titration with NO in polluted air masses along with low photochemical activity. The seasonal cycle of O_3 at KSL in the Caucasus, as well as at other stations in the Alps, showed a broad spring–summer maximum. Although the aforementioned stations are under the effects of European emissions, particularly from Po Basin, KSL is influenced by semi-polluted air masses from the regions of the northern Caspian, southern Urals, and Volga, which causes photochemical O_3 production in these air masses, thereby resulting in seasonal O_3 maxima (Tarasova et al. 2003).

Biomass burning

Biomass burning is a significant global source of gaseous and particulate species emissions to the troposphere. Emissions from biomass burning are known to be an important source of GHGs and chemically active gases on regional and global scales (e.g., Andreae and Merlet 2001). Interannual variations in biomass burning can be dramatic, depending on natural and socioeconomic factors such as rainfall and political incentives to clear land. In some regions of the world, biomass burning occurs throughout the year, even though on the global scale it usually peaks in March and again in September (Duncan et al. 2003). The peak in December to April during the dry season in the Northern Hemisphere is predominately associated with burning in the tropical regions of North Africa and Southeast Asia, with much smaller contributions from Central America and Mexico and northern South America. The peak in August to October during the Southern Hemisphere dry season is associated with burning in South Africa and Brazil, with smaller contributions from Indonesia and Malaysia. Although the Indonesia and Malaysia region straddles the equator, the burning season generally occurs in the latter half of the year. Figure 9 shows a schematic overview of the long-range transport of trace gases and aerosols emitted from biomass-burning sources.

MKN is rarely influenced directly by African biomass burning emissions, which are most prominent in the western part of the continent. Henne et al. (2008) attributed the boreal summer maximum of CO at MKN to advection of Southern Hemispheric air loaded with emissions from biomass burning in South Africa. They analyzed fire counts and fire radiative power (FRP) recorded by Moderate Resolution Imaging Spectroradiometer (MODIS) sensors and concluded that the interannual variability of this summer maximum could be mostly explained by a combination of changes in transport patterns and biomass burning intensity.

Biomass burning is a seasonally important source of emissions in Central Europe (Lanz et al. 2010). Cristofanelli et al. (2009b) identified the transport of a biomass-burning plume with mineral dust from North Africa by means of air mass circulation analysis and aerosol chemical characterization. Cristofanelli et al. (2013) determined that biomass-burning effects on CMN were maximized during the warm months from July to September. Moreover, they analyzed the source regions of biomass burning events by using FLEXPART and identified transport at the local scale in the central Alps, North Africa, southern Italy, and Greece; that at the regional scale in Russia; and that at the global scale in North America and western equatorial Africa.

CO and BC influences from Siberian boreal forest fires have been observed at HPO (Kato et al. 2002; Liu et al. 2013; Pochanart et al. 2004), and aerosol influences have been observed at FWS (Kaneyasu et al. 2007). It is considered likely that biomass burning contributed to the mass concentration of BC values at HPO, particularly in spring (Liu et al. 2013). An increase in the observed mass concentration of BC values in April and May 2008 suggested substantial effects of very active biomass burning in Siberia. Wang et al. (2006) investigated the influence of biomass burning activities on the levels of trace gases at WLG. They concluded that forest fires in central Asia affected WLG observations during spring. In contrast, in eastern Siberia, forest fires occurred mainly during summer, and those air masses were rarely transported to WLG.

LLN has been influenced by Southeast Asian biomass burning activities in spring (Chang et al. 2013; Chen et al. 2013; Chi et al. 2010; Lee et al. 2011; Lin et al. 2010; Ou Yang et al. 2012, 2014; Sheu et al. 2010). Spring is the major biomass-burning season in the Indochina Peninsula (Streets et al. 2003). Lee et al. (2011) determined that $PM_{2.5}$ at LLN was highest during the biomass-burning season, particularly in March. They also concluded, based on back trajectory analysis, that the observed high $PM_{2.5}$ levels were attributed mainly to the biomass-burning events. Backward trajectory analysis by Lin et al. (2010) showed that most air masses observed by LLN originated from India, the Indochina Peninsula, and southern coastal China, which together accounted for 85 % of the total trajectory. A different transport mechanism that favors CO transport from Indochina to the downwind Taiwan area was identified via a Weather Research and Forecasting (WRF) meteorological model simulation (Cheng et al. 2013). The results indicated the formation of a thermal forcing-induced low-pressure system in Indochina and that the high terrain located in the northern part of Southeast Asia further forced the uplift of biomass-burning emissions. Contrastingly, a sufficiently strong northeasterly monsoonal flow intruding into Indochina would hinder the development of the thermal low and would weaken the upward movement, which would, in turn, prevent the transport of biomass-burning emissions from Indochina to the Taiwan area. During the dry period of the year, the biomass burning in Sumatra normally begins around May and lasts until September or October. The mass concentration of PM_{10} at TAR in the study of Streets et al. (2003) showed a cycle similar to that of O_3, with two minima in March or April and November or December, and a maximum during the summer monsoon, thereby indicating that the O_3 and PM_{10} precursors had a common source. Toh et al. (2013) showed that the transport of air pollutants from biomass burning in Sumatra released large amounts of precursors and led to increases in O_3 and PM_{10}.

Occasionally, MLO has been influenced by biomass burning plumes transported from Southeast Asia and

the Indian subcontinent across the Pacific (Karl et al. 2003), and from North America (Perry et al. 1999). Karl et al. (2003) measured the levels of methanol (CH_3OH), acetonitrile (CH_3CN), acetone (C_3H_6O), C_5H_8, methyl vinyl ketone (MVK), and methacrolein (MACR) in spring 2001 and found high correlations among CO, C_3H_6O, and CH_3CN during the event.

WHI has been influenced by regional biomass burning, particularly in northern California, Oregon, Alaska, and Yukon Territory (Macdonald et al. 2011; McKendry et al. 2010, 2011). MBO has also experienced numerous events associated with biomass-burning emission originating from Alaska (Weiss-Penzias et al. 2007) and the northwestern USA including California and Oregon (Finley et al. 2009; Primbs et al. 2008a, b; Weiss-Penzias et al. 2007). In July and August 2008, two regional biomass-burning events induced increases of CO and O_3 concentrations at both WHI and MBO (McKendry et al. 2011). Takahama et al. (2011) analyzed the organic functional groups of aerosols collected during those biomass-burning periods and showed a large contribution of ketones, at 26 % on average, to the organic aerosol mass in addition to sharp peaks of ketones attributed to plant wax. Macdonald et al. (2011) examined the influence of different transport and source regions on the O_3 and CO concentrations at WHI. They noted little difference between trans-Pacific air masses and the clean background in summer. The air masses from North America showed the greatest increases in O_3 and CO concentrations above the background values during years when the largest areas of western North America area burned. Finley et al. (2009) reported that regional wildfire events produced larger enhancement of CO (ΔCO), aerosol scatter coefficient ($\Delta\sigma_{sp}$), and NOy (ΔNO_y) values than the Asian long-range transport events due to the significantly shorter transport times from source to receptor, which meant less plume dilution, photochemical removal, and wet particle deposition. Jaffe et al. (2008) showed that the area of summer burning in the western USA was significantly correlated with daytime summer O_3 concentrations at LAV and YEL, which indicates that the presence of fire played an important role in increasing the summer O_3 in the western USA. Chalbot et al. (2013) indicated that regional fire incidents might trigger high O_3 episodes. They estimated a 3 ppb increase in the MDA8 O_3 concentration at CHA in Arizona by such incidents within 400 km of the sites. McKendry et al. (2010) emphasized the importance of permanent lidar installations in mountainous locations for understanding the vertical transport process and the analysis of the chemical time series.

In past decades, significant intercontinental transport of air masses containing abundant biomass burning emissions from North America to Europe and the North Atlantic have been reported in many studies. Emission transport from North American and Siberian boreal wild fires has substantially affected the concentrations of trace gases at PMO (Helmig et al. 2008; Honrath et al. 2004; Lapina et al. 2008; Pfister et al. 2006; Val Martín et al. 2006; Val Martin et al. 2008a, b). The NO_x/CO emission ratio is related to the relative amounts of smoldering and flaming combustion because CO concentrations typically show maxima during smoldering combustion while NO_x concentrations show maxima during flaming combustion (Lobert et al. 1991). The NO_x/CO emission ratios from boreal fires had higher values in early summer and lower values in late summer, which is consistent with the smoldering combustion variation (Lapina et al. 2008). Lapina et al. (2008) suggested that this change in fuel properties affects the results for the O_3 production rate in model calculations because it impacts the relative properties of the species released from fires and an increase in the overall fuel consumption. During summer 2004, extensive wildfires in Alaska and western Canada released large amounts of trace gases and aerosols into the atmosphere. For example, CO emitted from mid-June to August was in the order of anthropogenic CO emissions for the entire continental USA during the same period (Pfister et al. 2005; Turquety et al. 2007). Intense boreal wildfires plumes were observed at PMO during the International Consortium for Atmospheric Research on Transport and Transformation (ICARTT) study (Pfister et al. 2006; Val Martín et al. 2006). This long-range transport of boreal wildfire emissions resulted in large enhancements of CO, BC, NO_y, and NO_x (Val Martín et al. 2006). Emissions from these wildfires frequently affected PMO downwind 6 to 15 days later. The enhancement ratios relative to CO were variable in the plumes sampled due to variations in wildfire emissions and removal processes during transport. Analyses of ΔBC/ΔCO, $\Delta NO_y/\Delta$CO, and $\Delta NO_x/\Delta$CO ratios indicated that NO_y and BC were, on average, efficiently exported in these plumes, and suggested that the decomposition of PAN to NO_x was a significant source of NO_x. High levels of NO_x suggested the continuing formation of O_3 in these well-aged plumes. Pfister et al. (2006) simulated the O_3 production from boreal forest fires based on a case study of wildfires in Alaska and Canada in summer 2004 by using a chemistry transport model, the Model for O_3 and Related Chemical Tracers (MOZART-4). Their results indicate that fires in the boreal region could have a significant impact on the O_3 production over large parts of the Northern Hemisphere.

Dust and volcanic emissions

Every year, massive amounts of mineral dust are uplifted into the atmosphere (1950 to 2400 Tg year^{-1}; Ginoux

et al. 2004). The desert region of North Africa (65 % of the global dust emissions) is the largest source of soil dust suspended in the atmosphere while Asia's deserts are the second largest source (25 %). Saharan dust has significant climatic and environmental impacts in the North Atlantic and in Europe (Fig. 9). Mineral dust is transported from North Africa along three pathways: westward across the Atlantic to the Americas, northward across the eastern Mediterranean to Europe, and eastward across the eastern Mediterranean to the Middle East and Asia (Middleton and Goudie 2001). Saharan dust events have often been observed at IZO (Alastuey et al. 2005; Arimoto et al. 1995; Díaz et al. 2006; Kandler et al. 2007; Maring et al. 2000; Rodríguez et al. 2011; Salisbury et al. 2006; Schmitt and Volz-Thomas 1997; Smirnov et al. 1998), CMN (Bonasoni et al. 1997, 2004; Cristofanelli and Bonason 2009; Cristofanelli et al. 2009b; de Reus et al. 2005; Gobbi et al. 2003; Hanke et al. 2003; Marenco et al. 2006; Putaud et al. 2004; Van Dingenen et al. 2005), and JFJ (Chou et al. 2011; Collaud Coen et al. 2004; Cozic et al. 2008; Fierz-Schmidhauser et al. 2010; Nyeki et al. 1998b; Schwikowski et al. 1995; Zieger et al. 2012). Furthermore, long-range transport of Saharan dust over a pathway spanning from Asia and the Pacific to western North America has been identified at WHI by McKendry et al. (2007).

Mineral dust affects the gas phase chemistry in the troposphere by providing a reactive surface that is able to support heterogeneous trace gas reactions (e.g., Usher et al. 2003). Hanisch and Crowley (2003) investigated the heterogeneous reaction between O_3 and Saharan dust surfaces in a Knudsen reactor and observed the destruction of O_3 on the dust surface and the formation of O_2. The phenomena of low O_3 and high dust concentrations have been observed in the field (e.g., Bonasoni et al. 1997; Prospero et al. 1995). As part of the Mineral Dust and Tropospheric Chemistry (MINATROC) project, which was an intensive field measurement campaign conducted at CMN from June 1 to July 5, 2000 (Balkanski et al. 2003; Bauer et al. 2004; Bonasoni et al. 2004; de Reus et al. 2005; Fischer et al. 2003; Gobbi et al. 2003; Hanke et al. 2003; Putaud et al. 2004; Van Dingenen et al. 2005) and at IZO from July 15 to August 15, 2002 (de Reus et al. 2005; Salisbury et al. 2006; Umann et al. 2005). Their aim was to fully characterize gas and aerosol species with a complete set of measurements in order to identify the heterogeneous reactions of dust. Bonasoni et al. (2004) showed that the O_3 concentrations during the dust events at CMN were 4 to 21 % lower than the de-trended monthly mean dust transport values, thus suggesting that Saharan dust has a substantial influence on the O_3 levels, even in a polluted region of Southern Europe. During the Saharan dust advection period, mixing of fine particles from anthropogenic particles and coarse particles from the Saharan region was observed at CMN (Putaud et al. 2004). Putaud et al. (2004) suggested that NO_3^- was shifted toward the aerosol super-μm fraction in the presence of dust. Hanke et al. (2003) and Umann et al. (2005) observed an efficient uptake of gaseous HNO_3 by mineral dust aerosol particles, thereby suggesting that mineral dust might be a significant sink for HNO_3 in the troposphere. Hence, it could affect the photochemical cycles and O_3 production. Bauer et al (2004) estimated the impact of heterogeneous chemical reactions at the surface of mineral dust on global O_3 chemistry using a global general circulation model, coupled online with atmospheric chemistry and mineral aerosol modules that were evaluated based on observational data during the MINATROC campaign. The model simulated a decrease in global tropospheric O_3 mass by ~5 % due to heterogeneous reactions, and implied that the most important heterogeneous reaction was the uptake of HNO_3 on the dust surface. Salisbury et al. (2006) observed the concentrations of the organic compounds CO, CH_3OH, formaldehyde (HCHO), acetaldehyde (CH_3CHO), C_3H_6O, C_3H_8, C_5H_8, and toluene ($C_6H_5CH_3$) under both normal conditions and during large dust storms, in order to investigate the effects of mineral dust on oxygenated organic species. However, no clear production for CH_3CHO or HCHO on dust particles was ascertained. By using the Module Efficiency Calculating the Chemistry of the Atmosphere (MECCA) chemistry box model, de Reus et al. (2005) concluded that the reduced RO_x and NO_x concentrations in the Saharan dust plume contributed to a reduced net O_3 production rate, which likely explains the observed relatively low O_3 concentrations.

After reaching CMN, Saharan dust plumes often move farther northward and eastward to eventually reach northern Italy, the Alps, and central Europe. At JFJ, Saharan dust events have been detected as a pronounced change in aerosol properties compared with the background conditions (Chou et al. 2011; Collaud Coen et al. 2004; Cozic et al. 2008; Fierz-Schmidhauser et al. 2010; Nyeki et al. 1998b; Schwikowski et al. 1995; Zieger et al. 2012). Collaud Coen et al. (2004) summarized the annual distribution of Saharan dust events in Europe, the Mediterranean basin, West Africa, and over the Atlantic Ocean and explained that Saharan dust events frequently occurred during spring and less frequently in July and August. Figure 10a shows the seasonal variation of Ca^{2+} (a component of mineral dust) concentration in total suspended particles (TSP) at JFJ. Associated with relatively large monthly variability caused by occasional intense events, seasonal variations are not very distinct. However, the annual maximum is seen in February (~0.10 μg m^{-3}) associated with large variability.

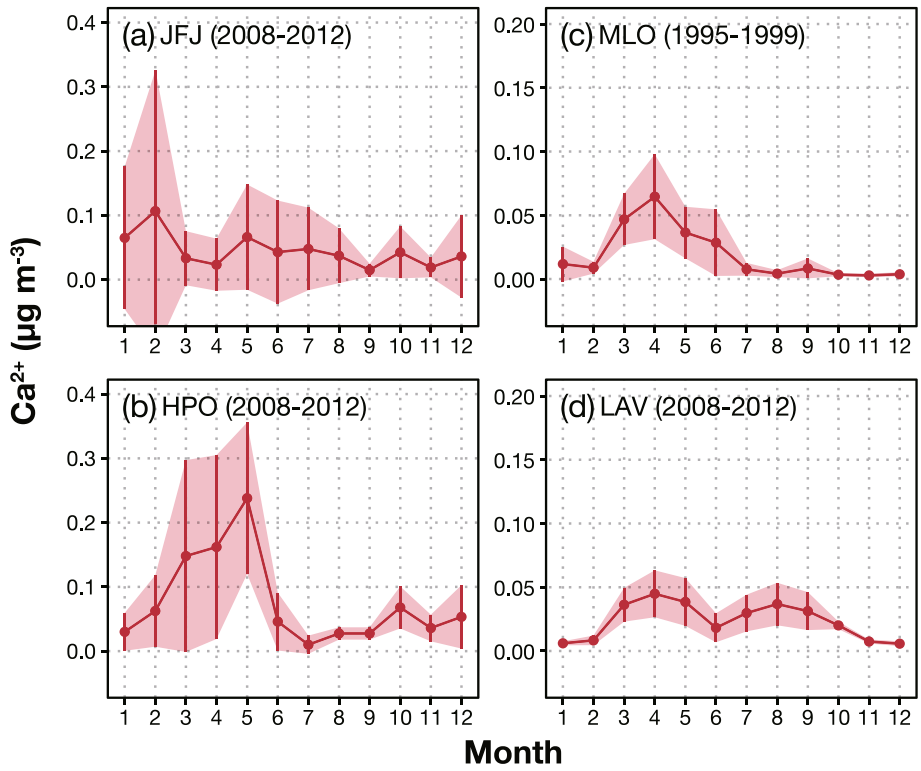

Fig. 10 Seasonal variations in Ca^{2+} concentrations at four mountain stations. The *lines with circles* denote the average observed Ca^{2+} concentrations during a particular period. The *years in parenthesis* denote the averaging period. The *red shaded bands* and *error bars* denote the standard deviations. The concentrations of Ca^{2+} in TSP were measured at JFJ (**a**) and HPO (**b**) and those in $PM_{2.5}$ were measured at MLO (**c**) and LAV (**d**)

Asian dust particles known collectively as "Kosa" are generated when the surface soil particles in the arid and semi-arid regions of inland Asia (such as Taklamakan and Gobi deserts) are lifted by the winds and transported over long distances by strong westerly winds. Intense Asian dust events are observed each spring in China, Korea, Japan, and even occasionally in Hawaii and North America (Fig. 9). This phenomenon normally occurs in spring. Weak dust layers occur in the FT over Japan during periods with no evident dust outbreaks or even in seasons other than spring (e.g., Iwasaka et al. 1983). Asian dust events have been observed at FWS (Suzuki et al. 2008, 2010), MLO (Bodhaine 1995; Clarke and Charlson 1985; Darzi and Winchester 1982; Holmes and Zoller 1996; Hyslop et al. 2013; Parrington et al. 1983; Parrington and Zoller 1984; Perry et al. 1999; VanCuren and Cahill 2002; Zieman et al. 1995), LAV (Jaffe et al. 2003b; Liu et al. 2003a; VanCuren 2003; VanCuren and Cahill 2002; VanCuren et al. 2005), and WHI (Leaitch et al. 2009; McKendry et al. 2008). A distinct seasonal cycle with a spring maximum of Ca^{2+} concentration can be seen at HPO (~0.25 μg m^{-3}; Fig. 10b) and MLO (~0.05 μg m^{-3}; Fig. 10c). At LAV, two peaks can be seen in spring (~0.05 μg m^{-3}) and summer (Fig. 10d). The concentrations at two IMPROVE stations (MLO and LAV) and at HPO were determined by $PM_{2.5}$ and TSP analyses, respectively. VanCuren and Cahill (2002) found that the tropical wind bands were displaced to the south of Hawaii and that strong westerly circulation can reach the islands to deliver Asian aerosols, particularly at MLO from December to May. Other studies have reported that in January or February, many elements associated with continental crust experienced an increase in the mass of samples. The aerosol concentration of crustal elements remained elevated until June or July, suggesting that the dust season is from late winter to mid-summer (Parrington et al. 1983; Zieman et al. 1995). VanCuren et al. (2005) concluded that Asian aerosols influence LAV throughout spring, summer, and fall.

Mineral dust is a major component of PM_{10} observed at PYR by Decesari et al. (2010). They suggested that the increase in mineral components in the pre-monsoon season is due mainly to an increase in the background concentration. This increase is likely related to changes in their long-range transport from the arid regions of western India, possibly to upwind regions such as the Arabian deserts. Aerosols at MAB are dominated by mineral dust (Kumar and Sarin 2009, 2010; Ram et al. 2008; Rastogi and Sarin 2005). Kumar and Sarin (2009)

showed that the mass concentration of $PM_{10-2.5}$ at MAB is influenced by the uniform contribution of dust (60 to 80 %) throughout the year. The predominant of sources of MAB are the Thar and Arabian deserts during summer months and the Indo–Gangetic Plain during winter months (Kumar and Sarin 2009).

Volcanic emissions such as ash clouds, aerosols, and volcanic gases often affect local or regional air quality (e.g., Huebert et al. 2001). Furthermore, the volcanic aerosols released by explosive eruption affect the stratospheric aerosol layer (Deshler 2008), which is important for radiation (e.g., Solomon et al. 2011) and atmospheric chemistry, particularly O_3 depletion (e.g., Solomon 1999). In the later part of the twentieth century, the signatures of major volcanic eruptions such as El Chichón in 1982 and Mt. Pinatubo in 1991 were identified in the total O_3 records at ISK (Visheratin et al. 2006) and ARO (Rieder et al. 2010a, b) and in the total column NO_2 records at JFJ (De Mazière et al. 1998). The oxidizing capacity of the troposphere can also be affected because the amount of UV radiation reaching the troposphere decreases due to the enhanced stratospheric aerosols and SO_2. Bândă et al. (2015) showed that the sulfur emissions from Pinatubo significantly affected the CH_4 budget using a 3D global chemistry model.

In spring 2010, eruptions of Eyjafjallajökull volcano (63.63° N, 19.62° W) in Iceland had a major impact on aviation because ash from the April–May summit eruption was transported with northwesterly winds toward Europe and the North Atlantic. The volcanic plume resulting from that eruption was observed at CMN (Sandrini et al. 2014), KVV (Beeston et al. 2012), ZSF (Flentje et al. 2010; Schäfer et al. 2011), and JFJ (Bukowiecki et al. 2011). Moreover, enhanced PM_{10} and SO_2 concentrations were observed at ZSF and JFJ. Monthly mean SO_2 concentrations in the spring of 2010 at JFJ were higher than those in other years (Fig. 11a). These observations suggest that the large volcanic eruption had a significant impact on the sulfur cycle on a regional scale.

On July 8, 2000, Miyake-jima volcano (34.09° N, 139.53° E), located in the northwest Pacific Ocean, began to erupt. In winter, volcanic emissions were transported southeastward to the Pacific Ocean due to the prevailing northwesterly wind, while in summer volcanic emissions were transported southwestward to Japan, Korea, and Taiwan due to the subtropical high-pressure system (Kajino et al. 2004). At FWS, Naoe et al. (2003) showed that the large fraction of the SO_4^{2-} concentrations in aerosols was most likely produced in the volcanic plume from Miyake-jima. At HPO, aerosols, precipitation, and gaseous pollutants including O_3, SO_2, NO, and NO_2 were observed prior to the eruption, and short-term aerosol sampling was conducted by Satsumabayashi et al. (2004). They reported unchanged O_3 levels, a fourfold enhancement of SO_2 concentration, and increased SO_4^{2-} and NH_4^+ levels in aerosols following the eruption. When the volcanic plume was transported directly, the atmospheric SO_2 and SO_4^{2-} concentrations in the aerosols increased simultaneously, and the NO_3^- and chlorine (Cl^-) concentrations decreased. Monthly mean SO_2 concentrations at HPO for the period from the summer of 2000 to the spring of 2001 were higher than those in other years (Fig. 11b). Kajino et al. (2005) quantitatively estimated the indirect acidification of nonvolcanic NO_3^- and Cl^- as a result of the increase in SO_4^{2-} aerosol concentration from the eruption. They concluded that the contribution of indirect acidification could not be negligible and that this effect should be considered in general air pollution because SO_2 emissions could be expected to continue increasing—especially in Asia.

Recommendations for future atmospheric monitoring

This paper has provided a comprehensive review on the seasonal and long-term variations and long-range transports of tropospheric O_3 and its precursors based on past observations made at mountain sites. The main

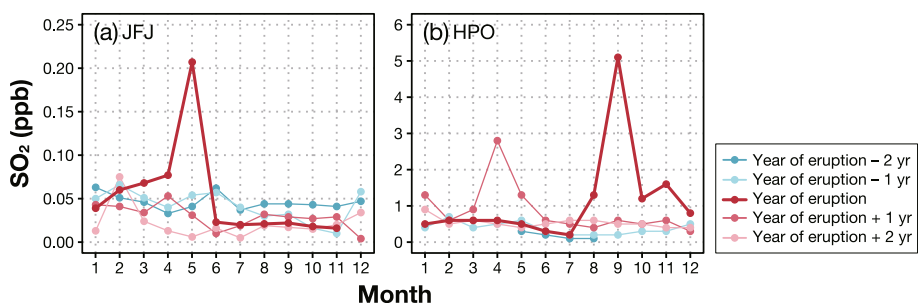

Fig. 11 Seasonal variations in SO_2 concentrations at two mountain stations. The *thick* and *thin lines with circles* denote the monthly average SO_2 in the year of the volcanic eruption and in the pre- and post-eruption years, respectively. The eruptions of Eyjafjallajökull volcano and Miyake-jima volcano occurred in 2010 (**a**) and in 2000 (**b**), respectively

recommendations for future atmospheric monitoring are summarized as follows:

1) Expanding the continuous measurements of trace species other than O_3 at high-altitude stations.

The observed species and temporal coverage differ among stations and research programs for which individual stations are operated. For example, O_3 and CO data are available, even though the data of other components are limited. Continuous measurements of NO_x and NMHCs are carried out mainly in Europe. For example, the number and mass concentrations, AOD, and visibility of aerosols have been reported extensively, but observations of their chemical properties are currently limited to high-altitude stations. Because of this bias in observations of aerosol parameters at high-altitude stations, it is still unfeasible to provide a regionally consistent summary on their long-term trends and seasonal variations. Accordingly, observations of trace species and parameters ancillary to tropospheric O_3 such as NO_x, SO_2, NMHCs, and aerosols should be increased in the future.

2) Expanding the global atmospheric observational capability through the establishment of high-altitude stations.

The geographical locations of the current high-altitude stations are not well distributed across the globe. Many are located in the northern mid-latitudes including North America, Europe, and Asia, and several are located in Africa. In contrast, few stations are located in Siberia, in spite of the importance of its role. In the Southern Hemisphere, there are severe data limitations because only a few sites are located in South America; and none are located in Oceania regions. Recently, two new stations were established in the South Hemisphere. One is located on Mt. Mäido, Réunion Island, which is a volcanic island located in the southwestern part of the Indian Ocean (Baray et al. 2013). The second is located in a high-altitude basin known as the Altiplano, Bolivia (Rose et al. 2015). Sofen et al. (2016) indicated that the current monitoring network of surface O_3 (including low-altitude stations) is insufficient for measurements in key regions (China, India, Amazon, Africa, tropical oceans, and Southern Ocean) and suggested the establishment of 20 possible sites (10 island and 10 continental). A strategy should be implemented to facilitate observations of key species in areas in which few observatories are located. It should also be noted that continuous observational data at mountain sites are useful for checking the consistency between sondes and regular aircraft, which cannot perform continuous ambient sampling (Tanimoto et al. 2015), when making globally consistent datasets for tropospheric species such as tropospheric O_3.

3) Building an objective and homogenous classification for assessment of the spatial representativeness of specific pollutants.

Remote mountainous sites are important because they are designed to provide representative data on continental to hemispheric scales and data for the lower FT. However, except for some European stations, most sites have never been assessed. In general, chemical species with strong surface sources or sinks, and with short atmospheric lifetimes due to photochemistry and deposition, show stronger spatial variability. Therefore, these species have smaller areas of representativeness than species with weak surface fluxes and long lifetimes. It is beneficial for any analysis, such as validation of satellite data, comparison of model outputs, and evaluation of long-term trends to consider the representativeness of atmospheric observational data.

4) Building a filtering method that can be applied to the observational data at baseline sites in the same way.

Filtered data are the most ideal for the analysis of long-term changes. Depending on the purpose, different filtering methods should be applied. For the estimation of "background" concentrations, the influences of local pollution (e.g., buoyant upslope flow) and long-range transport should be excluded, while for the estimation of "baseline" concentrations, only local pollution should be excluded. In most cases, unfiltered data have been used for trend analysis on regional or global scales because it is difficult to make determinations on baseline concentrations at individual stations (e.g., Logan et al. 2012; Parrish et al. 2012). The specifications of each observational site should be determined before handling the data, which primarily represent the regional and intercontinental scale concentrations. For example, Logan et al. (2012) confirmed that local influence was not of great concern for their analysis based on the amplitudes of diurnal variation and comparison to ozone sonde data. Meanwhile, Parrish et al. (2012) showed that the long-term trends derived from the unfiltered data were similar to those from filtered data analyzed by different methods at seven elevated sites including JFJ, ZUG/ZSF, and LAV, even though the trend for unfiltered data was different from that for filtered data at Mace Head, which receives air masses recirculated from the local continent. As the influences of local pollution levels were negligible, these two studies examined the trends for baseline concentrations. However, this does not mean that filtering is

unnecessary. Calculated trends for CO at JFJ for the period from 1996 to 2007 were different between background data (-2.65 ± 0.04 ppb year^{-1}; Zellweger et al. 2009) and unfiltered data (-3.36 ± 1.08 ppb year^{-1}; Gilge et al. 2010).

It is important to consider all of the above recommendations because observational data at remote sites can contribute to improvements in satellite observations, model simulations, and emission inventories. Observations at mountain sites have often been used for comparison with the outputs of global and regional chemistry-transport models when evaluating their performance levels. This tests our understanding of key processes and mechanisms in the troposphere such as the long-range transport of dust and biomass burning from the source regions, photochemistry in the FT, and the budget of reactive species. Although chemistry-transport models are useful for obtaining a better understanding of the mechanisms causing spatiotemporal variations in trace gases and aerosols, and for deriving their global/regional budget and assessing the impacts to human health and ecosystems, the current models still have limitations (e.g., Fiore et al. 2014). Disagreements between observation and model results might lead to improvements in existing models, although such guidance remains unclear. In addition, the role of mountain-based observations in filling the gap between the views from the ground and those from space should be enhanced in the future. Satellite observations have emerged as a useful technique for the long-term monitoring of tropospheric compositions of species such as O_3, CO, and NO_2 (e.g., Chehade et al. 2014; van der A et al. 2008; Worden et al. 2013). Its capability to make reliable observations in the FT has been demonstrated over the last decades. The spatial and temporal resolution of satellite observations has been improved in recent years, and the number of observable species has increased from basic chemical species such as O_3 and CO to other minor but important species such as NO_2, HCHO, and CH_3CN (Streets et al. 2013). It is important to expand the mountain-based platforms in a systematic manner to complement satellite observations, and thus to improve our understanding of the chemistry and dynamics in the FT.

The greatest advantage of models and satellite observations is their global coverage. However, this fact does not necessarily indicate a lack of interest in mountain-based observations. Indeed, observations in mountainous regions have several advantages. The uncertainty is significantly lower for in situ observations at mountainous sites than that for satellites. In addition, mountain-based observations have the capability to observe multiple components simultaneously with a higher time-resolution than is possible by satellites, and in most cases, those measurements are continuous. This advantage enables the capturing of occasional events as well as climatological features, which helps us to examine the chemical and physical processes in greater detail. Moreover, direct sampling for the analysis of ultra-trace components such as isotopes is possible at mountainous sites. Therefore, even though it is difficult to construct, operate, and maintain stations on remote mountains, the assistance they provide in tackling the above issues makes the effort and expense worthwhile.

Conclusions

Herein, we summarized the findings from past and ongoing field measurements and analyses of atmospheric constituents conducted at mountainous sites across the globe. Observations at mountain-based stations could provide representative data at continental to hemispheric scales and the lower FT. Many species in the FT have longer lifetimes than those in the PBL due to the lower temperatures and the lack of deposition in the FT. In addition, most of the transport of chemical species within the atmosphere occurs in the FT. The combination of long-range transport and longer chemical lifetimes indicate that the chemistry of the FT is important in determining the chemical compositions of regions remote from pollutant source regions. We identified observations at 31 mountain stations on the continents of Europe, North and South America, Eurasia, and Africa and islands in the Pacific, Indian, and Atlantic Oceans. These stations were selected because of their reliable observational data and because many previous studies have utilized these data. Furthermore, we adopted the stations located in regions in which few atmospheric observations have been conducted thus far, thereby covering the entire world, except for the Antarctic and the Arctic regions. Particular emphasis was placed on reactive species including tropospheric O_3 and its precursors such as CO, NO_x, NO_y, and NMHCs.

Numerous studies have shown that the tropospheric O_3 maximum occurs during spring in wide regions across the mid-latitudes in the Northern Hemisphere, including the remote islands in the North Pacific and North Atlantic Oceans. The seasonal cycle of O_3 at European stations has a minimum in winter and a broad maximum in spring–summer that represents a combination of a spring maximum with a secondary maximum in summer. This broad summer maximum is caused by enhanced regional pollution in Europe. Largely influenced by the Asian monsoon, the seasonal cycle of O_3 in the margin of East Asia and Himalayan region has a deep minimum in summer. In contrast, surface O_3 over the Qinghai–Tibetan Plateau and central Asia exhibits a summertime maximum. In North America, the seasonal cycle of O_3 shows a broad spring–summer peak or two peaks in spring and summer. The seasonal cycle of O_3 in Africa shows a minimum in boreal autumn and a broad maximum in boreal summer. In the Northern Hemisphere,

the mean concentration of O_3 and the amplitude of the seasonal cycle depend on latitude, with larger values at higher latitudes. The mean concentrations are ~50 ppb in Europe and 30 to 45 ppb in Africa. The tropical sites differ from other mid-latitude sites, with small variability shown over the course of the year. The seasonal amplitudes in East Asia and South Asia are substantially larger than those found at other stations, likely due to the intense photochemical production in spring and the Asian monsoon influence in summer.

In the Northern Hemisphere, the seasonal maximum and minimum for CO occur in late winter–early spring and in summer, respectively. The summer CO minimum is caused by the maximum occurrence of OH radicals, which are the main sink for CO in the troposphere. The CO maximum in late winter–early spring reflects the combined effects of the minimum in OH radical concentration and the enhancement of winter CO emissions. The maximum and minimum concentrations of CO and the amplitude of the CO seasonal cycle depend on latitude, with lower values found at higher altitudes. This indicates that the emission sources for CO are located at the ground surface. The means are between 120 and 180 ppb in Europe and Asia and 100 ppb in Africa. The maxima in East Asia are higher than those at other sites owing to intense springtime air pollution. The seasonal amplitude at the 15 stations falls into the range of 85 to 180 ppb, except for LLN in Taiwan. This large seasonal amplitude for CO can be attributed to the combination of a high spring maximum and summer low, at ~215 ppb, caused by the effect of the Asian monsoon and biomass burning activity in Southeast Asia.

Unlike O_3 and CO, NMHCs, NO_x, and NO_y have only been observed continuously at very few stations. The seasonal cycles of C_2H_6, C_2H_2, C_3H_8, and C_6H_6 in the Northern Hemisphere generally show a maximum in winter and a minimum in summer owing to reaction with the OH radical. The seasonal cycle at MKN in the equatorial region shows a different cycle with two minima and two maxima corresponding with the climate pattern in equatorial East Africa induced by the displacement of the ITCZ. Although NMHC concentration ratios are useful indicators of the degree of photochemical processing or aging (e.g., Helmig et al. 2008), such studies have been rarely conducted at mountainous sites. Generally, the amplitudes of the seasonal cycles of C_2H_6 and C_3H_8 depend on the latitude, with smaller amplitudes at the lower-latitude sites and higher amplitudes at the higher-latitude sites. The annual maximum concentrations of C_2H_6 and C_3H_8 at higher-altitude stations are higher than those at lower-altitude stations within each latitudinal band.

NO_y measurements show a broad spring and summer maximum, whereas NO_x shows a minimum during these seasons at SNB, ZUG, and JFJ. The seasonal cycle of NO_y at HPO show a spring and early summer maximum. The NO_x and NO_y concentrations are low on remote islands such as IZO and MLO. At MLO, the seasonal cycle of both NO_x and NO_y shows a spring maximum, but their concentrations are fairly invariant over the year, which implies that the partitioning of NO_y is almost steady state. NO_x observations at PMO exhibit a distinct seasonal cycle from July to October that is larger than those in other months, while NO_y observations exhibit a distinct seasonal cycle which is larger from June to September than from November to March, primarily due to boreal forest wildfires and more efficient export and transport from eastern North America. Despite the importance of the photochemistry of tropospheric O_3, continuous measurements of these species, which are precursors and by-products of O_3 photochemistry at high-altitude stations, are very limited.

The observations at European stations in the 1990s show increases in tropospheric O_3. The O_3 concentrations at these stations peak in the late 1990s or early 2000s before exhibiting a decreasing trend. The long-term trends for surface O_3 observed at SNB, ZUG/ZSF, and JFJ are 0.22 ± 0.17 ppb year^{-1} (1989–2007), 0.42 ± 0.09 ppb year^{-1} (1975–2007), and 0.26 ± 0.16 ppb year^{-1} (1986–2007), respectively. The mean rate of O_3 decrease at the seven European alpine sites including SNB, ZUG/ZSF, and JFJ for the period from 2000 to 2009 is -0.16 ± 0.14 ppb year^{-1}. In the North Atlantic, the surface O_3 record at IZO shows a slightly positive trend with a rate of 0.09 ± 0.02 ppb year^{-1} for the period from 1988 to 2009. In particular, a rapid increase is found between 1996 and 1998 that coincides with the phase shift of the NAO. In East Asia, a positive trend of surface O_3 at 0.25 ± 0.17 ppb year^{-1} is observed at WLG for the period from 1994 to 2013. Of particular note, the strongest increase is found in autumn. HPO in Japan experiences a generally large increase in spring O_3 of ~1 ppb year^{-1} for the period from 1998 to 2006. In the western USA, the mean spring O_3 at MBO shows a significant increase of 0.73 ± 0.54 ppb year^{-1} for the period from 2004 to 2013. At HPO and MBO, which are significantly influenced by East Asian outflow in spring, larger increasing trends in the levels of O_3 occur in higher percentiles than in lower percentile levels.

In the Northern Hemisphere, the CO levels observed at mountainous sites increase from the 1950s until the 1980s, and then decrease beginning in the late 1980s. The decreasing rate of the global mean CO concentrations was estimated to be -0.52 ± 0.10 ppb year^{-1} for the period from 1991 to 2001. The trend for CO at JFJ for the period from 1996 to

2007 is about −3 ppb year^{-1}. At MBO in the western USA, the mean spring CO shows a significant decrease for the period from 2004 to 2013, whereas the annual average CO did not show a significant trend. This result is consistent with satellite observations of total column CO, which show a continued decreasing trend from 2000 through 2011 in the Northern Hemisphere.

There are few long-term measurements of NO_y and NO_x at high-altitude stations. In European countries, NO_x emissions declined significantly in the early 1990s due to the mandated installation of catalytic converters in vehicles and other emission reduction measures. For the period from 1998 to 2002, the trend in NO_y was positive but not significant, whereas in the period 2004 to 2009, a significant decreasing tendency was observed at a rate of -0.048 ± 0.012 ppb year^{-1}. The overall annual averages of O_3 and NO_y were the highest in 2003, which was the hottest year in recorded European history due to an exceptional prolonged summer heat wave.

List of stations

ARO, Arosa
ASK, Assekrem
CHA, Chiricahua National Monument
CMN, Monte Cimone
FWS, Mt. Fuji
GRB, Great Basin National Park
HPO, Mt. Happo
ISK, Issyk-Kul
IZO, Izãna
JFJ, Jungfraujoch
KSL, Kislovodsk
KVV, Krvavec
LAV, Lassen Volcanic National Park
LLN, Lulin
LQO, La Quiaca Observatorio
MAB, Mt. Abu
MBO, Mt. Bachelor Observatory
MDY, Mondy
MKN, Mt. Kenya
MLO, Mauna Loa
NWR, Niwot Ridge
PMO, Pico Mountain Observatory
PYR, Nepal Climate Observatory–Pyramid
SNB, Sonnblick
TAR, Tanah Rata
WHI, Whistler Mountain
WLG, Mt. Walliguan
YEL, Yellowstone National Park
YOS, Yosemite National Park
ZSF, Zugspitze–Schneefernerhaus
ZUG, Zugspitze–Gipfel

Abbreviations

ABC: Atmospheric brown cloud; ACE-2: Second Aerosol Characterization Experiment; AEMET: Agencia Estatal de Meteorología; CASTNET: Clean Air Status and Trends Network; CLRTAP: Convention on Long-Range Transboundary Air Pollution; CMA: China Meteorological Administration; CONTRACE: Convective Transport of Trace Gases into the Middle and Upper Troposphere over Europe; DWD: German Weather Service (Deutscher Wetterdienst); EANET: Acid Deposition Monitoring Network in East Asia; ECMWF: European Centre for Medium-Range Weather Forecasts; EMEP: European Monitoring and Evaluation Programme; Empa: Swiss Federal Laboratories for Materials Science and Technology; EPA: US Environmental Protection Agency; ESRL: Earth System Research Laboratory; Ev-K2-CNR: Everest-K2 National Research Council; FOEN: Swiss Federal Office for the Environment; FREETEX: Free Tropospheric Experiments; GAW: Global Atmosphere Watch; GMD: Global Monitoring Division; HIS: Hydrometeorological Institute of Slovenia; ICARTT: International Consortium for Atmospheric Research on Transport and Transformation; IFA: Oboukhov Institute of Atmospheric Physics; IMPROVE: Interagency Monitoring of Protected Visual Environments; INTEX-B: Intercontinental Chemical Transport Experiment Phase B; ISAC-CNR: Institute of Atmospheric Sciences and Climate of the National Research Council of Italy; JMA: Japan Meteorological Agency; KMD: Kenya Meteorological Department; LTER: Long-Term Ecological Research; MINATROC: Mineral Dust and Tropospheric Chemistry; MLOPEX: Mauna Loa Observatory Photochemistry Experiment; MMD: Malaysian Meteorological Department; MOE: Ministry of the Environment (Japan); MONARPOP: Monitoring Network in the Alpine Region for Persistent and Other Organic Pollutants; NABEL: Swiss National Air Pollution Monitoring Network; NCU: National Central University; NOAA: National Oceanic and Atmospheric Administration; NPS: National Park Service; ONM: Déportent Météorologique Régional Sud of the Office National de la Météorologie; PSI: Paul Scherrer Institute; SHARE: Stations at High Altitude for Research on the Environment; SMNA: Servicio Meteorológico Nacional; TCCON: Total Column Carbon Observation Network; UBA: Federal Environmental Agency (Umweltbundesamt); UNEP: United Nations Environmental Programme; WACS 2010: Whistler Aerosol and Cloud Study 2010; WDCGG: World Data Centre for Greenhouse Gases; WMO: World Meteorological Organization

Acknowledgements

The authors thank the Acid Deposition Monitoring Network in East Asia (EANET, http://www.eanet.asia/), EBAS (http://ebas.nilu.no), the US Environmental Protection Agency Clean Air Markets Division Clean Air Status and Trends Network (CASTNET, http://www.epa.gov/castnet), the Interagency Monitoring of Protected Visual Environments (IMPROVE, http://vista.cira.colostate.edu/improve/), and the World Data Centre for Greenhouse Gases (WDCGG, http://ds.data.jma.go.jp/gmd/wdcgg/) for providing the observational data. The Office National de la Météorologie (ONM), Algeria and the Earth System Research Laboratory, NOAA (NOAA/ESRL) provided the Assekrem data. The Kenya Meteorological Department (KMD) provided the Mt. Kenya data. The Izana Atmospheric Research Center, Meteorological State Agency of Spain (AEMET) provided the Izaña data. The China Meteorological Administration (CMA) and NOAA/ESRL provided the Mt. Waliguan data. The Kyrgyz National University (KSNU) provided the Issyk-Kul data. The National Research Council, Institute of Atmospheric Sciences and Climate (ISAC) in collaboration with Department of Pure and Applied Science, University of Urbino, provided the Pyramid and Monte Cimone data. Prof. Neng-Huei Lin at the National Central University, which is managed by the Taiwan Environmental Protection Administration, provided the Lulin data. EANET provided the Mondy data. Dr. Manish Naja at the Aryabhatta Research Institute for Observational Sciences and Dr. Shyam Lal at the Physical Research Laboratory provided the Mt. Abu data. Dr. Shungo Kato at Tokyo Metropolitan University and EANET provided the Mt. Happo data. The National Weather Service (SMNA) provided the La Quiaca Observatorio data. Environment and Climate Change Canada provided the Whistler Mountain data. Dr. Dan Jaffe at the University of Washington provided the Mt. Bachelor Observatory data. NOAA/ESRL provided the Niwot Ridge and Mauna Loa data. CASTNET and IMPROVE provided the Chiricahua NM, Great Basin NP, Lassen Volcanic NP, Yellowstone NP, and Yosemite NP data. The Malaysian Meteorological Department (MMD) provided the Tanah Rata data. The Environment Agency Austria provided the Sonnblick data. The Federal Environmental Agency Germany provided the Zugspitze data. The Slovenian Environment Agency (ARSO) provided the Krvavec data. Swiss Federal Laboratories for Materials Testing and Research (Empa) and the Laboratory of Atmospheric Chemistry of the Paul Scherrer Institute (PSI) provided the Jungfraujoch data. The data at Pico Mountain Observatory were collected in a collaboration among Michigan

Technological University, the University of Colorado and NOAA/ESRL. The NMHC sampling at Assekrem, Mt. Kenya, Izaña, and Mauna Loa is a component of the NOAA Global Greenhouse Gas Reference Network, with NMHC in the collected whole air samples being analyzed by the Institute of Arctic and Alpine Research at the University of Colorado. The authors also thank Dr. Edit Nagy-Tanaka, Dr. Hajime Akimoto of the National Institute of Environmental Studies (NIES), along with the editor and anonymous reviewers for providing valuable comments.

Funding
Not applicable.

Authors' contributions
SO reviewed the literature data and conducted the experimental study. SO and HT proposed the topic, conceived, and then designed the study. Both authors have read and approved the final manuscript.

Competing interests
The authors declare that they have no competing interests.

Received: 20 November 2015 Accepted: 6 October 2016
Published online: 26 October 2016

References

Acid Deposition Monitoring Network in East Asia (EANET). http://www.eanet.asia/. Accessed 15 Jan 2016

Ahlm L, Shakya KM, Russell LM, Schroder JC, Wong JPS, Sjostedt SJ, Hayden KL, Liggio J, Wentzell JJB, Wiebe HA, Mihele C, Leaitch WR, Macdonald AM (2013) Temperature-dependent accumulation mode particle and cloud nuclei concentrations from biogenic sources during WACS 2010. Atmos Chem Phys 13:3393–3407. doi:10.5194/acp-13-3393-2013

Alastuey A, Querol X, Castillo S, Escudero M, Avila A, Cuevas E, Torres C, Romero P-M, Exposito F, García O, Diaz JP, Van Dingenen R, Putaud JP (2005) Characterisation of TSP and PM2.5 at Izaña and Sta. Cruz de Tenerife (Canary Islands, Spain) during a Saharan Dust Episode (July 2002). Atmos Environ 39:4715–4728. doi:10.1016/j.atmosenv.2005.04.018

Ambrose JL, Reidmiller DR, Jaffe DA (2011) Causes of high O_3 in the lower free troposphere over the Pacific Northwest as observed at the Mt. Bachelor Observatory. Atmos Environ 45:5302–5315. doi:10.1016/j.atmosenv.2011.06.056

Andreae MO, Merlet P (2001) Emission of trace gases and aerosols from biomass burning. Glob Biogeochem Cycles 15:955–966. doi:10.1029/2000GB001382

Andrews E, Ogren JA, Bonasoni P, Marinoni A, Cuevas E, Rodríguez S, Sun JY, Jaffe DA, Fischer EV, Baltensperger U, Weingartner E, Collaud Coen M, Sharma S, Macdonald AM, Leaitch WR, Lin N-H, Laj P, Arsov T, Kalapov I, Jefferson A, Sheridan P (2011) Climatology of aerosol radiative properties in the free troposphere. Atmos Res 102:365–393. doi:10.1016/j.atmosres.2011.08.017

Angelbratt J, Mellqvist J, Blumenstock T, Borsdorff T, Brohede S, Duchatelet P, Forster F, Hase F, Mahieu E, Murtagh D, Petersen AK, Schneider M, Sussmann R, Urban J (2011a) A new method to detect long term trends of methane (CH_4) and nitrous oxide (N_2O) total columns measured within the NDACC ground-based high resolution solar FTIR network. Atmos Chem Phys 11:6167–6183. doi:10.5194/acp-11-6167-2011

Angelbratt J, Mellqvist J, Simpson D, Jonson JE, Blumenstock T, Borsdorff T, Duchatelet P, Forster F, Hase F, Mahieu E, De Mazière M, Notholt J, Petersen AK, Raffalski U, Servais C, Sussmann R, Warneke T, Vigouroux C (2011b) Carbon monoxide (CO) and ethane (C_2H_6) trends from ground-based solar FTIR measurements at six European stations, comparison and sensitivity analysis with the EMEP model. Atmos Chem Phys 11:9253-9269. doi:10.5194/acp-11-9253-2011

Aref'ev VN, Semenov VK (1994) Spectral transparency of the atmosphere in the center of the European-Asian continent. Atmos Environ 28:997–999. doi:10.1016/1352-2310(94)90259-3

Aref'ev VN, Kamenogradskiy NY, Semyonov VK, Sinyakov VP (1995) Ozone and nitrogen dioxide in the atmosphere above the Northern Tien Shan. Izv Atmos Ocean Phys 31:15–20

Aref'ev VN, Kashin FV, Krasnosel'tsev AV, Semenov VK, Sinyakov VP (2008) Structure of time variations in the atmospheric transparency in Central Eurasia (Issyk Kul monitoring station). Izv Atmos Ocean Phys 44:615–620. doi:10.1134/S0001433808050071

Aref'ev VN, Kashin FV, Semenov VK, Sinyakov VP (2009) Variations in nitrogen dioxide in the atmosphere over central Eurasia (Issyk Kul monitoring station). Izv Atmos Ocean Phys 45:575–582. doi:10.1134/S0001433809050053

Aref'ev VN, Kashin FV, Orozaliev MD, Sizov NI, Sinyakov VP, Sorokina LI (2013) Structure of carbon monoxide time variations in the atmospheric thickness over central Eurasia (Issyk Kul monitoring station). Izv Atmos Ocean Phys 49:148–153. doi:10.1134/S0001433813020047

Arimoto R, Duce RA, Ray BJ, Ellis WG Jr, Cullen JD, Merrill JT (1995) Trace elements in the atmosphere over the North Atlantic. J Geophys Res 100:1199–1213. doi:10.1029/94JD02618

Armerding W, Comes FJ, Crawack HJ, Forberich O, Gold G, Ruger C, Spiekermann M, Walter J, Cuevas E, Redondas A, Schmitt R, Matuska P (1997) Testing the daytime oxidizing capacity of the troposphere: 1994 OH field campaign at the Izaña observatory, Tenerife. J Geophys Res 102:10603–10611. doi:10.1029/96JD03714

Assonov SS, Brenninkmeijer CAM, Schuck TJ, Taylor P (2010) Analysis of ^{13}C and ^{18}O isotope data of CO_2 in CARIBIC aircraft samples as tracers of upper troposphere/lower stratosphere mixing and the global carbon cycle. Atmos Chem Phys 10:8575–8599. doi:10.5194/acp-10-8575-2010

Atkinson R (2000) Atmospheric chemistry of VOCs and NO_x. Atmos Environ 34:2063–2101. doi:10.1016/s1352-2310(99)00460-4

Atkinson R, Arey J (2003) Atmospheric degradation of volatile organic compounds. Chem Rev 103:4605–4638. doi:10.1021/cr0206420

Atlas E, Ridley B, Walega J, Greenberg J, Kok G, Staffelbach T, Schauffler S, Lind J, Hübler G, Norton R, PEM-West Science Team GTE, Dlugokeneky E, Elkins J, Oltmans S, Mackay G, Karecki D (1996) A comparison of aircraft and ground-based measurements at Mauna Loa Observatory, Hawaii, during GTE PEM-West and MLOPEX 2. J Geophys Res 101:14599–14612. doi:10.1029/96JD00213

Balkanski Y, Bauer SE, Van Dingenen R, Bonasoni P, Schultz M, Fischer H, Gobbi GP, Hanke M, Hauglustaine D, Putaud JP, Stohl A, Raes F (2003) The Mt Cimone, Italy, free tropospheric campaign: principal characteristics of the gaseous and aerosol composition from European pollution, Mediterranean influences and during African dust events. Atmos Chem Phys Discuss 3:1753–1776. doi:10.5194/acpd-3-1753-2003

Baltensperger U, Gäggeler HW, Jost DT, Lugauer M, Schwikowski M, Weingartner E, Seibert P (1997) Aerosol climatology at the high-alpine site Jungfraujoch, Switzerland. J Geophys Res 102:19707–19715. doi:10.1029/97JD00928

Balzani Lööv JM, Henne S, Legreid G, Staehelin J, Reimann S, Prévôt ASH, Steinbacher M, Vollmer MK (2008) Estimation of background concentrations of trace gases at the Swiss Alpine site Jungfraujoch (3580 m asl). J Geophys Res 113:D22305. doi:10.1029/2007JD009751

Bândă N, Krol M, van Noije T, van Weele M, Williams JE, Le Sager P, Niemeier U, Thomason L, Röckmann T (2015) The effect of stratospheric sulfur from Mount Pinatubo on tropospheric oxidizing capacity and methane. J Geophys Res 120:1202–1220. doi:10.1002/2014JD022137

Baray J-L, Courcoux Y, Keckhut P, Portafaix T, Tulet P, Cammas J-P, Hauchecorne A, Godin Beekmann S, De Mazière M, Hermans C, Desmet F, Sellegri K, Colomb A, Ramonet M, Sciare J, Vuillemin C, Hoareau C, Dionisi D, Duflot V, Vérèmes H, Porteneuve J, Gabarrot F, Gaudo T, Metzger J-M, Payen G, Leclair de Bellevue J, Barthe C, Posny F, Ricaud P, Abchiche A et al (2013) Maïdo observatory: a new high-altitude station facility at Reunion Island (21°S, 55°E) for long-term atmospheric remote sensing and in situ measurements. Atmos Meas Tech 6:2865–2877. doi:10.5194/amt-6-2865-2013

Barret B, De Mazière M, Demoulin P (2002) Retrieval and characterization of ozone profiles from solar infrared spectra at the Jungfraujoch. J Geophys Res 107:4788. doi:10.1029/2001JD001298

Barret B, De Mazière M, Demoulin P (2003a) Correction to "Retrieval and characterization of ozone profiles from solar infrared spectra at the Jungfraujoch." J Geophys Res 108:4372. doi:10.1029/2003JD003809

Barret B, De Mazière M, Mahieu E (2003b) Ground-based FTIR measurements of CO from the Jungfraujoch: characterisation and comparison with in situ surface and MOPITT data. Atmos Chem Phys 3:2217-2223. doi:10.5194/acp-3-2217-2003

Bauer SE, Balkanski Y, Schulz M, Hauglustaine DA, Dentener F (2004) Global modeling of heterogeneous chemistry on mineral aerosol surfaces: influence on tropospheric ozone chemistry and comparison to observations. J Geophys Res 109:D02304. doi:10.1029/2003JD003868

Beeston M, Grgić I, van Elteren JT, Iskra I, Kapun G, Močnik G (2012) Chemical and morphological characterization of aerosol particles at Mt. Krvavec, Slovenia, during the Eyjafjallajökull Icelandic volcanic eruption. Environ Sci Pollut Res 19:235–243. doi:10.1007/s11356-011-0563-8

Bey I, Jacob DJ, Logan JA, Yantosca RM (2001) Asian chemical outflow to the Pacific in spring: Origins, pathways, and budgets. J Geophys Res 106:23097–23113. doi:10.1029/2001JD000806

Bianchi F, Tröstl J, Junninen H, Frege C, Henne S, Hoyle CR, Molteni U, Herrmann E, Adamov A, Bukowiecki N, Chen X, Duplissy J, Gysel M, Hutterli M, Kangasluoma J, Kontkanen J, Kürten A, Manninen HE, Münch S, Peräkylä O, Petäjä T, Rondo L, Williamson C, Weingartner E, Curtius J, Worsnop DR, Kulmala M, Dommen J,

Baltensperger U (2016) New particle formation in the free troposphere: a question of chemistry and timing. Science 26. doi:10.1126/science.aad5456.
Bodhaine BA (1995) Aerosol absorption measurements at Barrow, Mauna Loa and the south pole. J Geophys Res 100:8967–8975. doi:10.1029/95JD00513
Bollasina M, Bertolani L, Tartari G (2002) Meteorological observations at high altitude in the Khumbu Valley, Nepal Himalayas, 1994-1999. Bull Glaciol Res 19:1–11
Bonasoni P, Calzolari F, Colombo T, Corazza E, Santaguida R, Tesi G (1997) Continuous CO and H_2 measurements at Mt. Cimone (Italy): preliminary results. Atmos Environ 31:959–967. doi:10.1016/S1352-2310(96)00259-2
Bonasoni P, Evangelisti F, Bonafe U, Ravegnani F, Calzolari F, Stohl A, Tositti L, Tubertini O, Colombo T (2000a) Stratospheric ozone intrusion episodes recorded at Mt. Cimone during the VOTALP project: case studies. Atmos Environ 34:1355-1365. doi:10.1016/S1352-2310(99)00280-0
Bonasoni P, Stohl A, Cristofanelli P, Calzolari F, Colombo T, Evangelisti F (2000b) Background ozone variations at Mt. Cimone Station. Atmos Environ 34:5183-5189. doi:10.1016/S1352-2310(00)00268-5
Bonasoni P, Cristofanelli P, Calzolari F, Bonafè U, Evangelisti F, Stohl A, Zauli Sajani S, van Dingenen R, Colombo T, Balkanski Y (2004) Aerosol-ozone correlations during dust transport episodes. Atmos Chem Phys 4:1201–1215. doi:10.5194/acp-4-1201-2004
Bonasoni P, Laj P, Angelini F, Arduini J, Bonafè U, Calzolari F, Cristofanelli P, Decesari S, Facchini MC, Fuzzi S, Gobbi GP, Maione M, Marinoni A, Petzold A, Roccato F, Roger JC, Sellegri K, Sprenger M, Venzac H, Verza GP, Villani P, Vuillermoz E (2008) The ABC-Pyramid Atmospheric Research Observatory in Himalaya for aerosol, ozone and halocarbon measurements. Sci Total Environ 391:252–261. doi:10.1016/j.scitotenv.2007.10.024
Bonasoni P, Laj P, Marinoni A, Sprenger M, Angelini F, Arduini J, Bonafè U, Calzolari F, Colombo T, Decesari S, Di Biagio C, di Sarra AG, Evangelisti F, Duchi R, Facchini MC, Fuzzi S, Gobbi GP, Maione M, Panday A, Roccato F, Sellegri K, Venzac H, Verza GP, Villani P, Vuillermoz E, Cristofanelli P (2010) Atmospheric Brown Clouds in the Himalayas: first two years of continuous observations at the Nepal Climate Observatory-Pyramid (5079 m). Atmos Chem Phys 10:7515–7531. doi:10.5194/acp-10-7515-2010
Bond TC, Bhardwaj E, Dong R, Jogani R, Jung S, Roden C, Streets DG, Trautmann NM (2007) Historical emissions of black and organic carbon aerosol from energy-related combustion, 1850-2000. Glob Biogeochem Cycles 21:GB2018. doi:10.1029/2006GB002840
Bowman KW, Shindell DT, Worden HM, Lamarque JF, Young PJ, Stevenson DS, Qu Z, de la Torre M, Bergmann D, Cameron-Smith PJ, Collins WJ, Doherty R, Dalsøren SB, Faluvegi G, Folberth G, Horowitz LW, Josse BM, Lee YH, MacKenzie IA, Myhre G, Nagashima T, Naik V, Plummer DA, Rumbold ST, Skeie RB, Strode SA, Sudo K, Szopa S, Voulgarakis A, Zeng G et al (2013) Evaluation of ACCMIP outgoing longwave radiation from tropospheric ozone using TES satellite observations. Atmos Chem Phys 13:4057–4072. doi:10.5194/acp-13-4057-2013
Bracci A, Cristofanelli P, Sprenger M, Bonafé U, Calzolari F, Duchi R, Laj P, Marinoni A, Roccato F, Vuillermoz E, Bonasoni P (2012) Transport of stratospheric air masses to the Nepal Climate Observatory-Pyramid (Himalaya; 5079 m MSL): a synoptic-scale investigation. J Appl Meteorol 51:1489–1507. doi:10.1175/jamc-d-11-0154.1
Brasseur GP, Hauglustaine DA, Walters S (1996) Chemical compounds in the remote Pacific troposphere: comparison between MLOPEX measurements and chemical transport model calculations. J Geophys Res 101:14795–14813. doi:10.1029/95JD03520
Brönnimann S, Buchmann B, Wanner H (2002) Trends in near-surface ozone concentrations in Switzerland: the 1990s. Atmos Environ 36:2841–2852. doi:10.1016/S1352-2310(02)00145-0
Brönnimann S, Cain JC, Staehelin J, Farmer SFG (2003) Total ozone observations prior to the IGY. II: data and quality. Q J R Meteorol Soc 129:2819–2843. doi:10.1256/qj.02.145
Bukowiecki N, Zieger P, Weingartner E, Jurányi Z, Gysel M, Neininger B, Schneider B, Hueglin C, Ulrich A, Wichser A, Henne S, Brunner D, Kaegi R, Schwikowski M, Tobler L, Wienhold FG, Engel I, Buchmann B, Peter T, Baltensperger U (2011) Ground-based and airborne in-situ measurements of the Eyjafjallajökull volcanic aerosol plume in Switzerland in spring 2010. Atmos Chem Phys 11:10011–10030. doi:10.5194/acp-11-10011-2011
Bukowiecki N, Weingartner E, Gysel M, Collaud Coen M, Zieger P, Herrmann E, Steinbacher M, Gäggeler HW, Baltensperger U (2016) A review of more than 20 years of aerosol observation at the High Altitude Research Station Jungfraujoch, Switzerland (3580 m asl). Aerosol Air Qual Res 16:764–788. doi:10.4209/aaqr.2015.05.0305
Calvert JG (1990) Glossary of atmospheric chemistry terms. Pure Appl Chem 62:2167–2219. doi:10.1351/pac199062112167
Campana M, Li Y, Staehelin J, Prevot ASH, Bonasoni P, Loetscher H, Peter T (2005) The influence of south foehn on the ozone mixing ratios at the high alpine site Arosa. Atmos Environ 39:2945–2955. doi:10.1016/j.atmosenv.2005.01.037
Carslaw N, Plane JMC, Coe H, Cuevas E (1997) Observations of the nitrate radical in the free troposphere at Izaña de Tenerife. J Geophys Res 102:10613–10622. doi:10.1029/96JD03512
Chalbot M-C, Kavouras IG, Dubois DW (2013) Assessment of the contribution of wildfires to ozone concentrations in the central US-Mexico border region. Aerosol Air Qual Res 13:1–11. doi:10.4209/aaqr.2012.08.0232
Chameides W, Walker JCG (1973) A photochemical theory of tropospheric ozone. J Geophys Res 78:8751–8760. doi:10.1029/JC078i036p08751
Chang YS, Carmichael GR, Kurita H, Ueda H (1989) The transport and formation of photochemical oxidants in central Japan. Atmos Environ 23:363–393. doi:10.1016/0004-6981(89)90584-2
Chang S-S, Lee W-J, Wang L-C, Lin N-H, Chang-Chien G-P (2013) Influence of the Southeast Asian biomass burnings on the atmospheric persistent organic pollutants observed at near sources and receptor site. Atmos Environ 78:184–194. doi:10.1016/j.atmosenv.2012.07.074
Chehade W, Weber M, Burrows JP (2014) Total ozone trends and variability during 1979-2012 from merged data sets of various satellites. Atmos Chem Phys 14:7059–7074. doi:10.5194/acp-14-7059-2014
Chen S-C, Hsu S-C, Tsai C-J, Chou CC-K, Lin N-H, Lee C-T, Roam G-D, Pui DYH (2013) Dynamic variations of ultrafine, fine and coarse particles at the Lu-Lin background site in East Asia. Atmos Environ 78:154–162. doi:10.1016/j.atmosenv.2012.05.029
Cheng H, Zhang G, Jiang JX, Li X, Liu X, Li J, Zhao Y (2007) Organochlorine pesticides, polybrominated biphenyl ethers and lead isotopes during the spring time at the Waliguan Baseline Observatory, northwest China: implication for long-range atmospheric transport. Atmos Environ 41:4734–4747. doi:10.1016/j.atmosenv.2007.03.023
Cheng F-Y, Yang Z-M, Ou-Yang C-F, Ngan F (2013) A numerical study of the dependence of long-range transport of CO to a mountain station in Taiwan on synoptic weather patterns during the Southeast Asia biomass-burning season. Atmos Environ 78:277–290. doi:10.1016/j.atmosenv.2013.03.020
Chevalier A, Gheusi F, Delmas R, Ordóñez C, Sarrat C, Zbinden R, Thouret V, Athier G, Cousin J-M (2007) Influence of altitude on ozone levels and variability in the lower troposphere: a ground-based study for western Europe over the period 2001–2004. Atmos Chem Phys 7:4311–4326. doi:10.5194/acp-7-4311-2007
Chi KH, Lin C-Y, Ou Yang C-F, Wang J-L, Lin N-H, Sheu G-R, Lee C-T (2010) PCDD/F measurement at a high-altitude station in central Taiwan: evaluation of long-range transport of PCDD/Fs during the Southeast Asia biomass burning event. Environ Sci Technol 44:2954–2960. doi:10.1021/es1000984
Chiapello I, Prospero JM, Herman JR, Hsu NC (1999) Detection of mineral dust over the North Atlantic Ocean and Africa with the Nimbus 7 TOMS. J Geophys Res 104:9277–9291. doi:10.1029/1998JD200083
Chou C, Stetzer O, Weingartner E, Jurányi Z, Kanji ZA, Lohmann U (2011) Ice nuclei properties within a Saharan dust event at the Jungfraujoch in the Swiss Alps. Atmos Chem Phys 11:4725–4738. doi:10.5194/acp-11-4725-2011
Clarke AD, Charlson RJ (1985) Radiative properties of the background aerosol: absorption component of extinction. Science 229:263–265. doi:10.1126/science.229.4710.263
Collaud Coen M, Weingartner E, Schaub D, Hueglin C, Corrigan C, Schwikowski M, Baltensperger U (2004) Saharan dust events at the Jungfraujoch: detection by wavelength dependence of the single scattering albedo and first climatology analysis. Atmos Chem Phys 4:2465–2480. doi:10.5194/acp-4-2465-2004
Collaud Coen M, Weingartner E, Nyeki S, Cozic J, Henning S, Verheggen B, Gehrig R, Baltensperger U (2007) Long-term trend analysis of aerosol variables at the high-alpine site Jungfraujoch. J Geophys Res 112:D13213. doi:10.1029/2006JD007995
Collaud Coen M, Weingartner E, Furger M, Nyeki S, Prévôt ASH, Steinbacher M, Baltensperger U (2011) Aerosol climatology and planetary boundary influence at the Jungfraujoch analyzed by synoptic weather types. Atmos Chem Phys 11:5931–5944. doi:10.5194/acp-11-5931-2011
Collaud Coen M, Andrews E, Asmi A, Baltensperger U, Bukowiecki N, Day D, Fiebig M, Fjaeraa AM, Flentje H, Hyvärinen A, Jefferson A, Jennings SG, Kouvarakis G, Lihavainen H, Lund Myhre C, Malm WC, Mihapopoulos N, Molenar JV, O'Dowd C, Ogren JA, Schichtel BA, Sheridan P, Virkkula A, Weingartner E, Weller R, Laj P (2013) Aerosol decadal trends-Part 1: in-situ optical measurements at GAW and IMPROVE stations. Atmos Chem Phys 13:869–894. doi:10.5194/acp-13-869-2013
Comes FJ, Armerding W, Spiekermann M, Walter J, Rüger C (1995) Point measurements of tropospheric trace gases at Tenerife by a laser absorption technique. Atmos Environ 29:169–174. doi:10.1016/1352-2310(94)00254-I

Comes FJ, Forberich O, Walter J (1997) OH field measurements: a critical input into model calculations on atmospheric chemistry. J Atmos Sci 54:1886–1894. doi:10.1175/1520-0469(1997)054<1886:OFMACI>2.0.CO;2

Cooper OR, Forster C, Parrish D, Trainer M, Dunlea E, Ryerson T, Hüber G, Fehsenfeld F, Nicks D, Holloway J, de Gouw J, Warneke C, Roberts JM, Flocke F, Moody J (2004) A case study transpacific warm conveyor belt transport: Influence of merging airstreams on trace gas import to North America. J Geophys Res 109:D23S08. doi:10.1029/2003JD003624

Cooper OR, Parrish DD, Ziemke J, Balashov NV, Cupeiro M, Galbally IE, Gilge S, Horowitz L, Jensen NR, Lamarque J-F, Naik V, Oltmans SJ, Schwab J, Shindell DT, Thompson AM, Thouret V, Wang Y, Zbinden RM (2014) Global distribution and trends of tropospheric ozone: an observation-based review. Elem Sci Anth 2:000029–28. doi:10.12952/journal.elementa.000029

Cozic J, Verheggen B, Weingartner E, Crosier J, Bower KN, Flynn M, Coe H, Henning S, Steinbacher M, Henne S, Collaud Coen M, Petzold A, Baltensperger U (2008) Chemical composition of free tropospheric aerosol for PM1 and coarse mode at the high alpine site Jungfraujoch. Atmos Chem Phys 8:407–423. doi:10.5194/acp-8-407-2008

Cristofanelli P, Bonasoni P (2009) Background ozone in the southern Europe and Mediterranean area: influence of the transport processes. Environ Pollut 157:1399–1406. doi:10.1016/j.envpol.2008.09.017

Cristofanelli P, Bonasoni P, Tositti L, Bonafè U, Calzolari F, Evangelisti F, Sandrini S, Stohl A (2006) A 6-year analysis of stratospheric intrusions and their influence on ozone at Mt. Cimone (2165 m above sea level). J Geophys Res 111:D03306. doi:10.1029/2005JD006553

Cristofanelli P, Bonasoni P, Bonafé U, Calzolari F, Duchi R, Marinoni A, Roccato F, Vuillermoz E, Sprenger M (2009a) Influence of lower stratosphere/upper troposphere transport events on surface ozone at the Everest-Pyramid GAW Station (Nepal): first year of analysis. Int J Remote Sens 30:4083-4097. doi:10.1080/01431160902821940

Cristofanelli P, Marinoni A, Arduini J, Bonafè U, Calzolari F, Colombo T, Decesari S, Duchi R, Facchini MC, Fierli F, Finessi E, Maione M, Chiari M, Calzolari F, Messina P, Orlandi E, Roccato F, Bonasoni P (2009b) Significant variations of trace gas composition and aerosol properties at Mt. Cimone during air mass transport from North Africa—contributions from wildfire emissions and mineral dust. Atmos Chem Phys 9:4603-4619. doi:10.5194/acp-9-4603-2009

Cristofanelli P, Fierli F, Marinoni A, Calzolari F, Duchi R, Burkhart J, Stohl A, Maione M, Arduini J, Bonasoni P (2013) Influence of biomass burning and anthropogenic emissions on ozone, carbon monoxide and black carbon at the Mt. Cimone GAW-WMO global station (Italy, 2165 m a.s.l.). Atmos Chem Phys 13:15–30. doi:10.5194/acp-13-15-2013

Cristofanelli P, Scheel H-E, Steinbacher M, Saliba M, Azzopardi F, Ellul R, Fröhlich M, Tositti L, Brattich E, Maione M, Calzolari F, Duchi R, Landi TC, Marinoni A, Bonasoni P (2015) Long-term surface ozone variability at Mt. Cimone WMO/GAW global station (2165 m a.s.l., Italy). Atmos Environ 101:23–33. doi:10.1016/j.atmosenv.2014.11.012

Crutzen P (1974) A review of upper atmospheric photochemistry. Can J Chem 52:1569–1581. doi:10.1016/S0140-6736(00)88507-4

Cuevas E, González Y, Rodríguez S, Guerra JC, Gómez-Peláez AJ, Alonso-Pérez S, Bustos J, Milford C (2013) Assessment of atmospheric processes driving ozone variations in the subtropical North Atlantic free troposphere. Atmos Chem Phys 13:1973–1998. doi:10.5194/acp-13-1973-2013

Cui J, Sprenger M, Staehelin J, Siegrist A, Kunz M, Henne S, Steinbacher M (2009) Impact of stratospheric intrusions and intercontinental transport on ozone at Jungfraujoch in 2005: comparison and validation of two Lagrangian approaches. Atmos Chem Phys 9:3371–3383. doi:10.5194/acp-9-3371-2009

Cui J, Pandey Deolal S, Sprenger M, Henne S, Staehelin J, Steinbacher M, Nédélec P (2011) Free tropospheric ozone changes over Europe as observed at Jungfraujoch (1990-2008): an analysis based on backward trajectories. J Geophys Res 116:D10304. doi:10.1029/2010JD015154

Danielsen EF (1968) Stratospheric-tropospheric exchange based on radioactivity, ozone and potential vorticity. J Atmos Sci 25:502–518. doi:10.1175/1520-0469(1968)025<0502:STEBOR>2.0.CO;2

Darzi M, Winchester JW (1982) Aerosol characteristics at Mauna Loa Observatory, Hawaii, after East Asian dust storm episodes. J Geophys Res 87:1251–1258. doi:10.1029/JC087iC02p01251

De Mazière M, Van Roozendael M, Hermans C, Simon PC, Demoulin P, Roland G, Zander R (1998) Quantitative evaluation of the post-Mount Pinatubo NO_2 reduction and recovery, based on 10 years of Fourier transform infrared and UV-visible spectroscopic measurements at Jungfraujoch. J Geophys Res 103:10849–10858. doi:10.1029/97JD03362

De Mazière M, Hennen O, Van Roozendael M, Demoulin P, De Backer H (1999) Daily ozone vertical profile model built on geophysical grounds, for column retrieval from atmospheric high-resolution infrared spectra. J Geophys Res 104:23855–23869. doi:10.1029/1999JD900347

de Reus M, Fischer H, Sander R, Gros V, Kormann R, Salisbury G, Van Dingenen R, Williams J, Zöllner M, Lelieveld J (2005) Observations and model calculations of trace gas scavenging in a dense Saharan dust plume during MINATROC. Atmos Chem Phys 5:1787–1803. doi:10.5194/acp-5-1787-2005

Decesari S, Facchini MC, Carbone C, Giulianelli L, Rinaldi M, Finessi E, Fuzzi S, Marinoni A, Cristofanelli P, Duchi R, Bonasoni P, Vuillermoz E, Cozic J, Jaffrezo JL, Laj P (2010) Chemical composition of PM_{10} and PM_1 at the high-altitude Himalayan station Nepal Climate Observatory-Pyramid (NCO-P) (5079 m a.s.l.). Atmos Chem Phys 10:4583–4596. doi:10.5194/acp-10-4583-2010

Deshler T (2008) A review of global stratospheric aerosol: measurements, importance, life cycle, and local stratospheric aerosol. Atmos Res 90:223–232. doi:10.1016/j.atmosres.2008.03.016

Díaz AM, Díaz JP, Expósito FJ, Hernández-Leal PA, Savoie D, Querol X (2006) Air masses and aerosols chemical components in the free troposphere at the subtropical Northeast Atlantic region. J Atmos Chem 53:63–90. doi:10.1007/s10874-006-2644-5

Dils B, Cui J, Henne S, Mahieu E, Steinbacher M, De Mazière M (2011) 1997-2007 CO trend at the high Alpine site Jungfraujoch: a comparison between NDIR surface in situ and FTIR remote sensing observations. Atmos Chem Phys 11:6735–6748. doi:10.5194/acp-11-6735-2011

Ding A, Wang T (2006) Influence of stratosphere-to-troposphere exchange on the seasonal cycle of surface ozone at Mount Waliguan in western China. Geophys Res Lett 33:L03803. doi:10.1029/2005GL024760

Duchatelet P, Mahieu E, Ruhnke R, Feng W, Chipperfield M, Demoulin P, Bernath P, Boone CD, Walker KA, Servais C, Flock O (2009) An approach to retrieve information on the carbonyl fluoride (COF_2) vertical distributions above Jungfraujoch by FTIR multi-spectrum multi-window fitting. Atmos Chem Phys 9:9027–9042. doi:10.5194/acp-9-9027-2009

Duchatelet P, Demoulin P, Hase F, Ruhnke R, Feng W, Chipperfield MP, Bernath PF, Boone CD, Walker KA, Mahieu E (2010) Hydrogen fluoride total and partial column time series above the Jungfraujoch from long-term FTIR measurements: impact of the line-shape model, characterization of the error budget and seasonal cycle, and comparison with satellite and model data. J Geophys Res 115:D22306. doi:10.1029/2010JD014677

Duncan BN, Martin RV, Staudt AC, Yevich R, Logan JA (2003) Interannual and seasonal variability of biomass burning emissions constrained by satellite observations. J Geophys Res 108:4100. doi:10.1029/2002JD002378

Duncan BN, Logan JA, Bey I, Megretskaia IA, Yantosca RM, Novelli PC, Jones NB, Rinsland CP (2007) Global budget of CO, 1988-1997: source estimates and validation with a global model. J Geophys Res 112:D22301. doi:10.1029/2007JD008459

Duncan BN, West JJ, Yoshida Y, Fiore AM, Ziemke JR (2008) The influence of European pollution on ozone in the Near East and northern Africa. Atmos Chem Phys 8:2267–2283. doi:10.5194/acp-8-2267-2008

EBAS. http://ebas.nilu.no. Accessed 9 Feb 2016

Elansky NF, Arabov AY, Elokhov AS, Makarov OV, Savastyuk VV, Senik IA (1995) Observations of minor species and UV radiation in atmosphere at high-mountain scientific station Kislovodsk. Izv Atmos Ocean Phys 31:5–14

Fahey DW, Hübler G, Parrsich DD, Williams EJ, Norton RB, Ridley BA, Singh HB, Liu SC, Fehsenfeld FC (1986) Reactive nitrogen species in the troposphere: measurements of NO, NO_2, HNO_3, particulate nitrate, peroxyacetyl nitrate (PAN), O_3, and total reactive odd nitrogen (NO_y) at Niwot Ridge, Colorado. J Geophys Res 91:9781–9793. doi:10.1029/JD091iD09p09781

Fehsenfeld FC, Dickerson RR, Hübler G, Luke WT, Nunnermacker LJ, Williams EJ, Roberts JM, Calvert JG, Curran CM, Delany AC, Eubank CS, Fahey DW, Fried A, Gandrud BW, Langford AO, Murphy PC, Norton RB, Pickering KE, Ridley BA (1987) A ground-based intercomparison of NO, NO_x, and NO_y measurement techniques. J Geophys Res 92:14710–14722. doi:10.1029/jd092id12p14710

Fenneteaux I, Colin P, Etienne A, Boudries H, Dutot AL, Perros PE, Toupance G (1999) Influence of continental sources on oceanic air composition at the eastern edge of the North Atlantic Ocean, TOR 1992-1995. J Atmos Chem 32:233–280. doi:10.1023/A:1006140223711Fierz-Schmidhauser R, Zieger P, Gysel M, Kammermann L, DeCarlo PF, Baltensperger U, Weingartner E (2010) Measured and predicted aerosol light scattering enhancement factors at the high alpine site Jungfraujoch. Atmos Chem Phys 10:2319–2333. doi:10.5194/acp-10-2319-2010

Finley BD, Swartzendruber PC, Jaffe DA (2009) Particulate mercury emissions in regional wildfire plumes observed at the Mount Bachelor Observatory. Atmos Environ 43:6074–6083. doi:10.1016/j.atmosenv.2009.08.046

Fiore AM, Dentener FJ, Wild O, Cuvelier C, Schultz MG, Hess P, Textor C, Schulz M, Doherty RM, Horowitz LW, MacKenzie IA, Sanderson MG, Shindell DT, Stevenson DS, Szopa S, Van Dingenen R, Zeng G, Atherton C, Bergmann D, Bey I, Carmichael G, Collins WJ, Duncan BN, Faluvegi G, Folberth G, Gauss M, Gong S, Hauglustaine D, Holloway T, Isaksen ISA et al (2009) Multimodel estimates of intercontinental source-receptor relationships for ozone pollution. J Geophys Res 114:D04301–21. doi:10.1029/2008JD010816

Fiore AM, Oberman JT, Lin MY, Zhang L, Clifton OE, Jacob DJ, Naik V, Horowitz LW, Pinto JP, Milly GP (2014) Estimating North American background ozone in U.S. surface air with two independent global models: variability, uncertainties, and recommendations. Atmos Environ 96:284–300. doi:10.1016/j.atmosenv.2014.07.045

Fischer H, Kormann R, Klüpfel T, Gurk C, Königstedt R, Parchatka U, Mühle J, Rhee TS, Brenninkmeijer CAM, Bonasoni P, Stohl A (2003) Ozone production and trace gas correlations during the June 2000 MINATROC intensive measurement campaign at Mt. Cimone. Atmos Chem Phys 3:725–738. doi:10.5194/acp-3-725-2003

Fischer EV, Jaffe DA, Marley NA, Gaffney JS, Marchany-Rivera A (2010a) Optical properties of aged Asian aerosols observed over the U.S. Pacific Northwest. J Geophys Res 115:D20209. doi:10.1029/2010JD013943

Fischer EV, Jaffe DA, Reidmiller DR, Jaeglé L (2010b) Meteorological controls on observed peroxyacetyl nitrate at Mount Bachelor during the spring of 2008. J Geophys Res 115:D03302. doi:10.1029/2009JD012776

Flentje H, Claude H, Elste T, Gilge S, Köhler U, Plass-Dülmer C, Steinbrecht W, Thomas W, Werner A, Fricke W (2010) The Eyjafjallajökull eruption in April 2010—detection of volcanic plume using in-situ measurements, ozone sondes and lidar-ceilometer profiles. Atmos Chem Phys 10:10085–10092. doi:10.5194/acp-10-10085-2010

Folini D, Kaufmann P, Ubl S, Henne S (2009) Region of influence of 13 remote European measurement sites based on modeled carbon monoxide mixing ratios. J Geophys Res 114:D08307. doi:10.1029/2008JD011125

Forrer J, Rüttimann R, Schneiter D, Fischer A, Buchmann B, Hofer P (2000) Variability of trace gases at the high-Alpine site Jungfraujoch caused by meteorological transport processes. J Geophys Res 105:12241–12251. doi:10.1029/1999JD901178

Francis T (2012) Temporal trends in ambient SO_2 at a high altitude site in semi-arid western India: observations versus chemical transport modeling. J Environ Prot 03:657–680. doi:10.4236/jep.2012.37079

Fu XW, Feng X, Liang P, Deliger ZH, Ji J, Liu P (2012) Temporal trend and sources of speciated atmospheric mercury at Waliguan GAW station, Northwestern China. Atmos Chem Phys 12:1951–1964. doi:10.5194/acp-12-1951-2012

Furger M, Dommen J, Graber WK, Poggio L, Prévôt ASH, Emeis S, Grell G, Trickl T, Gomiscek B, Neininger B, Wotawa G (2000) The VOTALP Mesolcina Valley Campaign 1996-concept, background and some highlights. Atmos Environ 34:1395–1412. doi:10.1016/S1352-2310(99)00377-5

Gaiero DM, Simonella L, Gassó S, Gili S, Stein AF, Sosa P, Becchio R, Arce J, Marelli H (2013) Ground/satellite observations and atmospheric modeling of dust storms originating in the high Puna-Altiplano deserts (South America): implications for the interpretation of paleo-climatic archives. J Geophys Res 118:3817–3831. doi:10.1002/jgrd.50036

Gallagher JP, McKendry IG, Macdonald AM, Leaitch WR (2011) Seasonal and diurnal variations in aerosol concentration on Whistler Mountain: boundary layer influence and synoptic-scale controls. J Appl Meteorol Climatol 50:2210–2222. doi:10.1175/JAMC-D-11-028.1

Gallagher JP, McKendry IG, Strawbridge K, Macdonald AM, Leaitch WR, Cottle PW (2012) Application of lidar data to assist airmass discrimination at the Whistler Mountaintop Observatory. J Appl Meteorol Climatol 51:1733–1739. doi:10.1175/JAMC-D-12-067.1

García OE, Schneider M, Redondas A, González Y, Hase F, Blumenstock T, Sepúlveda E (2012) Investigating the long-term evolution of subtropical ozone profiles applying ground-based FTIR spectrometry. Atmos Meas Tech 5:2917–2931. doi:10.5194/amt-5-2917-2012

Garreaud R, Vuille M, Clement AC (2003) The climate of the Altiplano: observed current conditions and mechanisms of past changes. Palaeogeogr Palaeoclimatol Palaeoecol 194:5–22. doi:10.1016/S0031-0182(03)00269-4

Genualdi SA, Massey Simonich SL, Primbs TK, Bidleman TF, Jantunen LM, Ryoo K-S, Zhu T (2009) Enantiomeric signatures of organochlorine pesticides in Asian, trans-Pacific, and western U.S. air masses. Environ Sci Technol 43:2806–2811. doi:10.1021/es803402q

Gil M, Puentedura O, Yela M, Cuevas E (2000) Behavior of NO_2 and O_3 columns during the eclipse of February 26, 1998, as measured by visible spectroscopy. J Geophys Res 105:3583–3593. doi:10.1029/1999JD900973

Gil M, Yela M, Gunn LN, Richter A, Alonso I, Chipperfield MP, Cuevas E, Iglesias J, Navarro M, Puentedura O, Rodríguez S (2008) NO_2 climatology in the northern subtropical region: diurnal, seasonal and interannual variability. Atmos Chem Phys 8:1635–1648. doi:10.5194/acp-8-1635-2008

Gilge S, Plass-Duelmer C, Fricke W, Kaiser A, Ries L, Buchmann B, Steinbacher M (2010) Ozone, carbon monoxide and nitrogen oxides time series at four alpine GAW mountain stations in central Europe. Atmos Chem Phys 10:12295–12316. doi:10.5194/acp-10-12295-2010

Ginoux P, Prospero JM, Torres O, Chin M (2004) Long-term simulation of global dust distribution with the GOCART model: correlation with North Atlantic Oscillation. Environ Model Softw 19:113–128. doi:10.1016/S1364-8152(03)00114-2

Gobbi GP, Barnaba F, Van Dingenen R, Putaud JP, Mircea M, Facchini MC (2003) Lidar and in situ observations of continental and Saharan aerosol: closure analysis of particles optical and physical properties. Atmos Chem Phys 3:2161–2172. doi:10.5194/acp-3-2161-2003

Gobbi GP, Angelini F, Bonasoni P, Verza GP, Marinoni A, Barnaba F (2010) Sunphotometry of the 2006–2007 aerosol optical/radiative properties at the Himalayan Nepal Climate Observatory-Pyramid (5079 m a.s.l.). Atmos Chem Phys 10:11209–11221. doi:10.5194/acp-10-11209-2010

Gomez-Pelaez AJ, Ramos R, Gomez-Trueba V, Novelli PC, Campo-Hernandez R (2013) A statistical approach to quantify uncertainty in carbon monoxide measurements at the Izaña global GAW station: 2008–2011. Atmos Meas Tech 6:787–799. doi:10.5194/amt-6-787-2013

Gratz LE, Jaffe DA, Hee JR (2015) Causes of increasing ozone and decreasing carbon monoxide in springtime at the Mt. Bachelor Observatory from 2004 to 2013. Atmos Environ 109:323–330. doi:10.1016/j.atmosenv.2014.05.076

Graustein WC, Turekian KK (1996) ^{7}Be and ^{210}Pb indicate an upper troposphere source for elevated ozone in the summertime subtropical free troposphere of the eastern North Atlantic. Geophys Res Lett 23:539–542. doi:10.1029/96GL00304

Greally BR, Manning AJ, Reimann S, McCulloch A, Huang J, Dunse BL, Simmonds PG, Prinn RG, Fraser PJ, Cunnold DM, O'Doherty S, Porter LW, Stemmler K, Vollmer MK, Lunder CR, Schmidbauer N, Hermansen O, Arduini J, Salameh PK, Krummel PB, Wang RHJ, Folini D, Weiss RF, Maione M, Nickless G, Stordal F, Derwent RG (2007) Observations of 1,1-difluoroethane (HFC-152a) at AGAGE and SOGE monitoring stations in 1994-2004 and derived global and regional emission estimates. J Geophys Res 112:D06308. doi:10.1029/2006JD007527

Greenberg JP, Helmig D, Zimmerman PR (1996) Seasonal measurements of nonmethane hydrocarbons and carbon monoxide at the Mauna Loa Observatory during the Mauna Loa Observatory Photochemistry Experiment 2. J Geophys Res 101:14581–14598. doi:10.1029/95JD01543

Gros V, Bräunlich M, Röckmann T, Jöckel P, Bergamaschi P, Brenninkmeijer CAM, Rom W, Kutschera W, Kaiser A, Scheel HE, Mandl M, van der Plicht J, Possnert G (2001) Detailed analysis of the isotopic composition of CO and characterization of the air masses arriving at Mount Sonnblick (Austrian Alps). J Geophys Res 106:3179–3193. doi:10.1029/2000JD900509

Guerova G, Bey I, Attié J-L, Martin RV, Cui J, Sprenger M (2006) Impact of transatlantic transport episodes on summertime ozone in Europe. Atmos Chem Phys 6:2057–2072. doi:10.5194/acp-6-2057-2006

Haagen-Smit AJ (1952) Chemistry and physiology of Los Angeles smog. Ind Eng Chem 44:1342–1346. doi:10.1021/ie50510a045

Haagenson PL (1979) Meteorological and climatological factors affecting Denver air quality. Atmos Environ 13:79–85. doi:10.1016/0004-6981(79)90247-6

Hahn CJ (1981) A study of the diurnal behavior of boundary-layer winds at the Boulder Atmospheric Observatory. Boundary-Layer Meteorol 21:231–245. doi:10.1007/BF02033941

Hahn CJ, Merrill JT, Mendonca BG (1992) Meteorological influences during MLOPEX. J Geophys Res 97:10291–10309. doi:10.1029/91JD02299

Hanisch F, Crowley JN (2003) Ozone decomposition on Saharan dust: an experimental investigation. Atmos Chem Phys 11:119–130. doi:10.5194/acp-3-119-2003

Hanke M, Umann B, Uecker J, Arnold F, Bunz H (2003) Atmospheric measurements of gas-phase HNO_3 and SO_2 using chemical ionization mass spectrometry during the MINATROC field campaign 2000 on Monte Cimone. Atmos Chem Phys 3:417–436. doi:10.5194/acp-3-417-2003

Hauglustaine DA, Madronich S, Ridley BA, Flocke SJ, Cantrell CA, Eisele FL, Shetter RE, Tanner DJ, Ginoux P, Atlas EL (1999) Photochemistry and budget of ozone during the Mauna Loa Observatory Photochemistry Experiment (MLOPEX 2). J Geophys Res 104:30275–30307. doi:10.1029/91JD02298

Heikkilä U, Beer J, Alfimov V (2008) Beryllium-10 and beryllium-7 in precipitation in Dübendorf (440 m) and at Jungfraujoch (3580 m), Switzerland (1998–2005). J Geophys Res 113:D11104. doi:10.1029/2007JD009160

Helmig D, Tanner DM, Honrath RE, Owen RC, Parrish DD (2008) Nonmethane hydrocarbons at Pico Mountain, Azores: 1. Oxidation chemistry in the North Atlantic region. J Geophys Res 113:D20S91. doi:10.1029/2007JD008930

Helmig D, Muñoz M, Hueber J, Mazzoleni C, Mazzoleni L, Owen RC, Val-Martin M, Fialho P, Plass-Duelmer C, Palmer PI Lewis AC, Pfister G (2015) Climatology and atmospheric chemistry of the non-methane hydrocarbons ethane and propane over the North Atlantic. Elem Sci Anth 3:000054. doi:10.12952/journal.elementa.000054

Hemispheric Transport of Air Pollution (2007) Hemispheric Transport of Air Pollution 2007, Air Pollution Studies No. 16. United Nations, New York and Geneva

Henne S, Furger M, Nyeki S, Steinbacher M, Neininger B, de Wekker SFJ, Dommen J, Spichtinger N, Stohl A, Prévôt ASH (2004) Quantification of topographic venting of boundary layer air to the free troposphere. Atmos Chem Phys 4:497–509. doi:10.5194/acp-4-497-2004

Henne S, Furger M, Prévôt ASH (2005) Climatology of mountain venting-induced elevated moisture layers in the lee of the Alps. J Appl Meteorol 44:620–633. doi:10.1175/JAM2217.1

Henne S, Klausen J, Junkermann W, Kariuki JM, Aseyo JO, Buchmann B (2008) Representativeness and climatology of carbon monoxide and ozone at the global GAW station Mt. Kenya in equatorial Africa. Atmos Chem Phys 8:3119–3139. doi:10.5194/acp-8-3119-2008

Henne S, Brunner D, Folini D, Solberg S, Klausen J, Buchmann B (2010) Assessment of parameters describing representativeness of air quality in-situ measurement sites. Atmos Chem Phys 10:3561–3581. doi:10.5194/acp-10-3561-2010

Henning S, Weingartner E, Schwikowski M, Gäggeler HW, Gehrig R, Hinz K-P, Trimborn A, Spengler B, Baltensperger U (2003) Seasonal variation of water-soluble ions of the aerosol at the high-alpine site Jungfraujoch (3580 m asl). J Geophys Res 108:4030. doi:10.1029/2002JD002439

Hoegger B, Levrat G, Staehelin J, Schill H, Ribordy P (1992) Recent developments of the Light Climatic Observatory-ozone measuring station of the Swiss Meteorological Institute (LKO) at Arosa. J Atmos Terr Phys 54:497–505. doi:10.1016/0021-9169(92)90093-Z

Hoerling MP, Schaack TK, Lenzen AJ (1991) Global objective tropopause analysis. Mon Weather Rev 119:1816–1831. doi:10.1175/1520-0493(1991)119<1816:GOTA>2.0.CO;2

Holmes J, Zoller W (1996) The elemental signature of transported Asian dust at Mauna Loa observatory. Tellus B 48:83–92. doi:10.3402/tellusb.v48i1.15669

Holzinger R, Kasper-Giebl A, Staudinger M, Schauer G, Röckmann T (2010) Analysis of the chemical composition of organic aerosol at the Mt. Sonnblick observatory using a novel high mass resolution thermal-desorption proton-transfer-reaction mass-spectrometer (hr-TD-PTR-MS). Atmos Chem Phys 10:10111–10128. doi:10.5194/acp-10-10111-2010

Honrath RE, Owen RC, Val Martín M, Reid JS, Lapina K, Fialho P, Dziobak MP, Kleissl J, Westphal DL (2004) Regional and hemispheric impacts of anthropogenic and biomass burning emissions on summertime CO and O_3 in the North Atlantic lower free troposphere. J Geophys Res 109:D24310. doi:10.1029/2004JD005147

Honrath RE, Helmig D, Owen RC, Parrish DD, Tanner DM (2008) Nonmethane hydrocarbons at Pico Mountain, Azores: 2. Event-specific analyses of the impacts of mixing and photochemistry on hydrocarbon ratios. J Geophys Res 113:D20S92. doi:10.1029/2008JD009832

Hoyle CR, Webster CS, Rieder HE, Nenes A, Hammer E, Herrmann E, Gysel M, Bukowiecki N, Weingartner E, Steinbacher M, Baltensperger U (2016) Chemical and physical influences on aerosol activation in liquid clouds: a study based on observations from the Jungfraujoch, Switzerland. Atmos Chem Phys 16:4043–4061. doi:10.5194/acp-16-4043-2016

Huebert BJ, Phillips CA, Zhuang L, Kjellström E, Rodhe H, Feichter J, Land C (2001) Long-term measurements of free-tropospheric sulfate at Mauna Loa: comparison with global model simulations. J Geophys Res 106:5479–5492. doi:10.1029/2000JD900627

Huntrieser H, Heland J, Schlager H, Forster C, Stohl A, Aufmhoff H, Arnold F, Scheel HE, Campana M, Gilge S, Eixmann R, Cooper O (2005) Intercontinental air pollution transport from North America to Europe: experimental evidence from airborne measurements and surface observations. J Geophys Res 110:D01305. doi:10.1029/2004JD005045

Hyslop NP, Trzepla K, Wallis CD, Matzoll AK, White WH (2013) Technical note: a 23-year record of twice-weekly aerosol composition measurements at Mauna Loa Observatory. Atmos Environ 80:259–263. doi:10.1016/j.atmosenv.2013.07.038

Igarashi Y, Sawa Y, Yoshida K, Matsueda H, Fujii K, Dokiya Y (2004) Monitoring the SO_2 concentration at the summit of Mt. Fuji and a comparison with other trace gases during winter. J Geophys Res 109:D17304. doi:10.1029/2003JD004428

Igarashi Y, Sawa Y, Yoshioka K, Takahashi H, Matsueda H, Dokiya Y (2006) Seasonal variations in SO_2 plume transport over Japan: observations at the summit of Mt. Fuji from winter to summer. Atmos Environ 40:7018–7033. doi:10.1016/j.atmosenv.2006.06.017

Interagency Monitoring of Protected Visual Environments (IMPROVE). http://vista.cira.colostate.edu/improve/. Accessed 8 Feb 2016

Intergovermental Panel on Climate Change (2013) Climate Change 2013: The Physical Science Basis, Working Group I Contribution to the Fifth Assesment Report of the Intergovermental Panel on Climate Change. Cambridge University Press, Cambridge

Ionov DV, Timofeyev YM, Sinyakov VP, Semenov VK, Goutail F, Pommereau J-P, Bucsela EJ, Celarier EA, Kroon M (2008) Ground-based validation of EOS-Aura OMI NO_2 vertical column data in the midlatitude mountain ranges of Tien Shan (Kyrgyzstan) and Alps (France). J Geophys Res 113:D15S08. doi:10.1029/2007JD008659

Iwasaka Y, Minoura H, Nagaya K (1983) The transport and spacial scale of Asian dust-storm clouds: a case study of the dust-storm event of April 1979. Tellus B 35:189–196. doi:10.1111/j.1600-0889.1983.tb00023.x

Jabbar T, Steier P, Wallner G, Priller A, Kandler N, Kaiser A (2012) Iodine isotopes (^{127}I and ^{129}I) in aerosols at high altitude Alp stations. Environ Sci Technol 46:8637–8644. doi:10.1021/es300948t

Jaffe D (2011) Relationship between surface and free tropospheric ozone in the western U.S. Environ Sci Technol 45:432–438. doi:10.1021/es1028102

Jaffe D, Ray J (2007) Increase in surface ozone at rural sites in the western US. Atmos Environ 41:5452–5463. doi:10.1016/j.atmosenv.2007.02.034

Jaffe D, Mahura A, Kelley J, Atkins J, Novelli PC, Merrill J (1997) Impact of Asian emissions on the remote North Pacific atmosphere: Interpretation of CO data from Shemya, Guam, Midway and Mauna Loa. J Geophys Res 102:28627–28635. doi:10.1029/96JD02750

Jaffe D, McKendry I, Anderson T, Price H (2003a) Six "new" episodes of trans-Pacific transport of air pollutants. Atmospheric Environment 37:391-404. doi:10.1016/s1352-2310(02)00862-2

Jaffe D, Price H, Parrish D, Goldstein A, Harris J (2003b) Increasing background ozone during spring on the west coast of North America. Geophys Res Lett 30:1613. doi:10.1029/2003gl017024

Jaffe D, Prestbo E, Swartzendruber P, Weiss-Penzias P, Kato S, Takami A, Hatakeyama S, Kajii Y (2005) Export of atmospheric mercury from Asia. Atmos Environ 39:3029–3038. doi:10.1016/j.atmosenv.2005.01.030

Jaffe D, Chand D, Hafner W, Westerling A, Spracklen D (2008) Influence of fires on O_3 concentrations in the western U.S. Environ Sci Technol 42:5885–5891. doi:10.1021/es800084k

Joly M, Peuch V-H (2012) Objective classification of air quality monitoring sites over Europe. Atmos Environ 47:111–123. doi:10.1016/j.atmosenv.2011.11.025

Jonson JE, Stohl A, Fiore AM, Hess P, Szopa S, Wild O, Zeng G, Dentener FJ, Lupu A, Schultz MG, Duncan BN, Sudo K, Wind P, Schulz M, Marmer E, Cuvelier C, Keating T, Zuber A, Valdebenito A, Dorokhov V, De Backer H, Davies J, Chen GH, Johnson B, Tarasick DW, Stübi R, Newchurch MJ, von der Gathen P, Steinbrecht W, Claude H (2010) A multi-model analysis of vertical ozone profiles. Atmos Chem Phys 10:5759–5783. doi:10.5194/acp-10-5759-2010

Junge CE (1962) Global ozone budget and exchange between stratosphere and troposphere. Tellus 14:363–377. doi:10.3402/tellusa.v14i4.9563

Kaiser A (2009) Origin of polluted air masses in the Alps. An overview and first results for MONARPOP. Environ Pollut 157:3232–3237. doi:10.1016/j.envpol.2009.05.042

Kaiser A, Scheifinger H, Spangl W, Weiss A, Gilge S, Fricke W, Ries L, Cemas D, Jesenovec B (2007) Transport of nitrogen oxides, carbon monoxide and ozone to the Alpine Global Atmosphere Watch stations Jungfraujoch (Switzerland), Zugspitze and Hohenpeissenberg (Germany), Sonnblick (Austria) and Mt. Krvavec (Slovenia). Atmos Environ 41:9273–9287. doi:10.1016/j.atmosenv.2007.09.027

Kajii Y, Someno K, Tanimoto H, Hirokawa J, Akimoto H, Katsuno T, Kawara J (1998) Evidence for the seasonal variation of photochemical activity of tropospheric ozone: continuous observation of ozone and CO at Happo, Japan. Geophys Res Lett 25:3505–3508. doi:10.1029/98GL02602

Kajino M, Ueda H, Satsumabayashi H, An J (2004) Impacts of the eruption of Miyakejima Volcano on air quality over far east Asia. J Geophys Res 109: D21204. doi:10.1029/2004JD004762

Kajino M, Ueda H, Satsumabayashi H, Han Z (2005) Increase in nitrate and chloride deposition in east Asia due to increased sulfate associated with the eruption of Miyakejima Volcano. J Geophys Res 110:D18203. doi:10.1029/2005JD005879

Kanakidou M, Crutzen PJ (1999) The photochemical source of carbon monoxide: importance, uncertainties and feedbacks. Chemosphere 1:91–109. doi:10.1016/S1465-9972(99)00022-7

Kanakidou M, Mihalopoulos N, Kindap T, Im U, Vrekoussis M, Gerasopoulos E, Dermitzaki E, Unal A, Koçak M, Markakis K, Melas D, Kouvarakis G, Youssef AF, Richter A, Hatzianastassiou N, Hilboll A, Ebojie F, Wittrock F, von Savigny C,

Burrows JP, Ladstaetter-Weissenmayer A, Moubasher H (2011) Megacities as hot spots of air pollution in the East Mediterranean. Atmos Environ 45:1223–1235. doi:10.1016/j.atmosenv.2010.11.048

Kandler K, Benker N, Bundke U, Cuevas E, Ebert M, Knippertz P, Rodríguez S, Schütz L, Weinbruch S (2007) Chemical composition and complex refractive index of Saharan Mineral Dust at Izaña, Tenerife (Spain) derived by electron microscopy. Atmos Environ 41:8058–8074. doi:10.1016/j.atmosenv.2007.06.047

Kaneyasu N, Igarashi Y, Sawa Y, Takahashi H, Takada H, Kumata H, Höller R (2007) Chemical and optical properties of 2003 Siberian forest fire smoke observed at the summit of Mt. Fuji, Japan. J Geophys Res Atmos 112:D13214. doi:10.1029/2007JD008544

Karl T, Crutzen PJ, Mandl M, Staudinger M, Guenther A, Jordan A, Fall R, Lindinger W (2001a) Variability-lifetime relationship of VOCs observed at the Sonnblick Observatory 1999—estimation of HO-densities. Atmos Environ 35:5287-5300. doi:10.1016/S1352-2310(01)00341-7

Karl T, Fall R, Crutzen PJ, Jordan A, Lindinger W (2001b) High concentrations of reactive biogenic VOCs at a high altitude site in late autumn. Geophys Res Lett 28:507-510. doi:10.1029/2000GL012255

Karl T, Hansel A, Märk T, Lindinger W, Hoffmann D (2003) Trace gas monitoring at the Mauna Loa Baseline Observatory using Proton-Transfer Reaction Mass Spectrometry. Int J Mass Spectrom 223–224:527–538. doi:10.1016/S1387-3806(02)00874-6

Kashin FV, Aref'ev VN, Kamenogradskii NE, Semenov VK, Sinyakov VP (2007) Carbon dioxide content in the atmospheric thickness over central Eurasia (Issyk Kul Monitoring Station). Izv Atmos Ocean Phys 43:480–489. doi:10.1134/S0001433807040093

Kashin FV, Aref'ev VN, Semenov VK, Sinyakov VP, Upenek LB (2008) Structure of time variations in carbon dioxide in the atmospheric thickness over central Eurasia (Issyk Kul Monitoring Station). Izv Atmos Ocean Phys 44:94–103. doi:10.1134/S0001433808010106

Kasper A, Puxbaum H (1998) Seasonal variation of SO_2, HNO_3, NH_3 and selected aerosol components at Sonnblick (3106 m a.s.l.). Atmos Environ 32:3925–3939. doi:10.1016/S1352-2310(97)00031-9

Kato S, Kajii Y, Akimoto H, Bräunlich M, Röckmann T, Brenninkmeijer CAM (2000) Observed and modeled seasonal variations of ^{13}C, ^{18}O, and ^{14}C of atmospheric CO at Happo, a remote site in Japan, and a comparison with other records. J Geophys Res 105:8891–8900. doi:10.1029/1999JD901144

Kato S, Pochanart P, Hirokawa J, Kajii Y, Akimoto H, Ozaki Y, Obi K, Katsuno T, Streets DG, Minko NP (2002) The influence of Siberian forest fires on carbon monoxide concentrations at Happo, Japan. Atmos Environ 36:385–390. doi:10.1016/S1352-2310(01)00158-3

Keeling CD, Whorf TP, Wahlen M, van der Plicht J (1995) Interannual extremes in the rate of rise of atmospheric carbon dioxide since 1980. Nature 375:666–670. doi:10.1038/375666a0

Kentarchos AS, Roelofs GJ, Lelieveld J, Cuevas E (2000) On the origin of elevated surface ozone concentrations at Izana Observatory, Tenerife during late March 1996. Geophys Res Lett 27:3699–3702. doi:10.1029/2000GL011518

Khalil MAK, Rasmussen RA (1994) Global decrease in atmospheric carbon monoxide concentration. Nature 370:639–641. doi:10.1038/370639a0

Kivekäs N, Sun J, Zhan M, Kerminen V-M, Hyvärinen A, Komppula M, Viisanen Y, Hong N, Zhang Y, Kulmala M, Zhang X-C, Deli-Geer, Lihavainen H (2009) Long term particle size distribution measurements at Mount Waliguan, a high-altitude site in inland China. Atmos Chem Phys 9:5461–5474. doi:10.5194/acp-9-5461-2009

Kleissl J, Honrath RE, Dziobak MP, Tanner D, Val Martín M, Owen RC, Helmig D (2007) Occurrence of upslope flows at the Pico mountaintop observatory: a case study of orographic flows on a small, volcanic island. J Geophys Res 112:D10S35. doi:10.1029/2006JD007565

Klock R, Mullock J (2001) The weather of British Columbia: graphic area forecast 31. NAV Canada, Ottawa

Koch D, Rind D (1998) Beryllium 10/beryllium 7 as a tracer of stratospheric transport. J Geophys Res 103:3907–3917. doi:10.1029/97JD03117

Kovač-Andrić E, Šorgo G, Kezele N, Cvitaš T, Klasinc L (2010) Photochemical pollution indicators—an analysis of 12 European monitoring stations. Environ Monit Assess 165:577–583. doi:10.1007/s10661-009-0969-7

Krieg J, Nothholt J, Mahieu E, Rinsland CP, Zander R (2005) Sulphur hexafluoride (SF_6): comparison of FTIR-measurements at three sites and determination of its trend in the northern hemisphere. J Quant Spectrosc Radiat Transf 92:383–392. doi:10.1016/j.jqsrt.2004.08.005

Krzyścin JW (2000) Total ozone influence on the surface UV-B radiation in the late spring-summer 1963-1997: an analysis of multiple timescales. J Geophys Res 105:4993–5000. doi:10.1029/1999JD900265

Kuebler J, van den Bergh H, Russell AG (2001) Long-term trends of primary and secondary pollutant concentrations in Switzerland and their response to emission controls and economic changes. Atmos Environ 35:1351–1363. doi:10.1016/S1352-2310(00)00401-5

Kumar A, Sarin MM (2009) Mineral aerosols from western India: temporal variability of coarse and fine atmospheric dust and elemental characteristics. Atmos Environ 43:4005–4013. doi:10.1016/j.atmosenv.2009.05.014

Kumar A, Sarin MM (2010) Atmospheric water-soluble constituents in fine and coarse mode aerosols from high-altitude site in western India: long-range transport and seasonal variability. Atmos Environ 44:1245–1254. doi:10.1016/j.atmosenv.2009.12.035

Kumar A, Wu S, Weise MF, Honrath R, Owen RC, Helmig D, Kramer L, Val Martin M, Li Q (2013) Free-troposphere ozone and carbon monoxide over the North Atlantic for 2001-2011. Atmos Chem Phys 13:12537–12547. doi:10.5194/acp-13-12537-2013

Kurokawa J, Ohara T, Morikawa T, Hanayama S, Janssens-Maenhout G, Fukui T, Kawashima K, Akimoto H (2013) Emissions of air pollutants and greenhouse gases over Asian regions during 2000-2008: regional Emission inventory in ASia (REAS) version 2. Atmos Chem Phys 13:11019–11058. doi:10.5194/acp-13-11019-2013

Lal D, Peters B (1967) Cosmic ray produced radioactivity on the Earth. In: Sitte K (ed) Kosmische Strahlung II / Cosmic Rays II. Springer, Berlin Heidelberg

Lamarque J-F, Bond TC, Eyring V, Granier C, Heil A, Klimont Z, Lee D, Liousse C, Mieville A, Owen B, Schultz MG, Shindell D, Smith SJ, Stehfest E, Van Aardenne J, Cooper OR, Kainuma M, Mahowald N, McConnell JR, Naik V, Riahi K, van Vuuren DP (2010) Historical (1850-2000) gridded anthropogenic and biomass burning emissions of reactive gases and aerosols: methodology and application. Atmos Chem Phys 10:7017–7039. doi:10.5194/acp-10-7017-2010

Lanz VA, Henne S, Staehelin J, Hueglin C, Vollmer MK, Steinbacher M, Buchmann B, Reimann S (2009) Statistical analysis of anthropogenic non-methane VOC variability at a European background location (Jungfraujoch, Switzerland). Atmos Chem Phys 9:3445–3459. doi:10.5194/acp-9-3445-2009

Lanz VA, Prévôt ASH, Alfarra MR, Weimer S, Mohr C, DeCarlo PF, Gianini MFD, Hueglin C, Schneider J, Favez O, D'Anna B, George C, Baltensperger U (2010) Characterization of aerosol chemical composition with aerosol mass spectrometry in Central Europe: an overview. Atmos Chem Phys 10:10453–10471. doi:10.5194/acp-10-10453-2010

Lapina K, Honrath RE, Owen RC, Val Martín M, Hyer EJ, Fialho P (2008) Late summer changes in burning conditions in the boreal regions and their implications for NO_x and CO emissions from boreal fires. J Geophys Res 113:D11304. doi:10.1029/2007JD009421

Leaitch WR, Macdonald AM, Anlauf KG, Liu PSK, Toom-Sauntry D, Li S-M, Liggio J, Hayden K, Wasey MA, Russell LM, Takahama S, Liu S, van Donkelaar A, Duck T, Martin RV, Zhang Q, Sun Y, McKendry I, Shantz NC, Cubison M (2009) Evidence for Asian dust effects from aerosol plume measurements during INTEX-B 2006 near Whistler, BC. Atmos Chem Phys 9:3523–3546. doi:10.5194/acp-9-3523-2009

Leclair De Bellevue J, Réchou A, Baray JL, Ancellet G, Diab RD (2006) Signatures of stratosphere to troposphere transport near deep convective events in the southern subtropics. J Geophys Res 111:D24107. doi:10.1029/2005JD006947

Lee HN, Tositti L, Zheng X, Bonasoni P (2007) Analyses and comparisons of variations of ^{7}Be, ^{210}Pb, and $^{7}Be/^{210}Pb$ with ozone observations at two Global Atmosphere Watch stations from high mountains. J Geophys Res 112:D05303. doi:10.1029/2006JD007421

Lee C-T, Chuang M-T, Lin N-H, Wang J-L, Sheu G-R, Chang S-C, Wang S-H, Huang H, Chen H-W, Liu Y-L, Weng G-H, Lai H-Y, Hsu S-P (2011) The enhancement of $PM_{2.5}$ mass and water-soluble ions of biosmoke transported from Southeast Asia over the Mountain Lulin site in Taiwan. Atmos Environ 45:5784–5794. doi:10.1016/j.atmosenv.2011.07.020

Lee AKY, Hayden KL, Herckes P, Leaitch WR, Liggio J, Macdonald AM, Abbatt JPD (2012) Characterization of aerosol and cloud water at a mountain site during WACS 2010: secondary organic aerosol formation through oxidative cloud processing. Atmos Chem Phys 12:7103–7116. doi:10.5194/acp-12-7103-2012

Legreid G, Folini D, Staehelin J, Balzani Lööv J, Steinbacher M, Reimann S (2008) Measurements of organic trace gases including oxygenated volatile organic compounds at the high alpine site Jungfraujoch (Switzerland): seasonal variation and source allocations. J Geophys Res 113:D05307. doi:10.1029/2007JD008653

Lelieveld J, Berresheim H, Borrmann S, Crutzen PJ, Dentener FJ, Fischer H, Feichter J, Flatau PJ, Heland J, Holzinger R, Korrmann R, Lawrence MG, Levin Z, Markowicz KM, Mihalopoulos N, Minikin A, Ramanathan V, de Reus M, Roelofs GJ, Scheeren HA, Sciare J, Schlager H, Schultz M, Siegmund P, Steil B,

Stephanou EG, Stier P, Traub M, Warneke C, Williams J et al (2002) Global air pollution crossroads over the Mediterranean. Science 298:794–799. doi:10.1126/science.1075457

Levy II H (1971) Normal atmosphere: large radical and formaldehyde concentrations predicted. Science 173:141–143. doi:10.1126/science.173.3992.141

Levy II H, Moxim WJ (1989) Influence of long-range transport of combustion emissions on the chemical variability of the background atmosphere. Nature 338:326–328. doi:10.1038/338326a0

Li Y, Campana M, Reimann S, Schaub D, Stemmler K, Staehelin J, Peter T (2005) Hydrocarbon concentrations at the Alpine mountain sites Jungfraujoch and Arosa. Atmos Environ 39:1113–1127. doi:10.1016/j.atmosenv.2004.09.084

Li J, Wang Z, Akimoto H, Tang J, Uno I (2009) Modeling of the impacts of China's anthropogenic pollutants on the surface ozone summer maximum on the northern Tibetan Plateau. Geophys Res Lett 36:L24802. doi:10.1029/2009GL041123

Liang Q, Jaeglé L, Jaffe DA, Weiss-Penzias P, Heckman A, Snow JA (2004) Long-range transport of Asian pollution to the northeast Pacific: seasonal variations and transport pathways of carbon monoxide. J Geophys Res 109:D23S07. doi:10.1029/2003JD004402

Liang M-C, Tang J, Chan C-Y, Zheng XD, Yung YL (2008) Signature of stratospheric air at the Tibetan Plateau. Geophys Res Lett 35:L20816. doi:10.1029/2008GL035246

Lin YC, Lin CY, Hsu WT (2010) Observations of carbon monoxide mixing ratios at a mountain site in central Taiwan during the Asian biomass burning season. Atmos Res 95:270–278. doi:10.1016/j.atmosres.2009.10.006

Liu SC, Trainer M, Fehsenfeld FC, Parrish DD, Williams EJ, Fahey DW, Hübler G, Murphy PC (1987) Ozone production in the rural troposphere and the implications for regional and global ozone distributions. J Geophys Res 92:4191–4207. doi:10.1029/JD092iD04p04191

Liu H, Jacob DJ, Bey I, Yantosca RM, Duncan BN, Sachse GW (2003a) Transport pathways for Asian pollution outflow over the Pacific: interannual and seasonal variations. J Geophys Res 108:D20. doi:10.1029/2002JD003102

Liu W, Hopke PK, VanCuren RA (2003a) Origins of fine aerosol mass in the western United States using positive matrix factorization. J Geophys Res 108:D23. doi:10.1029/2003JD003678

Liu X, Kondo Y, Ram K, Matsui H, Nakagomi K, Ikeda T, Oshima N, Verma RL, Takegawa N, Koike M, Kajino M (2013) Seasonal variations of black carbon observed at the remote mountain site Happo in Japan. J Geophys Res 118:3709–3722. doi:10.1002/jgrd.50317

Lobert JM, Scharffe DH, Hao WM, Kuhlbusch TA, Seuwan R, Warneck P, Crutzen PJ (1991) Experimental evaluation of biomass burning emissions: nitrogen and carbon containing compounds. In: Levine JS (ed) Global Biomass Burning: Atmospheric, Climatic and Biospheric Implications. MIT Press, Cambridge, pp 289–304

Logan JA (1983) Nitrogen oxides in the troposphere: global and regional budgets. J Geophys Res 88:10785–10807. doi:10.1029/JC088iC15p10785

Logan JA, Staehelin J, Megretskaia IA, Cammas J-P, Thouret V, Claude H, De Backer H, Steinbacher M, Scheel H-E, Stübi R, Fröhlich M, Derwent R (2012) Changes in ozone over Europe: analysis of ozone measurements from sondes, regular aircraft (MOZAIC) and alpine surface sites. J Geophys Res 117:D09301. doi:10.1029/2011JD016952

Lugauer M, Baltensperger U, Furger M, Gäggeler HW, Jost DT, Schwikowski M, Wanner H (1998) Aerosol transport to the high Alpine sites Jungfraujoch (3454 m asl) and Colle Gnifetti (4452 m asl). Tellus B 50:76–92. doi:10.3402/tellusb.v50i1.16026

Luria M, Boatman JF, Harris J, Ray J, Straube T, Chin J, Gunter RL, Herbert G, Gerlach TM, Van Valin CC (1992) Atmospheric sulfur dioxide at Mauna Loa, Hawaii. J Geophys Res 97:6011–6022. doi:10.1029/91JD03126

Ma J, Tang J, Zhou X, Zhang X (2002) Estimates of the chemical budget for ozone at Waliguan Observatory. J Atmos Chem 41:21–48. doi:10.1023/A:1013892308983

Ma J, Zheng X, Xu X (2005) Comment on "Why does surface ozone peak in summertime at Waliguan?" by Bin Zhu et al. Geophys Res Lett 32:L01805. doi:10.1029/2004GL021683

Macdonald AM, Anlauf KG, Leaitch WR, Chan E, Tarasick DW (2011) Interannual variability of ozone and carbon monoxide at the Whistler high elevation site: 2002–2006. Atmos Chem Phys 11:11431–11446. doi:10.5194/acp-11-11431-2011

Mahieu E, Zander R, Delbouille L, Demoulin P, Roland G, Servais C (1997) Observed trends in total vertical column abundances of atmospheric gases from IR solar spectra recorded at the Jungfraujoch. J Atmos Chem 28:227–243. doi:10.1023/A:1005854926740

Marcq S, Laj P, Roger JC, Villani P, Sellegri K, Bonasoni P, Marinoni A, Cristofanelli P, Verza GP, Bergin M (2010) Aerosol optical properties and radiative forcing in the high Himalaya based on measurements at the Nepal Climate Observatory-Pyramid site (5079 m a.s.l.). Atmos Chem Phys 10:5859–5872. doi:10.5194/acp-10-5859-2010

Marenco A, Gouget H, Nédélec P, Pagés JP, Karcher F (1994) Evidence of a long-term increase in tropospheric ozone from Pic du Midi data series: consequences: positive radiative forcing. J Geophys Res 20:16617–16632. doi:10.1029/94JD00021

Marenco F, Bonasoni P, Calzolari F, Ceriani M, Chiari M, Cristofanelli P, D'Alessandro A, Fermo P, Lucarelli F, Mazzei F, Nava S, Piazzalunga A, Prati P, Valli G, Vecchi R (2006) Characterization of atmospheric aerosols at Monte Cimone, Italy, during summer 2004: source apportionment and transport mechanisms. J Geophys Res 111:D24202. doi:10.1029/2006JD007145

Maring H, Savoie DL, Izaguirre MA, McCormick C, Arimoto R, Prospero JM, Pilinis C (2000) Aerosol physical and optical properties and their relationship to aerosol composition in the free troposphere at Izaña, Tenetire, Canary Islands, during July 1995. J Geophys Res 105:14677–14700. doi:10.1029/2000JD900106

Marinoni A, Cristofanelli P, Laj P, Duchi R, Calzolari F, Decesari S, Sellegri K, Vuillermoz E, Verza GP, Villani P, Bonasoni P (2010) Aerosol mass and black carbon concentrations, a two year record at NCO-P (5079 m, Southern Himalayas). Atmos Chem Phys 10:8551–8562. doi:10.5194/acp-10-8551-2010

McKendry IG, Strawbridge KB, O'Neill NT, Macdonald AM, Liu PSK, Leaitch WR, Anlauf KG, Jaegle L, Fairlie TD, Westphal DL (2007) Trans-Pacific transport of Saharan dust to western North America: a case study. J Geophys Res 112:D01103. doi:10.1029/2006JD007129

McKendry IG, Macdonald AM, Leaitch WR, van Donkelaar A, Zhang Q, Duck T, Martin RV (2008) Trans-Pacific dust events observed at Whistler, British Columbia during INTEX-B. Atmos Chem Phys 8:6297–6307. doi:10.5194/acp-8-6297-2008

McKendry IG, Gallagher J, Campuzano Jost P, Bertram A, Strawbridge K, Leaitch R, Macdonald AM (2010) Ground-based remote sensing of an elevated forest fire aerosol layer at Whistler, BC: implications for interpretation of mountaintop chemistry. Atmos Chem Phys 10:11921–11930. doi:10.5194/acp-10-11921-2010

McKendry I, Strawbridge K, Karumudi ML, O'Neill N, Macdonald AM, Leaitch R, Jaffe D, Cottle P, Sharma S, Sheridan P, Ogren J (2011) Californian forest fire plumes over Southwestern British Columbia: lidar, sunphotometry, and mountaintop chemistry observations. Atmos Chem Phys 11:465–477. doi:10.5194/acp-11-465-2011

Melen F, Mahieu E, Zander R, Rinsland CP, Demoulin P, Roland G, Delbouille L, Servais C (1998) Vertical column abundances of COF_2 above the Jungfraujoch station, derived from ground-based infrared solar observations. J Atmos Chem 29:119–134. doi:10.1023/A:1005847829686

Meng Z-Y, Xu X-B, Wang T, Zhang X-Y, Yu X-L, Wang S-F, Lin W-L, Chen Y-Z, Jiang Y-A, An X-Q (2010) Ambient sulfur dioxide, nitrogen dioxide, and ammonia at ten background and rural sites in China during 2007-2008. Atmos Environ 44:2625–2631. doi:10.1016/j.atmosenv.2010.04.008

Middleton NJ, Goudie AS (2001) Saharan dust: sources and trajectories. Trans Inst Br Geogr 26:165–181. doi:10.1111/1475-5661.00013

Monks PS (2000) A review of the observations and origins of the spring ozone maximum. Atmos Environ 34:3545–3561. doi:10.1016/S1352-2310(00)00129-1

Monks PS, Granier C, Fuzzi S, Stohl A, Williams ML, Akimoto H, Amann M, Baklanov A, Baltensperger U, Bey I, Blake N, Blake RS, Carslaw K, Cooper OR, Dentener F, Fowler D, Fragkou E, Frost GJ, Generoso S, Ginoux P, Grewe V, Guenther A, Hansson HC, Henne S, Hjorth J, Hofzumahaus A, Huntrieser H, Isaksen ISA, Jenkin ME, Kaiser J et al (2009) Atmospheric composition change—global and regional air quality. Atmos Environ 43:5268–5350. doi:10.1016/j.atmosenv.2009.08.021

Mu Y, Pang X, Quan J, Zhang X (2007) Atmospheric carbonyl compounds in Chinese background area: a remote mountain of the Qinghai-Tibetan Plateau. J Geophys Res 112:D22302. doi:10.1029/2006JD008211

Nagashima T, Ohara T, Sudo K, Akimoto H (2010) The relative importance of various source regions on East Asian surface ozone. Atmos Chem Phys 10:11305–11322. doi:10.5194/acp-10-11305-2010

Naja M, Lal S, Chand D (2003) Diurnal and seasonal variabilities in surface ozone at a high altitude site Mt Abu (24.6°N, 72.7°E, 1680m asl) in India. Atmos Environ 37:4205–4215. doi:10.1016/s1352-2310(03)00565-x

Nakazawa T, Aoki S, Fukabori M, Tanaka M (1984) The concentration of atmospheric carbon dioxide on the summit of Mt. Fuji (3776m), Japan. J Meteorol Soc Japan 62:688–695

Naoe H, Heintzenberg J, Okada K, Zaizen Y, Hayashi K, Tateishi T, Igarashi Y, Dokiya Y, Kinoshita K (2003) Composition and size distribution of submicrometer aerosol particles observed on Mt. Fuji in the volcanic plumes from Miyakejima. Atmos Environ 37:3047–3055. doi:10.1016/S1352-2310(03)00295-4

Nappo CJ, Caneill JY, Furman RW, Gifford FA, Kaimal JC, Kramer ML, Lockhart TJ, Pendergast MM, Pielke RA, Randerson D, Shreffler JH, Wyngaard JC (1982)

The Workshop on the respresentativeness of meteorological observations, June 1981, Boulder, Colo. Bull Am Meteorol Soc 63:761–764

Narita D, Pochanart P, Matsumoto J, Someno K, Tanimoto H, Hirokawa J, Kajii Y, Akimoto H, Nakao M, Katsuno T, Kinjo Y (1999) Seasonal variation of carbon monoxide at remote sites in Japan. Chemospher 1:137–144. doi:10.1016/S1465-9972(99)00023-9

Novelli PC, Masarie KA, Lang PM (1998) Distributions and recent changes of carbon monoxide in the lower troposphere. J Geophys Res 103:19015–19033. doi:10.1029/98JD01366

Novelli PC, Masarie KA, Lang PM, Hall BD, Myers RC, Elkins JW (2003) Reanalysis of tropospheric CO trends: effects of the 1997-1998 wildfires. J Geophys Res 108:4464. doi:10.1029/2002JD003031

Nyeki S, Baltensperger U, Colbeck I, Jost DT, Weingartner E, Gäggeler HW (1998a) The Jungfraujoch high-alpine research station (3454 m) as a background clean continental site for the measurement of aerosol parameters. J Geophys Res 103:6097-6107. doi:10.1029/97JD03123

Nyeki S, Li F, Weingartner E, Streit N, Colbeck I, Gäggeler HW, Baltensperger U (1998b) The background aerosol size distribution in the free troposphere: an analysis of the annual cycle at a high-alpine site. J Geophys Res 103:31749-31761. doi:10.1029/1998JD200029

Nyeki S, Halios CH, Baum W, Eleftheriadis K, Flentje H, Gröbner J, Vuilleumier L, Wehrli C (2012) Ground-based aerosol optical depth trends at three high-altitude sites in Switzerland and southern Germany from 1995 to 2010. J Geophys Res 117:D18202. doi:10.1029/2012JD017493

Oliveira TS, Pio CA, Alves CA, Silvestre AJD, Evtyugina M, Afonso JV, Fialho P, Legrand M, Puxbaum H, Gelencsér A (2007) Seasonal variation of particulate lipophilic organic compounds at nonurban sites in Europe. J Geophys Res 112:D23S09. doi:10.1029/2007JD008504

Oltmans SJ, Levy II H (1994) Surface ozone measurements from a global network. Atmos Environ 28:9–24. doi:10.1016/1352-2310(94)90019-1

Oltmans SJ, Hofmann DJ, Lathrop JA, Harris JM, Komhyr WD, Kuniyuki D (1996a) Tropospheric ozone during Mauna Loa Observatory Photochemistry Experiment 2 compared to long-term measurements from surface and ozonesonde observations. J Geophys Res 101:14569-14580. doi:10.1029/95JD03004

Oltmans SJ, Levy II H, Harris JM, Merrill JT, Moody JL, Lathrop JA, Cuevas E, Trainer M, O'Neill MS, Prospero JM, Vömel H, Johnson BJ (1996b) Summer and spring ozone profiles over the North Atlantic from ozonesonde measurements. J Geophys Res 101:29179-29200. doi:10.1029/96JD01713

Oltmans SJ, Johnson BJ, Harris JM, Thompson AM, Liu HY, Chan CY, Vömel H, Fujimoto T, Brackett VG, Chang WL, Chen J-P, Kim JH, Chan LY, Chang H-W (2004) Tropospheric ozone over the North Pacific from ozonesonde observations. J Geophys Res 109:D15S01. doi:10.1029/2003JD003466

Oltmans SJ, Lefohn AS, Harris JM, Galbally I, Scheel HE, Bodeker G, Brunke E, Claude H, Tarasick D, Johnson BJ, Simmonds P, Shadwick D, Anlauf K, Hayden K, Schmidlin F, Fujimoto T, Akagi K, Meyer C, Nichol S, Davies J, Redondas A, Cuevas E (2006) Long-term changes in tropospheric ozone. Atmos Environ 40:3156–3173. doi:10.1016/j.atmosenv.2006.01.029

Oltmans SJ, Lefohn AS, Shadwick D, Harris JM, Scheel HE, Galbally I, Tarasick DW, Johnson BJ, Brunke EG, Claude H, Zeng G, Nichol S, Schmidlin F, Davies J, Cuevas E, Redondas A, Naoe H, Nakano T, Kawasato T (2013) Recent tropospheric ozone changes—a pattern dominated by slow or no growth. Atmos Environ 67:331–351. doi:10.1016/j.atmosenv.2012.10.057

Ou Yang C-F, Lin N-H, Sheu G-R, Lee C-T, Wang J-L (2012) Seasonal and diurnal variations of ozone at a high-altitude mountain baseline station in East Asia. Atmos Environ 46:279–288. doi:10.1016/j.atmosenv.2011.09.060

Ou-Yang C-F, Lin N-H, Lin C-C, Wang S-H, Sheu G-R, Lee C-T, Schnell RC, Lang PM, Kawasato T, Wang J-L (2014) Characteristics of atmospheric carbon monoxide at a high-mountain background station in East Asia. Atmos Environ 89:613–622. doi:10.1016/j.atmosenv.2014.02.060

Owen RC, Cooper OR, Stohl A, Honrath RE (2006) An analysis of the mechanisms of North American pollutant transport to the central North Atlantic lower free troposphere. J Geophys Res 111:D23S58. doi:10.1029/2006JD007062

Pandey Deolal S, Brunner D, Steinbacher M, Weers U, Staehelin J (2012) Long-term in situ measurements of NO_x and NO_y at Jungfraujoch 1998-2009: time series analysis and evaluation. Atmos Chem Phys 12:2551–2566. doi:10.5194/acp-12-2551-2012

Pandey Deolal S, Staehelin J, Brunner D, Cui J, Steinbacher M, Zellweger C, Henne S, Vollmer MK (2013) Transport of PAN and NO_y from different source regions to the Swiss high alpine site Jungfraujoch. Atmos Environ 64:103–115. doi:10.1016/j.atmosenv.2012.08.021

Parrington JR, Zoller WH (1984) Diurnal and longer-term temporal changes in the composition of atmospheric particles at Mauna Loa, Hawaii. J Geophys Res 89:2522–2534. doi:10.1029/JD089iD02p02522

Parrington JR, Zoller WH, Aras NK (1983) Asian dust: seasonal transport to the Hawaiian islands. Science 220:195–197. doi:10.1126/science.220.4593.195

Parrish DD, Stohl A, Forster C, Atlas EL, Blake DR, Goldan PD, Kuster WC, de Gouw JA (2007) Effects of mixing on evolution of hydrocarbon ratios in the troposphere. J Geophys Res 112:D10S34. doi:10.1029/2006JD007583

Parrish DD, Law KS, Staehelin J, Derwent R, Cooper OR, Tanimoto H, Volz-Thomas A, Gilge S, Scheel H-E, Steinbacher M, Chan E (2012) Long-term changes in lower tropospheric baseline ozone concentrations at northern mid-latitudes. Atmos Chem Phys 12:11485–11504. doi:10.5194/acp-12-11485-2012

Parrish DD, Law KS, Staehelin J, Derwent R, Cooper OR, Tanimoto H, Volz-Thomas A, Gilge S, Scheel H-E, Steinbacher M, Chan E (2013) Lower tropospheric ozone at northern midlatitudes: changing seasonal cycle. Geophys Res Lett 40:1631–1636. doi:10.1002/grl.50303

Parrish DD, Lamarque J-F, Naik V, Horowitz L, Shindell DT, Staehelin J, Derwent R, Cooper OR, Tanimoto H, Voltz-Thomas A, Gilge S, Scheel H-E, Steinbacher M, Fröhlich M (2014) Long-term changes in lower tropospheric baseline ozone concentrations: comparing chemistry-climate models and observations at northern midlatitudes. J Geophys Res 119:5719–5736. doi:10.1002/2013JD021435

Penkett SA, Brice KA (1986) The spring maximum in photo-oxidants in the Northern Hemisphere troposphere. Nature 319:655–657. doi:10.1038/319655a0

Perry KD, Cahill TA, Schnell RC, Harris JM (1999) Long-range transport of anthropogenic aerosols to the National Oceanic and Atmospheric Administration baseline station at Mauna Loa Observatory, Hawaii. J Geophys Res 104:18521–18533. doi:10.1029/1998JD100083

Peterson MC, Honrath RE, Parrish DD, Oltmans SJ (1998) Measurements of nitrogen oxides and a simple model of NO_y fate in the remote North Atlantic marine atmosphere. J Geophys Res 103:13489–13503. doi:10.1029/97JD02307

Pfister G, Hess PG, Emmons LK, Lamarque J-F, Wiedinmyer C, Edwards DP, Pétron G, Gille JC, Sachse GW (2005) Quantifying CO emissions from the 2004 Alaskan wildfires using MOPITT CO data. Geophys Res Lett 32:L11809. doi:10.1029/2005GL022995

Pfister GG, Emmons LK, Hess PG, Honrath R, Lamarque J-F, Val Martin M, Owen RC, Avery MA, Browell EV, Holloway JS, Nedelec P, Purvis R, Ryerson TB, Sachse GW, Schlager H (2006) Ozone production from the 2004 North American boreal fires. J Geophys Res 111:D24S07. doi:10.1029/2006JD007695

Pierce JR, Leaitch WR, Liggio J, Westervelt DM, Wainwright CD, Abbatt JPD, Ahlm L, Al-Basheer W, Cziczo DJ, Hayden KL, Lee AKY, Li S-M, Russell LM, Sjostedt SJ, Strawbridge KB, Travis M, Vlasenko A, Wentzell JJB, Wiebe HA, Wong JPS, Macdonald AM (2012) Nucleation and condensational growth to CCN sizes during a sustained pristine biogenic SOA event in a forested mountain valley. Atmos Chem Phys 12:3147–3163. doi:10.5194/acp-12-3147-2012

Pochanart P, Hirokawa J, Kajii Y, Akimoto H, Nakao M (1999) Influence of regional-scale anthropogenic activity in northeast Asia on seasonal variations of surface ozone and carbon monoxide observed at Oki, Japan. J Geophys Res 104:3621–3631. doi:10.1029/1998JD100071

Pochanart P, Akimoto H, Maksyutov S, Staehelin J (2001) Surface ozone at the Swiss Alpine site Arosa: the hemispheric background and the influence of large-scale anthropogenic emissions. Atmos Environ 35:5553–5566. doi:10.1016/S1352-2310(01)00236-9

Pochanart P, Akimoto H, Kajii Y, Potemkin VM, Khodzher TV (2003) Regional background ozone and carbon monoxide variations in remote Siberia/East Asia. J Geophys Res 108:4028. doi:10.1029/2001jd001412

Pochanart P, Kato S, Katsuno T, Akimoto H (2004) Eurasian continental background and regionally polluted levels of ozone and CO observed in northeast Asia. Atmos Environ 38:1325–1336. doi:10.1016/j.atmosenv.2003.11.014

Prather MJ (1996) Time scales in atmospheric chemistry: theory, GWPs for CH_4 and CO, and runaway growth. Geophys Res Lett 23:2597–2600. doi:10.1029/96GL02371

Primbs T, Piekarz A, Wilson G, Schmedding D, Higginbotham C, Field J, Simonich SM (2008a) Influence of Asian and western United States urban areas and fires on the atmospheric transport of polycyclic aromatic hydrocarbons, polychlorinated biphenyls, and fluorotelomer alcohols in the western United States. Environ Sci Technol 42:6385-6391. doi:10.1021/es702160d

Primbs T, Wilson G, Schmedding D, Higginbotham C, Simonich SM (2008b) Influence of Asian and western United States agricultural areas and fires on the atmospheric transport of pesticides in the western United States. Environ Sci Technol 42:6519-6525. doi:10.1021/es800511x

Prinn RG, Huang J, Weiss RF, Cunnold DM, Fraser PJ, Simmonds PG, McCulloch A, Harth C, Salameh P, O'Doherty S, Wang RHJ, Porter L, Miller BR (2001)

Evidence for substantial variations of atmospheric hydroxyl radicals in the past two decades. Science 292:1882–1888. doi:10.1126/science.1058673

Prospero JM, Schmitt R, Cuevas E, Savoie DL, Graustein WC, Turekian KK, Volz-Thomas A, Díaz A, Oltmans SJ, Levy II H (1995) Temporal variability of summer-time ozone and aerosols in the free troposphere over the eastern North Atlantic. Geophys Res Lett 22:2925–2928. doi:10.1029/95gl02791

Prospero JM, Ginoux P, Torres O, Nicholson S, Gill TE (2002) Environmental characterization of global sources of atmospheric soil dust identified with the Nimbus 7 Total Ozone Mapping Spectrometer (TOMS) absorbing aerosol product. Rev Geophys 40:1002. doi:10.1029/2000rg000095

Puentedura O, Gil M, Saiz-Lopez A, Hay T, Navarro-Comas M, Gómez-Pelaez A, Cuevas E, Iglesias J, Gomez L (2012) Iodine monoxide in the north subtropical free troposphere. Atmos Chem Phys 12:4909–4921. doi:10.5194/acp-12-4909-2012

Putaud J-P, Van Dingenen R, Dell'Acqua A, Raes F, Matta E, Decesari S, Facchini MC, Fuzzi S (2004) Size-segregated aerosol mass closure and chemical composition in Monte Cimone (I) during MINATROC. Atmos Chem Phys 4:889–902. doi:10.5194/acp-4-889-2004

Ram K, Sarin MM (2009) Absorption coefficient and site-specific mass absorption efficiency of elemental carbon in aerosols over urban, rural, and high-altitude sites in India. Environ Sci Technol 42:8233–8239. doi:10.1021/es9011542

Ram K, Sarin MM, Hegde P (2008) Atmospheric abundances of primary and secondary carbonaceous species at two high-altitude sites in India: Sources and temporal variability. Atmos Environ 42:6785–6796. doi:10.1016/j.atmosenv.2008.05.031

Ramanathan V, Crutzen PJ (2003) New directions: atmospheric brown "clouds". Atmos Environ 37:4033–4035. doi:10.1016/S1352-2310(03)00536-3

Rastogi N, Sarin MM (2005) Long-term characterization of ionic species in aerosols from urban and high-altitude sites in western India: role of mineral dust and anthropogenic sources. Atmos Environ 39:5541–5554. doi:10.1016/j.atmosenv.2005.06.011

Rastogi N, Sarin MM (2008) Atmospheric ^{210}Pb and ^{7}Be in ambient aerosols over low- and high-altitude sites in semiarid region: temporal variability and transport processes. J Geophys Res 113:D11103. doi:10.1029/2007jd009298

Reidmiller DR, Jaffe DA, Chand D, Strode S, Swartzendruber P, Wolfe GM, Thornton JA (2009) Interannual variability of long-range transport as seen at the Mt. Bachelor observatory. Atmos Chem Phys 9:557–572. doi:10.5194/acp-9-557-2009

Reidmiller DR, Jaffe DA, Fischer EV, Finley B (2010) Nitrogen oxides in the boundary layer and free troposphere at the Mt. Bachelor Observatory. Atmos Chem Phys 10:6043–6062. doi:10.5194/acp-10-6043-2010

Ridley BA, Robinson E (1992) The Mauna Loa Observatory photochemistry experiment. J Geophys Res 97:10285–10290. doi:10.1029/91jd00945

Ridley B, Walega J, Hübler G, Montzka D, Atlas E, Hauglustaine D, Grahek F, Lind J, Campos T, Norton R, Greenberg J, Schauffler S, Oltmans S, Whittlestone S (1998) Measurements of NO_x and PAN and estimates of O_3 production over the seasons during Mauna Loa Observatory Photochemistry Experiment 2. J Geophys Res 103:8323–8339. doi:10.1029/98JD00075

Rieder HE, Staehelin J, Maeder JA, Peter T, Ribatet M, Davison AC, Stübi R, Weihs P, Holawe F (2010a) Extreme events in total ozone over Arosa—part 1: application of extreme value theory. Atmos Chem Phys 10:10021-10031. doi:10.5194/acp-10-10021-2010

Rieder HE, Staehelin J, Maeder JA, Peter T, Ribatet M, Davison AC, Stübi R, Weihs P, Holawe F (2010b) Extreme events in total ozone over Arosa—part 2: fingerprints of atmospheric dynamics and chemistry and effects on mean values and long-term changes. Atmos Chem Phys 10:10033-10045. doi:10.5194/acp-10-10033-2010

Rinsland CP, Zander R, Demoulin P (1991) Ground-based infrared measurements of HNO_3 total column abundances: long-term trend and variability. J Geophys Res 96:9379–9389. doi:10.1029/91JD00609

Rinsland CP, Zander R, Mahieu E, Demoulin P, Goldman A, Ehhalt DH, Rudolph J (1992) Ground-based infrared measurements of carbonyl sulfide total column abundances: long-term trends and variability. J Geophys Res 97:5995–6002. doi:10.1029/92JD00040

Rinsland CP, Zander R, Demoulin P, Mahieu E (1996) $CLONO_2$ total vertical column abundances above the Jungfraujoch Station, 1986-1994: long-term trend and winter-spring enhancements. J Geophys Res 101:3891–3899. doi:10.1029/95JD03349

Rinsland CP, Mahieu E, Zander R, Demoulin P, Forrer J, Buchmann B (2000) Free tropospheric CO, C_2H_6, and HCN above central Europe: recent measurements from the Jungfraujoch station including the detection of elevated columns during 1998. J Geophys Res 105:24235–24249. doi:10.1029/2000JD900371

Rinsland CP, Mahieu E, Zander R, Jones NB, Chipperfield MP, Goldman A, Anderson J, Russell JM III, Demoulin P, Notholt J, Toon GC, Blavier J-F, Sen B, Sussmann R, Wood SW, Meier A, Griffith DWT, Chiou LS, Murcray FJ, Stephen TM, Hase F, Mikuteit S, Schulz A, Blumenstock T (2003) Long-term trends of inorganic chlorine from ground-based infrared solar spectra: past increases and evidence for stabilization. J Geophys Res 108:4252. doi:10.1029/2002JD003001

Rinsland CP, Chiou L, Mahieu E, Zander R, Boone CD, Bernath PF (2008) Measurements of long-term changes in atmospheric OCS (carbonyl sulfide) from infrared solar observations. J Quant Spectrosc Radiat Transf 109:2679–2686. doi:10.1016/j.jqsrt.2008.07.008

Rodríguez S, González Y, Cuevas E, Ramos R, Romero PM, Abreu-Afonso J, Redondas A (2009) Atmospheric nanoparticle observations in the low free troposphere during upward orographic flows at Izaña Mountain Observatory. Atmos Chem Phys 9:6319–6335. doi:10.5194/acp-9-6319-2009

Rodríguez S, Alastuey A, Alonso-Pérez S, Querol X, Cuevas E, Abreu-Afonso J, Viana M, Pérez N, Pandolfi M, de la Rosa J (2011) Transport of desert dust mixed with North African industrial pollutants in the subtropical Saharan Air Layer. Atmos Chem Phys 11:6663–6685. doi:10.5194/acp-11-6663-2011

Rodríguez S, Torres C, Guerra J-C, Cuevas E (2004) Transport pathways of ozone to marine and free-troposphere sites in Tenerife, Canary Islands. Atmos Environ 38:4733–4747. doi:10.1016/j.atmosenv.2004.05.021

Rose C, Sellegri K, Velarde F, Moreno I, Ramonet M, Weinhold K, Krejci R, Ginot P, Andrade M, Wiedensohler A, Laj P (2015) Frequent nucleation events at the high altitude station of Chacaltaya (5240 m a.s.l.), Bolivia. Atmos Environ 102:18–29. doi:10.1016/j.atmosenv.2014.11.015

Ruckstuhl AF, Henne S, Reimann S, Steinbacher M, Vollmer MK, O'Doherty S, Buchmann B, Hueglin C (2012) Robust extraction of baseline signal of atmospheric trace species using local regression. Atmos Meas Tech 5:2613–2624. doi:10.5194/amt-5-2613-2012

Salisbury G, Williams J, Gros V, Bartenbach S, Xu X, Fischer H, Kormann R, de Reus M, Zöllner M (2006) Assessing the effect of a Saharan dust storm on oxygenated organic compounds at Izaña, Tenerife (July-August 2002). J Geophys Res 111:D22303. doi:10.1029/2005JD006840

Sandrini S, Giulianelli L, Decesari S, Fuzzi S, Cristofanelli P, Marinori A, Bonasoni P, Chiari M, Calzolai G, Canepari S, Perrino C, Facchini MC (2014) In situ physical and chemical characterisation of the Eyjafjallajökull aerosol plume in the free troposphere over Italy. Atmos Chem Phys 14:1075–1092. doi:10.5194/acp-14-1075-2014

Satsumabayashi H, Kawamura M, Katsuno T, Futaki K, Murano K, Carmichael GR, Kajino M, Horiguchi M, Ueda H (2004) Effects of Miyake volcanic effluents on airborne particles and precipitation in central Japan. J Geophys Res 109:D19202. doi:10.1029/2003JD004204

Scarnato B, Staehelin J, Stübi R, Schill H (2010) Long-term total ozone observations at Arosa (Switzerland) with Dobson and Brewer instruments (1988-2007). J Geophys Res 115:D13306. doi:10.1029/2009JD011908

Schäfer K, Thomas W, Peters A, Ries L, Obleitner F, Schnelle-Kreis J, Birmili W, Diemer J, Fricke W, Junkermann W, Pitz M, Emeis S, Forkel R, Suppan P, Flentje H, Gilge S, Wichmann HE, Meinhardt F, Zimmermann R, Weinhold K, Soentgen J, Münkel C, Freuer C, Cyrys J (2011) Influences of the 2010 Eyjafjallajökull volcanic plume on air quality in the northern Alpine region. Atmos Chem Phys 11:8555–8575. doi:10.5194/acp-11-8555-2011

Schaub D, Brunner D, Boersma KF, Keller J, Folini D, Buchmann B, Berresheim H, Staehelin J (2007) SCIAMACHY tropospheric NO_2 over Switzerland: estimates of NO_x lifetimes and impact of the complex Alpine topography on the retrieval. Atmos Chem Phys 7:5971–5987. doi:10.5194/acp-7-5971-2007

Scheel HE, Areskoug H, Geiß H, Gomiscek B, Granby K, Haszpra L, Klasinc L, Kley D, Laurila T, Lindskog A, Roemer M, Schmitt R, Simmonds P, Solberg S, Toupance G (1997) On the spatial distribution and seasonal variation of lower-troposphere ozone over Europe. J Atmos Chem 28:11–28. doi:10.1023/A:1005882922435

Schmitt R, Volz-Thomas A (1997) Climatology of ozone, PAN, CO, and NMHC in the free troposphere over the southern North Atlantic. J Atmos Chem 28:245–262. doi:10.1023/A:1005801515531

Schneider M, Blumenstock T, Chipperfield MP, Hase F, Kouker W, Reddmann T, Ruhnke R, Cuevas E, Fischer H (2005a) Subtropical trace gas profiles determined by ground-based FTIR spectroscopy at Izaña (28°N, 16°W): five-year record, error analysis, and comparison with 3-D CTMs. Atmos Chem Phys 5:153-167. doi:10.5194/acp-5-153-2005

Schneider M, Blumenstock T, Hase F, Höpfner M, Cuevas E, Redondas A, Sancho JM (2005b) Ozone profiles and total column amounts derived at Izaña,

Tenerife Island, from FTIR solar absorption spectra, and its validation by an intercomparison to ECC-sonde and Brewer spectrometer measurements. J Quant Spectrosc Radiat Transf 91:245-274. doi:10.1016/j.jqsrt.2004.05.067

Schneider M, Redondas A, Hase F, Guirado C, Blumenstock T, Cuevas E (2008) Comparison of ground-based Brewer and FTIR total O_3 monitoring techniques. Atmos Chem Phys 8:5535–5550. doi:10.5194/acp-8-5535-2008

Schöner W, Böhm R, Auer I (2012) 125 years of high-mountain research at Sonnblick Observatory (Austrian Alps)—from "the house above the clouds" to a unique research platform. Theor Appl Climatol 110:491–498. doi:10.1007/s00704-012-0689-8

Schuepbach E, Davies TD, Massacand AC (1999) An unusual springtime ozone episode at high elevation in the Swiss Alps: contributions both from cross-tropopause exchange and from the boundary layer. Atmos Environ 33:1735–1744. doi:10.1016/S1352-2310(98)00232-5

Schuepbach E, Friedli TK, Zanis P, Monks PS, Penkett SA (2001) State space analysis of changing seasonal ozone cycles (1988–1997) at Jungfraujoch (3580 m above sea level) in Switzerland. J Geophys Res 106:20413–20427. doi:10.1029/2000JD900591

Schultz M, Schmitt R, Thomas K, Volz-Thomas A (1998) Photochemical box modeling of long-range transport from North America to Tenerife during the North Atlantic Regional Experiment (NARE) 1993. J Geophys Res 103:13477–13488. doi:10.1029/97JD01481

Schwikowski M, Seibert P, Baltensperger U, Gäggeler HW (1995) A study of an outstanding Saharan dust event at the high-alpine site Jungfraujoch, Switzerland. Atmos Environ 29:1829–1842. doi:10.1016/1352-2310(95)00060-C

Seibert P (1990) South foehn studies since the ALPEX experiment. Meteorol Atmos Phys 43:91–103. doi:10.1007/BF01028112

Seibert P, Kromp-Kolb H, Kasper A, Kalina M, Puxbaum H, Jost DT, Schwikowski M, Baltensperger U (1998) Transport of polluted boundary layer air from the Po Valley to high-alpine sites. Atmos Environ 32:3953–3965. doi:10.1016/S1352-2310(97)00174-X

Seinfeld JH, Pandis SN (2006) Atmospheric chemistry and physics: from air pollution to climate change, 2nd edn. Wiley, Hoboken

Sellegri K, Laj P, Venzac H, Boulon J, Picard D, Villani P, Bonasoni P, Marinoni A, Cristofanelli P, Vuillermoz E (2010) Seasonal variations of aerosol size distributions based on long-term measurements at the high altitude Himalayan site of Nepal Climate Observatory-Pyramid (5079 m), Nepal. Atmos Chem Phys 10:10679–10690. doi:10.5194/acp-10-10679-2010

Semenov VK, Smirnov A, Aref'ev VN, Sinyakov VP, Sorokina LI, Ignatova NI (2005) Aerosol optical depth over the mountainous region in central Asia (Issyk-Kul Lake, Kyrgyzstan). Geophys Res Lett 32:L05807. doi:10.1029/2004GL021746

Senik IA, Elansky NF (2001) Surface ozone concentration measurements at the Kislovodsk high-altitude scientific station: temporal variations and trends. Izv Atmos Ocean Phys 37:110–119

Senik IA, Elansky NF, Belikov IB, Lisitsyna LV, Galaktionov VV, Kortunova ZV (2005) Main patterns of the temporal variability of surface ozone in the region of the town of Kislovodsk at 870 and 2070 m above sea level. Izv Atmos Ocean Phys 41:67–79

Sepúlveda E, Schneider M, Hase F, García OE, Gomez-Pelaez A, Dohe S, Blumenstock T, Guerra JC (2012) Long-term validation of tropospheric column-averaged CH_4 mole fractions obtained by mid-infrared ground-based FTIR spectrometry. Atmos Meas Tech 5:1425–1441. doi:10.5194/amt-5-1425-2012

Sharma UK, Kajii Y, Akimoto H (2000) Seasonal variation of C_2–C_6 NMHCs at Happo, a remote site in Japan. Atmos Environ 34:4447–4458. doi:10.1016/S1352-2310(00)00162-X

Sheu G-R, Lin N-H, Wang J-L, Lee C-T, Ou Yang C-F, Wang S-H (2010) Temporal distribution and potential sources of atmospheric mercury measured at a high-elevation background station in Taiwan. Atmos Environ 44:2393–2400. doi:10.1016/j.atmosenv.2010.04.009

Sholkovitz ER, Sedwick PN, Church TM (2009) Influence of anthropogenic combustion emissions on the deposition of soluble aerosol iron to the ocean: empirical estimates for island sites in the North Atlantic. Geochim Cosmochim Acta 73:3981–4003. doi:10.1016/j.gca.2009.04.029

Škerlak B, Sprenger M, Wernli H (2014) A global climatology of stratosphere-troposphere exchange using the ERA-Interim data set from 1979 to 2011. Atmos Chem Phys 14:913–937. doi:10.5194/acp-14-913-2014

Smirnov A, Holben BN, Slutsker I, Welton EJ, Formenti P (1998) Optical properties of Saharan dust during ACE 2. J Geophys Res 103:28079–28092. doi:10.1029/98JD01930

Sofen ED, Bowdalo D, Evans MJ (2016) How to most effectively expand the global surface ozone observing network. Atmos Chem Phys 16:1445–1457. doi:10.5194/acp-16-1445-2016

Solomon S (1999) Stratospheric ozone depletion: a review of concepts and history. Rev Geophys 37:275–316. doi:10.1029/1999RG900008

Solomon S, Daniel JS, Neely RR III, Vernier J-P, Dutton EG, Thomason LW (2011) The persistently variable "background" stratospheric aerosol layer and global climate change. Science 333:866–870. doi:10.1126/science.1206027

Spangl W, Schneider J, Moosmann L, Nagl C (2007) Representativeness and classification of air quality monitoring stations. Final report. Umweltbundesamt, Vienna

Spivakovsky CM, Yevich R, Logan JA, Wofsy SC, McElroy MB (1990) Tropospheric OH in a three-dimensional chemical tracer model: An assessment based on observations of CH_3CCl_3. J Geophys Res Atmos 95:18441–18471. doi:10.1029/JD095iD11p18441

Staehelin J, Thudium J, Buehler R, Volz-Thomas A, Graber W (1994) Trends in surface ozone concentrations at Arosa (Switzerland). Atmos Environ 28:75–87. doi:10.1016/1352-2310(94)90024-8

Staehelin J, Kegel R, Harris NRP (1998a) Trend analysis of the homogenized total ozone series of Arosa (Switzerland), 1926–1996. J Geophys Res 103:8389-8399. doi:10.1029/97JD03650

Staehelin J, Renaud A, Bader J, McPeters R, Viatte P, Hoegger B, Bugnion V, Giroud M, Schill H (1998b) Total ozone series at Arosa (Switzerland): homogenization and data comparison. J Geophys Res 103:5827-5841. doi:10.1029/97JD02402

Stevenson DS, Dentener FJ, Schultz MG, Ellingsen K, van Noije TPC, Wild O, Zeng G, Amann M, Atherton CS, Bell N, Bergmann DJ, Bey I, Butler T, Cofala J, Collins WJ, Derwent RG, Doherty RM, Drevet J, Eskes HJ, Fiore AM, Gauss M, Hauglustaine DA, Horowitz LW, Isaksen ISA, Krol MC, Lamarque J-F, Lawrence MG, Montanaro V, Müller J-F, Pitari G et al (2006) Multimodel ensemble simulations of present-day and near-future tropospheric ozone. J Geophys Res 111:D08301. doi:10.1029/2005JD006338

Stohl A, Eckhardt S, Forster C, James P, Spichtinger N, Seibert P (2002) A replacement for simple back trajectory calculations in the interpretation of atmospheric trace substance measurements. Atmos Environ 36:4635–4648. doi:10.1016/S1352-2310(02)00416-8

Streets DG, Bond TC, Carmichael GR, Fernandes SD, Fu Q, He D, Klimont Z, Nelson SM, Tsai NY, Wang MQ, Woo J-H, Yarber KF (2003) An inventory of gaseous and primary aerosol emissions in Asia in the year 2000. J Geophys Res 108:8809. doi:10.1029/2002JD003093

Streets DG, Canty T, Carmichael GR, de Foy B, Dickerson RR, Duncan BN, Edwards DP, Haynes JA, Henze DK, Houyoux MR, Jacob DJ, Krotkov NA, Lamsal LN, Liu Y, Lu Z, Martin RV, Pfister GC, Pinder RW, Salawitch RJ, Wecht KJ (2013) Emissions estimation from satellite retrievals: a review of current capability. Atmos Environ 77:1011–1042. doi:10.1016/j.atmosenv.2013.05.051

Strode SA, Jaeglé L, Jaffe DA, Swartzendruber PC, Selin NE, Holmes C, Yantosca RM (2008) Trans-Pacific transport of mercury. J Geophys Res 113:D15305. doi:10.1029/2007JD009428

Sudo K, Akimoto H (2007) Global source attribution of tropospheric ozone: long-range transport from various source regions. J Geophys Res 112:D12302. doi:10.1029/2006JD007992

Suzuki I, Hayashi K, Igarashi Y, Takahashi H, Sawa Y, Ogura N, Akagi T, Dokiya Y (2008) Seasonal variation of water-soluble ion species in the atmospheric aerosols at the summit of Mt. Fuji. Atmos Environ 42:8027–8035. doi:10.1016/j.atmosenv.2008.06.014

Suzuki I, Igarashi Y, Dokiya Y, Akagi T (2010) Two extreme types of mixing of dust with urban aerosols observed in Kosa particles: "after" mixing and "on-the-way" mixing. Atmos Environ 44:858–866. doi:10.1016/j.atmosenv.2009.11.030

Swartzendruber PC, Jaffe DA, Prestbo EM, Weiss-Penzias P, Selin NE, Park R, Jacob DJ, Strode S, Jaeglé L (2006) Observations of reactive gaseous mercury in the free troposphere at the Mount Bachelor Observatory. J Geophys Res 111:D24301. doi:10.1029/2006JD007415

Takahama S, Schwartz RE, Russell LM, Macdonald AM, Sharma S, Leaitch WR (2011) Organic functional groups in aerosol particles from burning and non-burning forest emissions at a high-elevation mountain site. Atmos Chem Phys 11:6367–6386. doi:10.5194/acp-11-6367-2011

Tanimoto H (2009) Increase in springtime tropospheric ozone at a mountainous site in Japan for the period 1998–2006. Atmos Environ 43:1358–1363. doi:10.1016/j.atmosenv.2008.12.006

Tanimoto H, Sawa Y, Matsueda H, Uno I, Ohara T, Yamaji K, Kurokawa J, Yonemura S (2005) Significant latitudinal gradient in the surface ozone spring maximum over East Asia. Geophys Res Lett 32:L21805. doi:10.1029/2005GL023514

Tanimoto H, Mukai H, Sawa Y, Matsueda H, Yonemura S, Wang T, Poon S, Wong A, Lee G, Jung JY, Kim KR, Lee MH, Lin NH, Wang JL, Ou-Yang CF, Wu CF, Akimoto H, Pochanart P, Tsuboi K, Doi H, Zellweger C, Klausen J (2007) Direct assessment of international consistency of standards for ground-level ozone: strategy and implementation toward metrological traceability network in Asia. J Environ Monit 9:1183–1193. doi:10.1039/b701230f

Tanimoto H, Ohara T, Uno I (2009) Asian anthropogenic emissions and decadal trends in springtime tropospheric ozone over Japan: 1998–2007. Geophys Res Lett 36:L23802. doi:10.1029/2009GL041382

Tanimoto H, Zbinden RM, Thouret V, Nédélec P (2015) Consistency of tropospheric ozone observations made by different platforms and techniques in the global databases. Tellus B 67:27073. doi:10.3402/tellusb.v67.27073

Tarasova OA, Elansky NF, Kuznetsov GI, Kuznetsova IN, Senik IA (2003) Impact of air transport on seasonal variations and trends of surface ozone at Kislovodsk high mountain station. J Atmos Chem 45:245–249. doi:10.5194/acp-9-4157-2009

Tarasova OA, Brenninkmeijer CAM, Jöckel P, Zvyagintsev AM, Kuznetsov GI (2007) A climatology of surface ozone in the extra tropics: cluster analysis of observations and model results. Atmos Chem Phys 7:6099–6117. doi:10.5194/acp-7-6099-2007

Tarasova OA, Senik IA, Sosonkin MG, Cui J, Staehelin J, Prévôt ASH (2009) Surface ozone at the Caucasian site Kislovodsk High Mountain Station and the Swiss Alpine site Jungfraujoch: data analysis and trends (1990–2006). Atmos Chem Phys 9:4157–4175. doi:10.5194/acp-9-4157-2009

Thompson AM, Cicerone RJ (1986) Possible perturbations to atmospheric CO, CH_4, and OH. J Geophys Res 91:10853–10864. doi:10.1029/JD091iD10p10853

Thoning KW, Tans PP, Komhyr WD (1989) Atmospheric carbon dioxide at Mauna Loa Observatory 2. Analysis of the NOAA GMCC data, 1974–1985. J Geophys Res 94:8549–8565. doi:10.1029/JD094iD06p08549

Timonen H, Ambrose JL, Jaffe DA (2013) Oxidation of elemental Hg in anthropogenic and marine airmasses. Atmos Chem Phys 13:2827–2836. doi:10.5194/acp-13-2827-2013

Toh YY, Lim SF, von Glasow R (2013) The influence of meteorological factors and biomass burning on surface ozone concentrations at Tanah Rata, Malaysia. Atmos Environ 70:435–446. doi:10.1016/j.atmosenv.2013.01.018

Tressol M, Ordonez C, Zbinden R, Brioude J, Thouret V, Mari C, Nedelec P, Cammas J-P, Smit H, Patz H-W, Volz-Thomas A (2008) Air pollution during the 2003 European heat wave as seen by MOZAIC airliners. Atmos Chem Phys 8:2133–2150. doi:10.5194/acp-8-2133-2008

Trickl T, Cooper OR, Eisele H, James P, Mücke R, Stohl A (2003) Intercontinental transport and its influence on the ozone concentrations over central Europe: three case studies. J Geophys Res 108:8530. doi:10.1029/2002JD002735

Tsutsumi Y, Zaizen Y, Makino Y (1994) Tropospheric ozone measurement at the top of Mt. Fuji. Geophys Res Lett 21:1727–1730. doi:10.1029/94GL01107

Tsutsumi Y, Igarashi Y, Zaizen Y, Makino Y (1998) Case studies of tropospheric ozone events observed at the summit of Mount Fuji. J Geophys Res 103:16935–16951. doi:10.1029/98JD01152

Turekian KK, Nozaki Y, Benninger LK (1977) Geochemistry of atmospheric radon and radon products. Annu Rev Earth Planet Sci 5:227–255. doi:10.1146/annurev.ea.05.050177.001303

Turnbull JC, Lehman SJ, Miller JB, Sparks RJ, Southon JR, Tans PP (2007) A new high precision $^{14}CO_2$ time series for North American continental air. J Geophys Res 112:D11310. doi:10.1029/2006JD008184

Turquety S, Logan JA, Jacob DJ, Hudman RC, Leung FY, Heald CL, Yantosca RM, Wu S, Emmons LK, Edwards DP, Sachse GW (2007) Inventory of boreal fire emissions for North America in 2004: importance of peat burning and pyroconvective injection. J Geophys Res 112:D12S03. doi:10.1029/2006JD007281

Tuzson B, Henne S, Brunner D, Steinbacher M, Mohn J, Buchmann B, Emmenegger L (2011) Continuous isotopic composition measurements of tropospheric CO_2 at Jungfraujoch (3580 m a.s.l.), Switzerland: real-time observation of regional pollution events. Atmos Chem Phys 11:1685–1696. doi:10.5194/acp-11-1685-2011

U.S. Environmental Protection Agency (2006) Air quality criteria for ozone and related photochemical oxidants (2006 Final). U.S. Environmental Protection Agency, Washington, DC

U.S. Environmental Protection Agency Clean Air Markets Division Clean Air Status and Trends Network (CASTNET) [Ozone - Hourly, Filter Pack Concentration -Weekly]. http://www.epa.gov/castnet. Accessed 14 Jan 2016

Umann B, Arnold F, Schaal C, Hanke M, Uecker J, Aufmhoff H, Balkanski Y, Van Dingenen R (2005) Interaction of mineral dust with gas phase nitric acid and sulfur dioxide during the MINATROC II field campaign: first estimate of the uptake coefficient γ_{HNO3} from atmospheric data. J Geophys Res 110:D22306. doi:10.1029/2005JD005906

Usher CR, Michel AE, Grassian VH (2003) Reactions on mineral dust. Chem Rev 103:4883–4940. doi:10.1021/cr020657y

Val Martín M, Honrath RE, Owen RC, Pfister G, Fialho P, Barata F (2006) Significant enhancements of nitrogen oxides, black carbon, and ozone in the North Atlantic lower free troposphere resulting from North American boreal wildfires. J Geophys Res 111:D23S60. doi:10.1029/2006JD007530

Val Martin M, Honrath RE, Owen RC, Lapina K (2008a) Large-scale impacts of anthropogenic pollution and boreal wildfires on the nitrogen oxides over the central North Atlantic region. J Geophys Res 113:D17308. doi:10.1029/2007JD009689

Val Martin M, Honrath RE, Owen RC, Li QB (2008b) Seasonal variation of nitrogen oxides in the central North Atlantic lower free troposphere. J Geophys Res 113:D17307. doi:10.1029/2007JD009688

Van der A RJ, Eskes HJ, Boersma KF, van Noije TPC, Van Roozendae M, De Smedt I, Peters DHMU, Meijer EW (2008) Trends, seasonal variability and dominant NO_x source derived from a ten year record of NO_2 measured from space. J Geophys Res 113:D04302. doi:10.1029/2007JD009021

Van Dingenen R, Putaud J-P, Martins-Dos Santos S, Raes F (2005) Physical aerosol properties and their relation to air mass origin at Monte Cimone (Italy) during the first MINATROC campaign. Atmos Chem Phys 5:2203–2226. doi:10.5194/acp-5-2203-2005

VanCuren RA (2003) Asian aerosols in North America: extracting the chemical composition and mass concentration of the Asian continental aerosol plume from long-term aerosol records in the western United States. J Geophys Res 108:D20. doi:10.1029/2003JD003459

VanCuren RA, Cahill TA (2002) Asian aerosols in North America: frequency and concentration of fine dust. J Geophys Res 107:D24. doi:10.1029/2002JD002204

VanCuren RA, Cliff SS, Perry KD, Jimenez-Cruz M (2005) Asian continental aerosol persistence above the marine boundary layer over the eastern North Pacific: continuous aerosol measurements from Intercontinental Transport and Chemical Transformation 2002 (ITCT 2K2). J Geophys Res 110:D09S90. doi:10.1029/2004JD004973

Verheggen B, Cozic J, Weingartner E, Bower K, Mertes S, Connolly P, Gallagher M, Flynn M, Choularton T, Baltensperger U (2007) Aerosol partitioning between the interstitial and the condensed phase in mixed-phase clouds. J Geophys Res 112:D23202. doi:10.1029/2007JD008714

Verver G, Raes F, Vogelezang D, Johnson D (2000) The 2nd Aerosol Characterization Experiment (ACE-2): meteorological and chemical context. Tellus B 52:126–140. doi:10.1034/j.1600-0889.2000.00090.x

Viatte C, Schneider M, Redondas A, Hase F, Eremenko M, Chelin P, Flaud J-M, Blumenstock T, Orphal J (2011) Comparison of ground-based FTIR and Brewer O_3 total column with data from two different IASI algorithms and from OMI and GOME-2 satellite instruments. Atmos Meas Tech 4:535–546. doi:10.5194/amt-4-535-2011

Vigouroux C, De Mazière M, Errera Q, Mahieu E, Duchatelet P, Wood S, Smale D, Mikuteit S, Blumenstock T, Hase F, Jones N (2007) Comparisons between ground-based FTIR and MIPAS N_2O and HNO_3 profiles before and after assimilation in BASCOE. Atmos Chem Phys 7:377–396. doi:10.5194/acp-7-377-2007

Vigouroux C, De Mazière M, Demoulin P, Servais C, Hase F, Blumenstock T, Kramer I, Schneider M, Mellqvist J, Strandberg A, Velazco V, Notholt J, Sussmann R, Stremme W, Rockmann A, Gardiner T, Coleman M, Woods P (2008) Evaluation of tropospheric and stratospheric ozone trends over Western Europe from ground-based FTIR network observations. Atmos Chem Phys 8:6865–6886. doi:10.5194/acp-8-6865-2008

Vingarzan R (2004) A review of surface ozone background levels and trends. Atmos Environ 38:3431–3442. doi:10.1016/j.atmosenv.2004.03.030

Visheratin KN, Kamenogradskii NE, Kashin FV, Semenov VK, Sinyakov VP, Sorokina LI (2006) Spectral-temporal structure of variations in the atmospheric total ozone in central Eurasia. Izv Atmos Ocean Phys 42:184–202. doi:10.1134/S000143380602006X

Volz A, Kley D (1988) Evaluation of the Montsouris series of ozone measurements made in the nineteenth century. Nature 332:240–242. doi:10.1038/332240a0

Wai KM, Lin N-H, Wang S-H, Dokiya Y (2008) Rainwater chemistry at a high-altitude station, Mt. Lulin, Taiwan: comparison with a background station, Mt. Fuji. J Geophys Res 113:D06305. doi:10.1029/2006JD008248

Wainwright CD, Pierce JR, Liggio J, Strawbridge KB, Macdonald AM, Leaith RW (2012) The effect of model spatial resolution on Secondary Organic Aerosol predictions: a case study at Whistler, BC, Canada. Atmos Chem Phys 12:10911–10923. doi:10.5194/acp-12-10911-2012

Wang T, Wong HLA, Tang J, Ding A, Wu WS, Zhang XC (2006) On the origin of surface ozone and reactive nitrogen observed at a remote mountain site in the northeastern Qinghai-Tibetan Plateau, western China. J Geophys Res 111:D08303. doi:10.1029/2005JD006527

Weiss-Penzias P, Jaffe DA, Swartzendruber P, Dennison JB, Chand D, Hafner W, Prestbo E (2006) Observations of Asian air pollution in the free troposphere at Mount Bachelor Observatory during the spring of 2004. J Geophys Res 111:D10304. doi:10.1029/2005JD006522

Weiss-Penzias P, Jaffe D, Swartzendruber P, Hafner W, Chand D, Prestbo E (2007) Quantifying Asian and biomass burning sources of mercury using the Hg/CO ratio in pollution plumes observed at the Mount Bachelor observatory. Atmos Environ 41:4366–4379. doi:10.1016/j.atmosenv.2007.01.058

Welton EJ, Voss KJ, Gordon HR, Maring H, Smirnov A, Holben B, Schmid B, Livingston JM, Russell PB, Durkee PA, Formenti P, Andreae MO (2000) Ground-based lidar measurements of aerosols during ACE-2: instrument description, results, and comparisons with other ground-based and airborne measurements. Tellus B 52:636–651. doi:10.1034/j.1600-0889.2000.00025.x

Wild O, Pochanart P, Akimoto H (2004) Trans-Eurasian transport of ozone and its precursors. J Geophys Res 109:D11302. doi:10.1029/2003JD004501

Winkler P (1988) Surface ozone over the Atlantic ocean. J Atmos Chem 7:73–91. doi:10.1007/BF00048255

Wolfe GM, Thornton JA, McNeill VF, Jaffe DA, Reidmiller D, Chand D, Smith J, Swartzendruber P, Flocke F, Zheng W (2007) Influence of trans-Pacific pollution transport on acyl peroxy nitrate abundances and speciation at Mount Bachelor Observatory during INTEX-B. Atmos Chem Phys 7:5309–5325. doi:10.5194/acp-7-5309-2007

Wong JPS, Lee AKY, Slowik JG, Cziczo DJ, Leaitch WR, Macdonald A, Abbatt JPD (2011) Oxidation of ambient biogenic secondary organic aerosol by hydroxyl radicals: effects on cloud condensation nuclei activity. Geophys Res Lett 38:L22805. doi:10.1029/2011GL049351

Worden HM, Bowman KW, Worden JR, Eldering A, Beer R (2008) Satellite measurements of the clear-sky greenhouse effect from tropospheric ozone. Nat Geosci 1:305–308. doi:10.1038/ngeo182

Worden HM, Bowman KW, Kulawik SS, Aghedo AM (2011) Sensitivity of outgoing longwave radiative flux to the global vertical distribution of ozone characterized by instantaneous radiative kernels from Aura-TES. J Geophys Res 116:D14115. doi:10.1029/2010JD015101

Worden HM, Deeter MN, Frankenberg C, George M, Nichitiu F, Worden J, Aben I, Bowman KW, Clerbaux C, Coheur PF, de Laat ATJ, Detweiler R, Drummond JR, Edwards DP, Gille JC, Hurtmans D, Luo M, Martínez-Alonso S, Massie S, Pfister G, Warner JX (2013) Decadal record of satellite carbon monoxide observations. Atmos Chem Phys 13:837–850. doi:10.5194/acp-13-837-2013

World Data Centre for Greenhouse Gases, Tokyo. http://ds.data.jma.go.jp/gmd/wdcgg/. Accessed 15 Dec 2015

World Health Organization (2006) WHO Air quality guidelines for particulate matter, ozone, nitrogen dioxide and sulfur dioxide: global update 2005: summary of risk assessment. WHO Press, Geneva

World Meteorological Organization (2010) Guidelines for the measurement of atmospheric carbon monoxide, GAW Report No. 192. World Meteorological Organization, Geneva

World Meteorological Organization (2013) Guidelines for continuous measurements of ozone in the troposphere, GAW Report No. 209. World Meteorological Organization, Geneva

Wunch D, Toon GC, Blavier J-FL, Washenfelder RA, Notholt J, Connor BJ, Griffith DWT, Sherlock V, Wennberg PO (2011) The total carbon column observing network. Philos Trans R Soc A Math Phys Eng Sci 369:2087–2112. doi:10.1098/rsta.2010.0240

Xu WY, Lin WL, Xu XB, Tang J, Huang JQ, Wu H, Zhang XC (2015) Long-term trends of surface ozone and its influencing factors at the Mt. Waliguan GAW station, China—part 1: overall trends and characteristics. Atmos Chem Phys Discuss 15:30987–31024. doi:10.5194/acpd-15-30987-2015

Xue LK, Wang T, Zhang JM, Zhang XC, Poon CN, Ding AJ, Zhou XH, Wu WS, Tang J, Zhang QZ, Wang WX (2011) Source of surface ozone and reactive nitrogen speciation at Mount Waliguan in western China: new insights from the 2006 summer study. J Geophys Res 116:D07306. doi:10.1029/2010JD014735

Xue LK, Wang T, Guo H, Blake DR, Tang J, Zhang XC, Saunders SM, Wang WX (2013) Sources and photochemistry of volatile organic compounds in the remote atmosphere of western China: results from the Mt. Waliguan Observatory. Atmos Chem Phys 13:8551–8567. doi:10.5194/acp-13-8551-2013

Yienger J, Galanter M, Holloway TA, Phadnis MJ, Guttikunda SK, Carmichael GR, Moxim WJ, Levy II H (2000) The episodic nature of air pollution transport from Asia to North America. J Geophys Res 105:26931–26945. doi:10.1029/2000JD900309

Yonemura S, Tsuruta H, Kawashima S, Sudo S, Peng LC, Fook LS, Johar Z, Hayashi M (2002) Tropospheric ozone climatology over Peninsular Malaysia from 1992 to 1999. J Geophys Res 107:4229. doi:10.1023/A:1016152929037

Yurganov LN, Blumenstock T, Grechko EI, Hase F, Hyer EJ, Kasischke ES, Koike M, Kondo Y, Kramer I, Leung F-Y, Mahieu E, Mellqvist J, Notholt J, Novelli PC, Rinsland CP, Scheel HE, Schulz A, Strandberg A, Sussman R, Tanimoto H, Velazco V, Zander R, Zhao Y (2004) A quantitative assessment of the 1998 carbon monoxide emission anomaly in the Northern Hemisphere based on total column and surface concentration measurements. J Geophys Res 109:D15305. doi:10.1029/2004JD004559

Yurganov LN, Duchatelet P, Dzhola AV, Edwards DP, Hase F, Kramer I, Mahieu E, Mellqvist J, Notholt J, Novelli PC, Rockmann A, Scheel HE, Schneider M, Schulz A, Strandberg A, Sussmann R, Tanimoto H, Velazco V, Drummond JR, Gille JC (2005) Increased Northern Hemispheric carbon monoxide burden in the troposphere in 2002 and 2003 detected from the ground and from space. Atmos Chem Phys 5:563–573. doi:10.5194/acp-5-563-2005

Zander R, Demoulin P, Ehhalt DH, Schmidt U, Rinsland CP (1989) Secular increase of the total vertical column abundance of carbon monoxide above central Europe since 1950. J Geophys Res 94:11021–11028. doi:10.1029/JD094iD08p11021

Zander R, Mahieu E, Demoulin P, Duchatelet P, Roland G, Servais C, De Mazière M, Reimann S, Rinsland CP (2008) Our changing atmosphere: evidence based on long-term infrared solar observations at the Jungfraujoch since 1950. Sci Total Environ 391:184–195. doi:10.1016/j.scitotenv.2007.10.018

Zander R, Duchatelet P, Mahieu E, Demoulin P, Roland G, Servais C, Auwera JV, Perrin A, Rinsland CP, Crutzen PJ (2010) Formic acid above the Jungfraujoch during 1985-2007: observed variability, seasonality, but no long-term background evolution. Atmos Chem Phys 10:10047–10065. doi:10.5194/acp-10-10047-2010

Zanis P, Schuepbach E, Gäggeler HW, Hübener S, Tobler L (1999) Factors controlling beryllium-7 at Jungfraujoch in Switzerland. Tellus B 51:789–805. doi:10.1034/j.1600-0889.1999.t01-3-00004.x

Zanis P, Gerasopoulos E, Priller A, Schnabel C, Stohl A, Zerefos C, Gäggeler HW, Tobler L, Kubik PW, Kanter HJ, Scheel HE, Luterbacher J, Berger M (2003a) An estimate of the impact of stratosphere-to-troposphere transport (STT) on the lower free tropospheric ozone over the Alps using ^{10}Be and ^{7}Be measurements. J Geophys Res 108:8520. doi:10.1029/2002JD002604

Zanis P, Monks PS, Green TJ, Schuepbach E, Carpenter LJ, Mills GP, Rickard AR, Brough N, Penkett SA (2003b) Seasonal variation of peroxy radicals in the lower free troposphere based on observations from the FREE Tropospheric EXperiments in the Swiss Alps. Geophys Res Lett 30:1497. doi:10.1029/2003GL017122

Zanis P, Ganser A, Zellweger C, Henne S, Steinbacher M, Staehelin J (2007) Seasonal variability of measured ozone production efficiencies in the lower free troposphere of Central Europe. Atmos Chem Phys 7:223–236. doi:10.5194/acp-7-223-2007

Zellweger C, Ammann M, Buchmann B, Hofer P, Lugauer M, Rüttimann R, Streit N, Weingartner E, Baltensperger U (2000) Summertime NO_y speciation at the Jungfraujoch, 3580m above sea level, Switzerland. J Geophys Res 105:6655–6667. doi:10.1029/1999JD901126

Zellweger C, Forrer J, Hofer P, Nyeki S, Schwarzenbach B, Weingartner E, Ammann M, Baltensperger U (2003) Partitioning of reactive nitrogen (NO_y) and dependence on meteorological conditions in the lower free troposphere. Atmos Chem Phys 3:779–796. doi:10.5194/acp-3-779-2003

Zellweger C, Klausen J, Buchmann B (2007) System and performance audit for surface ozone and carbon monoxide at the Global GAW station Assekrem, Algeria, May 2007, WCC-Empa Report 07/2. Empa, Dübendorf

Zellweger C, Hüglin C, Klausen J, Steinbacher M, Vollmer M, Buchmann B (2009) Inter-comparison of four different carbon monoxide measurement techniques and evaluation of the long-term carbon monoxide time series of Jungfraujoch. Atmos Chem Phys 9:3491–3503. doi:10.5194/acp-9-3491-2009

Zenker T, Fischer H, Nikitas C, Parchatka U, Harris GW, Mihelcic D, Müsgen P, Pätz HW, Schultz M, Voltz-Thomas A, Schmitt R, Behmann T, Weißenmayer M, Burrows JP (1998) Intercomparison of NO, NO_2, NO_y, O_3, and RO_x measurements during the Oxidizing Capacity of the Tropospheric Atmosphere (OCTA) campaign 1993 at Izaña. J Geophys Res 103:13615–13634. doi:10.1029/97JD03739

Zhang L, Jacob DJ, Boersma KF, Jaffe DA, Olson JR, Bowman KW, Worden JR, Thompson AM, Avery MA, Cohen RC, Dibb JE, Flocke FM, Fuelberg HE, Huey LG, McMillan WW, Singh HB, Weinheimer AJ (2008) Transpacific transport of ozone pollution and the effect of recent Asian emission increases on air quality in North America: an integrated analysis using satellite, aircraft, ozonesonde, and surface observations. Atmos Chem Phys 8:6117–6136. doi:10.5194/acp-8-6117-2008

Zhang JM, Wang T, Ding AJ, Zhou XH, Xue LK, Poon CN, Wu WS, Gao J, Zuo HC, Chen JM, Zhang XC, Fan SJ (2009a) Continuous measurement of peroxyacetyl nitrate (PAN) in suburban and remote areas of western China. Atmos Environ 43:228-237. doi:10.1016/j.atmosenv.2008.09.070

Zhang L, Jacob DJ, Kopacz M, Henze DK, Singh K, Jaffe DA (2009b) Intercontinental source attribution of ozone pollution at western U.S. sites using an adjoint method. Geophys Res Lett 36:L11810. doi:10.1029/2009GL037950

Zhang F, Zhou LX, Novelli PC, Worthy DEJ, Zellweger C, Klausen J, Ernst M, Steinbacher M, Cai YX, Xu L, Fang SX, Yao B (2011) Evaluation of in situ measurements of atmospheric carbon monoxide at Mount Waliguan, China. Atmos Chem Phys 11:5195–5206. doi:10.5194/acp-11-5195-2011

Zhang B, Owen RC, Perlinger JA, Kumar A, Wu S, Val Martin M, Kramer L, Helmig D, Honrath RE (2014) A semi-Lagrangian view of ozone production tendency in North American outflow in the summers of 2009 and 2010. Atmos Chem Phys 14:2267–2287. doi:10.5194/acp-14-2267-2014

Zhu B, Akimoto H, Wang Z, Sudo K, Tang J, Uno I (2004) Why does surface ozone peak in summertime at Waliguan? Geophys Res Lett 31:L17104. doi:10.1029/2004GL020609

Zieger P, Kienast-Sjögren E, Starace M, Von Bismarck J, Bukowiecki N, Baltensperger U, Wienhold FG, Peter T, Ruhtz T, Collaud Coen M, Vuilleumier L, Maier O, Emili E, Popp C, Weingartner E (2012) Spatial variation of aerosol optical properties around the high-alpine site Jungfraujoch (3580 m a.s.l.). Atmos Chem Phys 12:7231–7249. doi:10.5194/acp-12-7231-2012

Zieman JJ, Holmes JL, Connor D, Jensen CR, Zoller WH, Hermann DM, Parrington JR, Gordon GE (1995) Atmospheric aerosol trace element chemistry at Mauna Loa Observatory 1. 1979–1985. J Geophys Res 100:25979–25994. doi:10.1029/93JD03316